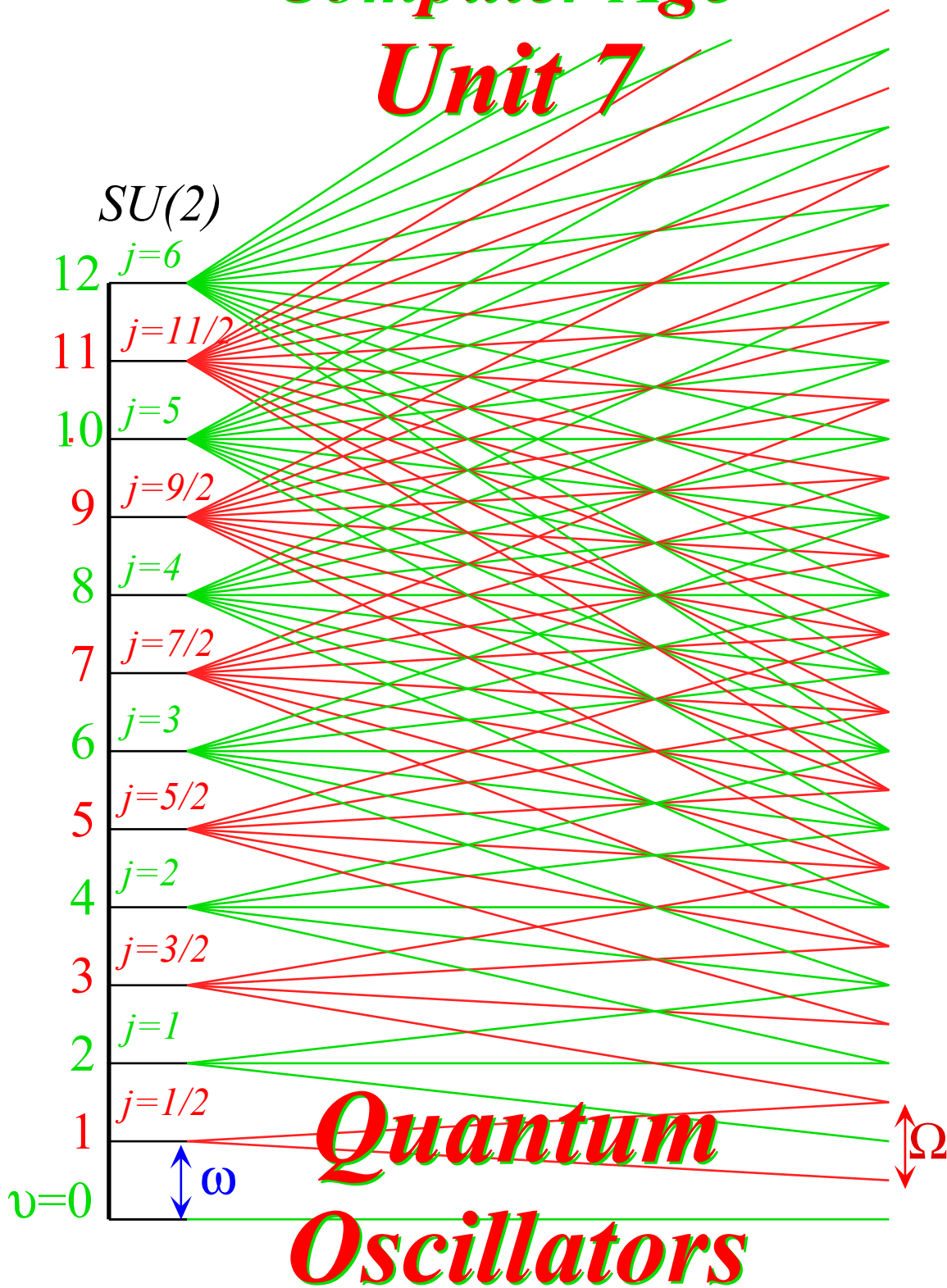


Quantum Theory for the Computer Age

Unit 7



Unit 7 Quantum Oscillators

Harmonic oscillation is the end-all and be-all of quantum theory. Planck's oscillation hypothesis begins it, and it's nothing but oscillation and resonance from there on. This unit begins the analysis of 1D oscillation in the non-relativistic Schrodinger context and then develops the creation-destruction ($a^\dagger a$) operator technology for multi-dimensional oscillators. Particular attention is paid to 2D oscillators that served as classical ABCD spin-and 2-state analogs in Chapter 10 of Unit 3. The quantum versions of the ABCD oscillator further elucidate the elegant $U(2)$ quantum mechanics of Schwinger used in the next unit to finesse angular momentum theory. It also begins the elementary quantum radiation ("photon") theory that is sometimes mistakenly referred to as "2nd quantization" if dimensions and "particles" get confused. Similar techniques are used to define "phonon" excitations for mechanical waves in solids, liquids, molecules, or molecular clusters.

W. G. Harter

Department of Physics

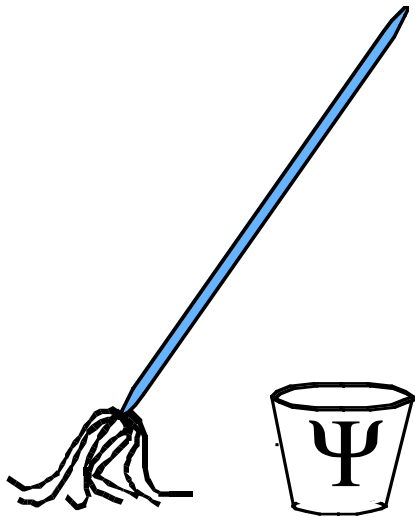
University of Arkansas

Fayetteville

Hardware and Software by

HARTER-Soft

Elegant Educational Tools Since 2001



QM for AMOP

Chapter 20

One-Dimensional

Oscillator States and Dynamics

W. G. Harter

Every continuous potential may be expanded in a Taylor polynomial about a minimum point so that the first variable term is quadratic: $V(x-x_{\min})=V_{\min}+1/2k(x-x_{\min})^2\dots$ This is just one of about a million reasons that harmonic oscillator analysis is useful in physics. The harmonic oscillator potential $V(x)=1/2kx^2$ gives a most symmetric non-relativistic Hamiltonian with the (rescaled) form: $H=P^2+X^2$. Because of this symmetry, its eigensolution analysis and application is extraordinarily convenient. We plan to take advantage of this here in Chapter 20 and in many of the later Chapters, as well.

CHAPTER 20. 1D-HARMONIC OSCILLATOR STATES AND DYNAMICS1

20.1 Harmonic Oscillator Equations1

- (a) Classical harmonic oscillator equations1
- (b) Quantum harmonic oscillator equations2
 - (1) Schrodinger oscillator equation2
 - (2) Hermite equations: Gaussians and zero point energy3

20.2 Harmonic Oscillator Eigensolutions5

- (a) Creation and destruction operators5
 - (1) Operator commutation relations5
 - (2) Eigenstate creationism (and destruction)6
 - (3) Wavefunction creationism7
- (b) Matrix and normalization calculations9
 - (1) Normalization and ladder operations10
 - (2) Number operator10
 - (3) Expectation values and uncertainty11
 - (4) Uncertainty approximation for anharmonic spectra12
- (c) High quantum oscillator states14

20.3 Harmonic Oscillator Dynamics and Coherent States15

- (a) Oscillator quantum beats15
 - (1) Energy expectation value16
 - (2) Position expectation values16
 - (3) Momentum expectation values18
- (b) Oscillator coherent states (“Shoved” and “kicked” states)18
 - (1) Translation operators and generators: (A “shove”)18
 - (2) Boost operators and generators: (A “kick”)20
 - (3) Applying boost-translation combinations21
 - (4) Time evolution of coherent states22
- (c) Classical and quantum dynamics of wavepackets25
 - (1) Classical action and phase25
 - (2) Quantum generating functions27
- (d) Shaped packet states (“Squeezed” states)27

Problems for Chapter 2032

CHAPTER 21. 2D-HARMONIC OSCILLATOR STATES AND DYNAMICS1

21.1 Two-Dimensional Harmonic Oscillator Hamiltonians and Bases1

- (a) 2D-Oscillator basics1
 - (1) Hamiltonians and operators1
 - (2) Commutation relations: Bosons and Fermions1
- (b) Two-dimensional (or 2-particle) base states3
- (c) Two-dimensional (or 2-particle) matrix operators5
- (d) 2D-Oscillator eigensolutions7
 - (1) Fundamental eigenstates7
 - (2) $U(2) \supset C2A$ eigenstates and wavefunctions10
 - (3) $U(2) \supset C2A$ oscillator wavefunctions11
- 21.2 2D Oscillator Symmetry, Spin, and Wavefunctions15**
 - (a) Angular momentum eigenstates: $C2C$ symmetry15
 - (1) Angular momentum labeling: Fundamental base states $\{|\uparrow\rangle, |\downarrow\rangle\}$ 16
 - (2) 3-Vector base states ($v=2$) or ($j=1$)19
 - (b) Polar coordinates: $C2C$ symmetry variable separation22
- 21.3 N-Dimensional Oscillator Levels25**
 - (a) Pascal triangle and $U(N)$ degeneracy25
- Problems for Chapter 2128**

Chapter 22 Quantum Electromagnetic Fields

22.1 QUANTUM ELECTROMAGNETIC FIELDS AND TRANSITIONS 2

- a. Classical Electromagnetic Fields and Operators 3
 - Classical Phasor Energy Relations 3
 - Classical Field Oscillator Variables 5
- b. Quantum Field Operators 6
- c. Electromagnetic Quantum States and Atomic Transitions 8
 - Single-Mode Atomic Dipole Transitions 9
 - Multimode Atomic Dipole Transitions 10
- c. "Impotence" of Photon Number States 13
- d. Coherent Radiation States 16
 - Do low-quantum fields make good coordinate frames? 17

22.2 SPECTRA OF ATOMS IN LASER CAVITY 19

- a. Jaynes-Cummings Hamiltonian 19
- b. Jaynes-Cummings Eigensolutions 22
- c. Transitions in the Jaynes-Cummings Model 24
 - Rayleigh scattering and fluorescence 25
 - Coherent Stokes Raman scattering 25

ADDITIONAL READING 29

Chapter 20. 1D-Harmonic Oscillator States and Dynamics

20.1 Harmonic Oscillator Equations

(a) Classical harmonic oscillator equations

To be *harmonic*, an oscillating body must return to a given initial position and velocity with the same frequency for a wide range of amplitudes. A sufficient (but not necessary) condition for this is that the body has a *linear* restoring force, that is, a Hooke's law force with a fixed *spring constant* k .

$$F = -kx \quad (20.1.1)$$

Then, and only then, will the classical motion of a body of mass M be purely sinusoidal with a single angular frequency ω totally independent of amplitude A .

$$x(t) = A \sin(\omega t + \alpha), \text{ where: } \omega = \sqrt{\frac{k}{m}} \quad (20.1.2)$$

The acceleration, and hence, by Newton II, the force is always proportional to the displacement $x(t)$,

$$\frac{d^2x}{dt^2} = \ddot{x}(t) = -\omega^2 A \sin(\omega t - \alpha) = -\omega^2 x(t), \quad (20.1.3a)$$

or

$$m\ddot{x}(t) = -\omega^2 A \sin(\omega t - \alpha) = -m\omega^2 x(t) = -kx(t). \quad (20.1.3b)$$

Given the proportionality or linearity between force and displacement, it follows that the work or potential energy associated with a Hooke-spring type force must be a *quadratic* potential.

$$V(x) = \int_0^x kx' dx' = \frac{1}{2} kx^2 = \frac{1}{2} m\omega^2 x^2 \quad (20.1.4)$$

From this follows the classical total energy or *Hamiltonian function* of the 1D harmonic oscillator.

$$E = H(x, p) = \frac{1}{2m} p^2 + \frac{1}{2} m\omega^2 x^2 \quad (20.1.5a)$$

Here the classical momentum is

$$p = m \frac{dx}{dt} = m\dot{x} \quad (20.1.5b)$$

It should be noted that the oscillator equations apply to a good deal more than a glob of lead on a coiled spring or pendulum. As pointed out in Chapter 10, harmonic oscillator equations of motion apply to any independent oscillator system such as a normal mode of vibration or a classical electromagnetic wave introduced in Chapter 4 or an electromagnetic mode such as we touched on in Chapter 6 (Sec. 6.3(d)) or for the classical electromagnetic Hamiltonian developed in Chapter 17.

It is these more complicated systems, primarily electromagnetic oscillation, that really make use of the oscillator quantum mechanics we are about to develop. However, just to get started, we can think of a (very small) blob of lead bouncing up and down on a (frictionless) spring as in Fig. 10.1.1 or a pendulum swinging back and forth at the end of a string as sketched in Fig. 16.1.1(a).

(b) Quantum harmonic oscillator equations

Converting the classical Hamiltonian H to a quantum Hamiltonian \mathbf{H} -operator is done in the same way for the oscillator as it was for a general potential $V(x)$ in equations (11.4.5). The first step is to convert all the coordinates and momenta to operators. At first, this just means just writing x and p with a thick pen to give \mathbf{x} and \mathbf{p} , something a five-year-old could do!

$$\mathbf{H}(\mathbf{x},\mathbf{p}) = \mathbf{p}^2/2M + V(\mathbf{x}) = \mathbf{p}^2/2M + M\omega^2\mathbf{x}^2/2 \quad (20.1.6)$$

However, we need to decide how to represent those thick-headed operators \mathbf{x} and \mathbf{p} , and right away we notice something unique about this Hamiltonian. Apart from scale factors $1/2M$ or $M\omega^2/2$, this Hamiltonian has a form $(\mathbf{P}^2 + \mathbf{X}^2)/2$ which is symmetric to interchange of position \mathbf{X} and momentum \mathbf{P} (or DeBroglie wavevector $\hbar\mathbf{k}$). It isn't going to make much difference whether we represent this problem in position x -space $\{..|x\rangle..\}$ or in momentum (Fourier wavevector) k -space $\{..|k\rangle..\}$.

So which do we use? The best answer turns out to be neither and both! We will solve this system's Schrodinger equations using discrete abstract algebra, but first, tie this to a standard historical approach to the harmonic oscillator that uses the calculus of continuous differential equations.

(1) Schrodinger oscillator equation

The commonly stated form of Schrodinger's equation is in the position x -space basis $\{..|x\rangle..\}$ for which the representation of the Hamiltonian is that given by (11.4.5c) with potential $V(x) = M\omega^2x^2/2$.

$$\begin{aligned} i\hbar\langle x|\frac{\partial}{\partial t}|\Psi\rangle &= \langle x|\mathbf{H}|\Psi\rangle = \langle x|\frac{\mathbf{p}^2}{2M} + \frac{M\omega^2\mathbf{x}^2}{2}|\Psi\rangle, \\ i\hbar\frac{\partial\Psi(x,t)}{\partial t} &= \frac{-\hbar^2}{2M}\frac{\partial^2\Psi(x,t)}{\partial x^2} + \frac{M\omega^2x^2}{2}\Psi(x,t) \end{aligned} \quad (20.1.7a)$$

The time dependent equation describes all the possible motion of a quantum oscillator, but first, we have to solve the time independent oscillator Schrodinger equation, that is, its *energy eigenvalue equations*,

$$\langle x|\mathbf{H}|E\rangle = E\langle x|E\rangle, \quad \text{or:} \quad \frac{-\hbar^2}{2M}\frac{\partial^2\psi_E(x)}{\partial x^2} + \frac{M\omega^2x^2}{2}\psi_E(x) = E\psi_E(x) \quad (20.1.7b)$$

where the latter follow from a simple substitution of a special time-dependent wavefunction

$$\Psi_{\text{special}}(x,t) = e^{-i\omega t}\psi_E(x) = e^{-iE t/\hbar}\psi_E(x) \quad (20.1.7c)$$

into (20.1.7a). Once we get the allowed energy (or frequency) eigenvalues $E=E_n$ and eigenfunctions

$$\psi_{E_n}(x) = \langle x|E_n\rangle = \langle x|n\rangle, \quad (20.1.7c)$$

then oscillator time behavior depends on linear combinations $\Psi_{\text{general}}(x,t)$ of eigenfunctions.

$$\Psi_{\text{general}}(x,t) = \sum_n a_n e^{-i\omega_n t}\psi_{E_n}(x) = \sum_n a_n e^{-iE_n t/\hbar}\psi_{E_n}(x), \quad (20.1.7d)$$

Each eigenfunction oscillates at its own (eigen) frequency and contributes to a Fourier time function.

The "special" wavefunctions $\Psi_{special}(x,t)$ or eigenfunctions $\psi_E(x)$ represent *stationary states*. Their probability distributions are motionless, that is, dead as a doornail.

$$\frac{d}{dt} \left(\Psi_{special}^* \Psi_{special} \right) = \frac{d|\psi_E(x)|^2}{dt} = 0 .$$

Motion and life as we know it comes only from a general wavefunction $\Psi_{general}(x,t)$ that is a combination of at least two such eigenfunctions with different (eigen)frequencies. Remember, the fundamental quantum time principle: "It takes two to Tango!" which was shown in Sec.4.4(a), 9.4(a), 10.2 (b) and 12.1(b).

(2) Hermite equations: Gaussians and zero point energy

The resulting eigenfunction differential equation is the Hermitian form of *Hermite's equation*.

$$H \cdot \psi_E(x) = \frac{d^2 \psi_E(x)}{dx^2} + (\varepsilon - ax^2) \psi_E(x) = 0 \quad \text{where: } a = \frac{M^2 \omega^2}{\hbar^2} \quad \text{and: } \varepsilon = \frac{2ME}{\hbar^2} \quad (20.1.8)$$

Historically, this is significant since Hermite's name appears on both this special equation and the concept of Hermitian (self-conjugate) operators ($H^\dagger = H$) which satisfy the Sturm-Liouville requirements discussed in Ch. 11 in equations (11.2.20) to (11.2.23). Gauss's name is significant, too, because it was known that a Gaussian function $e^{-\alpha x^2}$ is one very important solution to this equation as seen here. The derivatives

$$\frac{d}{dx} e^{-\alpha x^2} = -2\alpha x e^{-\alpha x^2}, \quad \frac{d^2}{dx^2} e^{-\alpha x^2} = -2\alpha e^{-\alpha x^2} + 4\alpha^2 x^2 e^{-\alpha x^2} \quad (20.1.9)$$

yield the following solution of (20.1.8)

$$\frac{d^2 \psi_E(x)}{dx^2} + (\varepsilon - ax^2) \psi_E(x) = 0 \quad \text{where: } \psi_E(x) = \frac{e^{-\alpha x^2}}{norm}, \quad a = 4\alpha^2 \quad \text{and: } \varepsilon = 2\alpha \quad (20.1.10a)$$

This gives the following Gaussian decay constant α and energy eigenvalue E .

$$\alpha = \frac{M\omega}{2\hbar}, \quad \text{and: } E = \frac{\hbar^2}{2M} \varepsilon = \frac{\hbar\omega}{2} \quad (20.1.10b)$$

The energy value $E = \hbar\omega/2$ is the ground state energy of a harmonic oscillator. It is called the *vacuum zero point energy* $E_0 = \hbar\omega/2$, and it has tremendous physical significance. It is related to the great "roar of the vacuum" at absolute zero temperature. It is the electromagnetic energy that remains after all "photons" and other excitation energies are as gone as is possible.

In spite of the overwhelming presence and significance of the zero-point wave, it is regarded as a nuisance for the treatment of differential equations. So the Gaussian is factored out by making it a scaling function $s(x) = e^{-\alpha x^2}$ such that the differential operator for a rescaled function $\psi(x) = s(x)\phi(x)$ is easier to

solve in polynomial form. Derivatives of a rescaled wavefunction convert the Hermite equation

$$(20.1.8) \quad \begin{aligned} \psi &= s \cdot \phi, & \psi' &= s' \cdot \phi + s \cdot \phi', & \psi'' &= s'' \cdot \phi + 2s' \cdot \phi' + s \cdot \phi'' \\ s \cdot \phi'' + 2s' \cdot \phi' + (s'' + \epsilon s - \alpha x^2 s) \phi &= 0 = e^{-\alpha x^2} \left[\phi'' - 4\alpha x \phi' + (-2\alpha + 4\alpha^2 x^2 + \epsilon - \alpha x^2) \phi \right] \end{aligned}$$

The rescaled equation is a standard form of Hermite's equation. Here we use $a=4\alpha^2$ from (20.1.10a).

$$K \cdot \phi = \phi'' - 4\alpha x \phi' + (\epsilon - 2\alpha) \phi = 0 \quad (20.1.11)$$

Putting in the ground state energy $\epsilon=2\alpha$ from (20.1.10a) gives two solutions: $\phi=const.$ and $\phi=\int dx e^{2\alpha x^2}$.

Only the first solution is of interest here, but it just gives back the Gaussian wavefunction

$$\psi(x)=s(x)\phi(x) = e^{-\alpha x^2} \text{ (const.)} \quad (20.1.12)$$

which was known (for centuries) before. The second solution blows up.

$$\psi(x)=s(x)\phi(x) = e^{-\alpha x^2} \int dx e^{2\alpha x^2} \rightarrow \infty \text{ as } x \rightarrow \infty \quad (20.1.13)$$

This "blow-up" solution is not wrong. It is the manifestation of the non-resonant eigenchannel wave or the "wrong" local-symmetry wavefunction discussed before in Sec. 14.1(c) (Fig. 14.1.13) and Sec.15.4(c). These waves are only needed if we plan to make "global" waves that flow in and out of the harmonic oscillator potential well. Since we are only dealing with local wavefunctions, this type of wave solution will not be considered in this section. The same applies to solution of (20.1.11) for other values of ϵ including other eigenvalues. (Only "quantized" eigenvalues give localized solutions.)

All local wavefunctions have an over-riding Gaussian envelope $e^{-\alpha x^2}$ with the constant $\alpha = M\omega/2\hbar$ proportional to mass M and natural frequency ω . The Gaussian width or "uncertainty" is proportional to the inverse square-root $1/\sqrt{\alpha}$ of this constant. (Just remember that $e^{-3}=5\%$ so the wave is down by 95% in a distance $x_{5\%}$ such that $\alpha(x_{5\%})^2 = 3$ or $x_{5\%} = \sqrt{3/\alpha}$.) So the quantum uncertainty fringe of the evanescent wave decreases exponentially with increasing mass or natural frequency.

The resulting standard Hermite equation (20.1.11) has some disadvantages over (20.1.8). The differential operator K is not Hermitian, that is, $(\mathbf{K}^\dagger \neq \mathbf{K})$. For these (and other) reasons we will go back to modern algebraic methods which deal with Hermitian Hamiltonian equations and unitary evolution operators. From time to time we will check our results with the differential equation (20.1.11).

20.2 Harmonic Oscillator Eigensolutions

(a) Creation and destruction operators

The key to the quantum oscillator eigensolutions is almost as simple as the factoring a^2-b^2 into $(a+b)(a-b)$. Actually, it involves factoring $\mathbf{P}^2+\mathbf{X}^2$ into $(\mathbf{X}+i\mathbf{P})(\mathbf{X}-i\mathbf{P})$ where operators

$$\mathbf{X} = \sqrt{M\omega} \mathbf{x} / \sqrt{2} \quad \text{and} \quad \mathbf{P} = \mathbf{p} / \sqrt{2M} \quad (20.2.1a)$$

are scaled position \mathbf{x} and momentum \mathbf{p} operators that square and sum to make the oscillator Hamiltonian (20.1.6). Since \mathbf{x} and \mathbf{p} do not commute the factorization is done symmetrically.

$$\mathbf{H}(\mathbf{x},\mathbf{p}) = \mathbf{P}^2+\mathbf{X}^2 = (\mathbf{X}-i\mathbf{P})(\mathbf{X}+i\mathbf{P})/2 + (\mathbf{X}+i\mathbf{P})(\mathbf{X}-i\mathbf{P})/2$$

Also, Planck's quantum oscillator energy $\hbar\omega$ is factored out as well.

$$\mathbf{H}(\mathbf{x},\mathbf{p}) = \mathbf{p}^2/2M + M\omega^2\mathbf{x}^2/2 = \hbar\omega (\mathbf{a}^\dagger\mathbf{a} + \mathbf{a}\mathbf{a}^\dagger)/2 \quad (20.2.1b)$$

The resulting operator factors include the following *destruction operator* \mathbf{a}

$$\mathbf{a} = \frac{(\mathbf{X} + i\mathbf{P})}{\sqrt{\hbar\omega}} = \frac{(\sqrt{M\omega} \mathbf{x} + i\mathbf{p} / \sqrt{M\omega})}{\sqrt{2\hbar}}, \quad (20.2.1c)$$

and the conjugate factor is called a *creation operator* \mathbf{a}^\dagger . This naming will make sense shortly.

$$\mathbf{a}^\dagger = \frac{(\mathbf{X} - i\mathbf{P})}{\sqrt{\hbar\omega}} = \frac{(\sqrt{M\omega} \mathbf{x} - i\mathbf{p} / \sqrt{M\omega})}{\sqrt{2\hbar}}, \quad (20.2.1d)$$

Recall from (11.3.10) and (11.3.11) that position \mathbf{x} and momentum \mathbf{p} are Hermitian operators.

$$\mathbf{x}^\dagger = \mathbf{x} \quad \mathbf{p}^\dagger = \mathbf{p} = \hbar\mathbf{k}$$

So the \mathbf{a} and \mathbf{a}^\dagger operators differ only by the sign of the imaginary i . Why the operator holding the dagger \dagger should be called a creation operator is like a murder mystery that will be revealed in due time!

The classical equivalent of the \mathbf{a} -operators are the *phasor coordinates* introduced in Ch. 10. The phasor coordinates $a_1=x_1+ip_1$ and $a_2=x_2+ip_2$ defined in (10.1.1c) related the classical phase space of a two-dimensional oscillator to the wave amplitudes of a 2-state quantum system. Later, we will discuss quantum oscillation of dimension-two, too, to do $SU(2)$ quantum theory using two independent sets of \mathbf{a} and \mathbf{a}^\dagger operators $\{\mathbf{a}_1=\mathbf{X}_1 + i\mathbf{P}_1, \mathbf{a}_1^\dagger=\mathbf{X}_1 - i\mathbf{P}_1\}$ and $\{\mathbf{a}_2=\mathbf{X}_2 + i\mathbf{P}_2, \mathbf{a}_2^\dagger=\mathbf{X}_2 - i\mathbf{P}_2\}$.

(1) Operator commutation relations

Operator algebra invariably involves questions of commutation or lack thereof. Here it starts with finding the basic commutation difference $\mathbf{x}\mathbf{p}-\mathbf{p}\mathbf{x}$ of position and momentum called a *commutator* $[\mathbf{x}, \mathbf{p}]$. One way to do this appeals to coordinate representations (11.3.10) and (11.3.11).

$$\begin{aligned} \langle x | \mathbf{x}\mathbf{p} - \mathbf{p}\mathbf{x} | \psi \rangle &= \frac{\hbar}{i} \left(x \frac{\partial}{\partial x} \psi(x) - \frac{\partial}{\partial x} x \psi(x) \right) = \frac{\hbar}{i} \left(x \frac{\partial}{\partial x} \psi(x) - x \frac{\partial}{\partial x} \psi(x) - \frac{\partial x}{\partial x} \psi(x) \right) \\ &= \langle x | [\mathbf{x}, \mathbf{p}] | \psi \rangle = -\frac{\hbar}{i} \psi(x) = \hbar i \psi(x) \end{aligned}$$

In abstract operator notation this is written simply as a *commutator* $[\mathbf{x}, \mathbf{p}]$ relation.

$$[\mathbf{x}, \mathbf{p}] \equiv \mathbf{x}\mathbf{p} - \mathbf{p}\mathbf{x} = \hbar i \mathbf{1} \quad (20.2.2)$$

Oscillator quantum mechanics involves commutation relations with \mathbf{a} and \mathbf{a}^\dagger .

$$\begin{aligned} [\mathbf{a}, \mathbf{a}^\dagger] &\equiv \mathbf{a}\mathbf{a}^\dagger - \mathbf{a}^\dagger\mathbf{a} \\ &= \frac{1}{2\hbar} \left(\sqrt{M\omega} \mathbf{x} + i\mathbf{p} / \sqrt{M\omega} \right) \left(\sqrt{M\omega} \mathbf{x} - i\mathbf{p} / \sqrt{M\omega} \right) - \left(\sqrt{M\omega} \mathbf{x} - i\mathbf{p} / \sqrt{M\omega} \right) \left(\sqrt{M\omega} \mathbf{x} + i\mathbf{p} / \sqrt{M\omega} \right) \end{aligned}$$

This is nicely simplified using (20.2.2) to give

$$[\mathbf{a}, \mathbf{a}^\dagger] = \frac{2i}{2\hbar} (\mathbf{p}\mathbf{x} - \mathbf{x}\mathbf{p}) = \frac{-i}{\hbar} [\mathbf{x}, \mathbf{p}] = \mathbf{1} \quad (20.2.3a)$$

or $\mathbf{a} \mathbf{a}^\dagger = \mathbf{a}^\dagger \mathbf{a} + \mathbf{1} \quad (20.2.3b)$

Just this simple relation by itself lets us simplify the Hamiltonian (20.2.1b) and expose the zero-point energy $E_0 = \hbar\omega/2$ first seen in (20.1.10b).

$$\begin{aligned} \mathbf{H}(\mathbf{x}, \mathbf{p}) &= \hbar\omega (\mathbf{a}^\dagger\mathbf{a} + \mathbf{a}\mathbf{a}^\dagger)/2 = \hbar\omega (\mathbf{a}^\dagger\mathbf{a} + \mathbf{a}^\dagger\mathbf{a} + \mathbf{1})/2 \\ &= \hbar\omega \mathbf{a}^\dagger\mathbf{a} + \hbar\omega/2 \end{aligned} \quad (20.2.4)$$

(2) Eigenstate creationism (and destruction)

Let us define the *ground state* $|0\rangle$ as the eigenstate of $\mathbf{H}(\mathbf{x}, \mathbf{p})$ with the zero point eigenvalue E_0 .

$$\mathbf{H}(\mathbf{x}, \mathbf{p}) |0\rangle = \hbar\omega/2 |0\rangle \quad \langle 0| \mathbf{H}(\mathbf{x}, \mathbf{p}) = \hbar\omega/2 \langle 0| \quad (20.2.5a)$$

From (20.2.4) action by \mathbf{a} on the ground ket $|0\rangle$ (or \mathbf{a}^\dagger on ground bra $\langle 0|$) gives *nothing* (zero vectors).

$$\mathbf{a} |0\rangle = \mathbf{0} \quad \langle 0| \mathbf{a}^\dagger = \mathbf{0} \quad (20.2.5b)$$

However, \mathbf{a}^\dagger acting on the ground ket gives a non-zero vector whose eigenvalue is $\hbar\omega$ greater than E_0 .

$$\mathbf{H}(\mathbf{x}, \mathbf{p}) \mathbf{a}^\dagger |0\rangle = \hbar\omega \mathbf{a}^\dagger \mathbf{a} \mathbf{a}^\dagger |0\rangle + \hbar\omega/2 \mathbf{a}^\dagger |0\rangle$$

Commutation (20.2.3b) gives the following since $\mathbf{a} |0\rangle = \mathbf{0}$ by (20.2.5b).

$$\begin{aligned} \mathbf{H}(\mathbf{x}, \mathbf{p}) \mathbf{a}^\dagger |0\rangle &= \hbar\omega \mathbf{a}^\dagger (\mathbf{a}^\dagger \mathbf{a} + \mathbf{1}) |0\rangle + \hbar\omega/2 \mathbf{a}^\dagger |0\rangle \\ &= (\hbar\omega + \hbar\omega/2) \mathbf{a}^\dagger |0\rangle \end{aligned} \quad (20.2.5c)$$

This is the *one-quantum* or *first excited eigenket* $|1\rangle$ and *eigenbra* $\langle 1|$ defined as follows.

$$|1\rangle = \mathbf{a}^\dagger |0\rangle \quad \langle 0| \mathbf{a} = \langle 1| \quad (20.2.5d)$$

For kets, \mathbf{a}^\dagger is a creation operator since it creates higher level kets while \mathbf{a} does the reverse.

$$\mathbf{a} |1\rangle = \mathbf{a} \mathbf{a}^\dagger |0\rangle = (\mathbf{a}^\dagger \mathbf{a} + \mathbf{1}) |0\rangle = |0\rangle \quad (20.2.5d)$$

Perhaps, the \dagger that \mathbf{a}^\dagger carries shouldn't be thought of as a dagger but more like a magic wand. But, beware of its dark side. For bras, \mathbf{a}^\dagger is the destructor, and it is \mathbf{a} that does the creation in "bra-space."

A semi-infinite sequence $\{|0\rangle, |1\rangle, |2\rangle, |3\rangle, |4\rangle, \dots, |n\rangle, \dots\}$ of eigenkets with $n=0, 1, 2, 3, \dots$ quanta can be built this way using repeated applications of this magic creation operator \mathbf{a}^\dagger . Before we do this, we need to check that this more than just formalistic posturing. It remains to be shown whether the operator algebra can yield wavefunctions and solutions to the old-fashioned differential equations (20.1.10) of yore.

(3) *Wavefunction creationism*

The coordinate representation of the “nothing” equation (20.2.5b) is as follows.

$$\langle x | \mathbf{a} | 0 \rangle = 0 \quad (20.2.6)$$

Expanding the destruction operator using (20.2.1c) gives

$$\langle x | \mathbf{a} | 0 \rangle = \frac{1}{\sqrt{2\hbar}} \left(\sqrt{M\omega} \langle x | \mathbf{x} | 0 \rangle + i \langle x | \mathbf{p} | 0 \rangle / \sqrt{M\omega} \right) = 0 \quad (20.2.7a)$$

The operator coordinate representations turn this into a simple differential equation for ground state wavefunction $\psi_0(x) = \langle x | 0 \rangle$.

$$\sqrt{M\omega} x \psi_0(x) + i \frac{\hbar}{i} \frac{\partial \psi_0(x)}{\partial x} / \sqrt{M\omega} = 0 \quad (20.2.7b)$$

$$\psi_0'(x) = \frac{M\omega}{\hbar} x \psi_0(x) \quad (20.2.7c)$$

Integrating this gives the familiar Gaussian wave mentioned before (20.1.9) and (20.1.10).

$$\int \frac{d\psi}{\psi} = \int \frac{M\omega}{\hbar} x dx, \quad \ln \psi + \ln \text{const.} = \frac{-M\omega}{\hbar} \frac{x^2}{2}, \quad \psi = \frac{e^{-M\omega x^2/2\hbar}}{\text{const.}} \quad (20.2.7d)$$

The normalization *const.* is evaluated using a standard Gaussian integral $\int_{-\infty}^{\infty} dx e^{-\alpha x^2} = \sqrt{\frac{\pi}{\alpha}}$.

$$\langle \psi_0 | \psi_0 \rangle = 1 = \int_{-\infty}^{\infty} dx \frac{e^{-M\omega x^2/\hbar}}{\text{const.}^2} = \sqrt{\frac{\pi \hbar}{M\omega}} / \text{const.}^2 \Rightarrow \text{const.} = \left(\frac{\pi \hbar}{M\omega} \right)^{1/4} \quad (20.2.7e)$$

The first excited state wavefunction $\psi_1(x) = \langle x | 1 \rangle$ is derived using a representation of (20.2.5d).

$$\langle x | \mathbf{a}^\dagger | 0 \rangle = \langle x | 1 \rangle = \psi_1(x) \quad (20.2.8a)$$

Expanding the creation operator using (20.2.1d) gives

$$\langle x | \mathbf{a}^\dagger | 0 \rangle = \frac{1}{\sqrt{2\hbar}} \left(\sqrt{M\omega} \langle x | \mathbf{x} | 0 \rangle - i \langle x | \mathbf{p} | 0 \rangle / \sqrt{M\omega} \right) = \langle x | 1 \rangle = \psi_1(x). \quad (20.2.8b)$$

The operator coordinate representations generate the first excited state wavefunction.

$$\begin{aligned} \langle x | 1 \rangle = \psi_1(x) &= \frac{1}{\sqrt{2\hbar}} \left(\sqrt{M\omega} x \psi_0(x) - i \frac{\hbar}{i} \frac{\partial \psi_0(x)}{\partial x} / \sqrt{M\omega} \right) \\ &= \frac{1}{\sqrt{2\hbar}} \left(\sqrt{M\omega} x \frac{e^{-M\omega x^2/2\hbar}}{\text{const.}} - i \frac{\hbar}{i} \frac{\partial}{\partial x} \frac{e^{-M\omega x^2/2\hbar}}{\text{const.}} / \sqrt{M\omega} \right) \\ &= \frac{1}{\sqrt{2\hbar}} \frac{e^{-M\omega x^2/2\hbar}}{\text{const.}} \left(\sqrt{M\omega} x + i \frac{\hbar}{i} \frac{M\omega x}{\hbar} / \sqrt{M\omega} \right) \\ &= \frac{\sqrt{M\omega}}{\sqrt{2\hbar}} \frac{e^{-M\omega x^2/2\hbar}}{\text{const.}} (2x) = \left(\frac{M\omega}{\pi \hbar} \right)^{3/4} \sqrt{2\pi} \left(x e^{-M\omega x^2/2\hbar} \right) \end{aligned} \quad (20.2.8c)$$

Plots of wavefunctions (20.2.7d) and (20.2.8c) are shown in Fig. 20.2.1a and Fig. 20.2.1b, respectively. (These were constructed using an $N=1$ well of $P=24$ -pendulum model of Bloch waves as described in Sec. 3.8.) Note the even and odd symmetry, respectively, of the $\psi_0(x)$ and $\psi_1(x)$ waves.

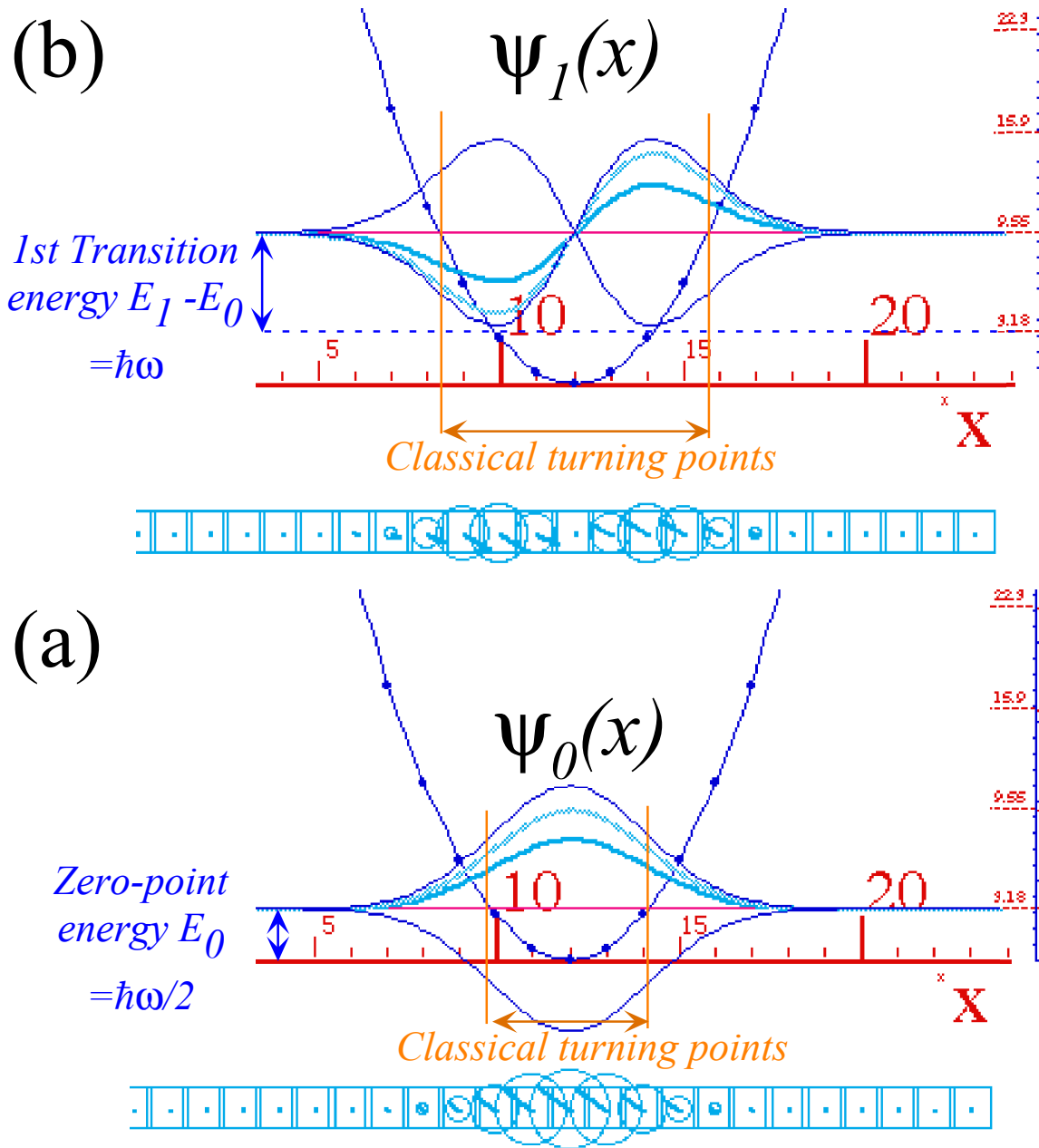


Fig. 20.2.1 Harmonic oscillator wavefunctions (a) Ground state, (a) First excited state.

Fig. 20.2.1 shows the points where the total energy equals the potential ($V=E$) and kinetic energy is zero. These are the *classical turning points* of an energy eigenstate. Beyond these points the wave becomes evanescent like a dying exponential. In this case it is a dying Gaussian $e^{-\alpha x^2}$ that dies even faster than $e^{-\alpha x}$. By Schrodinger's equation $\psi'' + \frac{2\hbar^2}{M} [E - V(x)]\psi = 0$, eigenfunction curvature ψ_n'' is zero at turning points where $E-V=0$. Turning points of square wells are *fixed* walls. Here our "walls" vary with E .

(b) Matrix and normalization calculations

The main advantage of the algebraic approach is that bra-ket calculations of matrix components like $\langle m|\mathbf{x}^k|n\rangle$ or $\langle m|\mathbf{a}^k|n\rangle$ generally do not have to involve coordinate (or momentum) integration. To facilitate the algebra of \mathbf{a} and \mathbf{a}^\dagger matrices it helps to reorder them using commutator identity $\mathbf{AB} = [\mathbf{A}, \mathbf{B}] + \mathbf{BA}$. In a matrix such as follows, it helps to move destructive \mathbf{a} operators to the right so they zero out.

$$\langle 0|f(\mathbf{a})g(\mathbf{a}^\dagger)|0\rangle = \langle 0|[f(\mathbf{a}), g(\mathbf{a}^\dagger)]|0\rangle + \langle 0|g(\mathbf{a}^\dagger)f(\mathbf{a})|0\rangle$$

Then only the commutator matrix $\langle 0|[f(\mathbf{a}), g(\mathbf{a}^\dagger)]|0\rangle$ needs to be evaluated.

For example, the following generalizations of the basic (20.3.3) relation $[\mathbf{a}, \mathbf{a}^\dagger] = \mathbf{1}$ are useful.

$$[\mathbf{a}, \mathbf{a}^{\dagger 2}] = 2\mathbf{a}^\dagger, \quad [\mathbf{a}, \mathbf{a}^{\dagger 3}] = 3\mathbf{a}^{2\dagger}, \dots, \quad [\mathbf{a}, \mathbf{a}^{\dagger n}] = n\mathbf{a}^{\dagger n-1} \tag{20.2.9a}$$

These are special cases of applying what might be called the *commutator derivative identity*.

$$\begin{aligned} [\mathbf{A}, \mathbf{BC}] &= \mathbf{ABC} - \mathbf{BCA} = [\mathbf{A}, \mathbf{B}]\mathbf{C} + \mathbf{BAC} - \mathbf{BCA} \\ &= [\mathbf{A}, \mathbf{B}]\mathbf{C} + \mathbf{B}[\mathbf{A}, \mathbf{C}] \end{aligned} \tag{20.2.9b}$$

The name recognizes the similarity between these relations and power-law derivatives. It goes either way.

$$\begin{aligned} [\mathbf{AB}, \mathbf{C}] &= -[\mathbf{C}, \mathbf{AB}] = -[\mathbf{C}, \mathbf{A}]\mathbf{B} - \mathbf{A}[\mathbf{C}, \mathbf{B}] \\ &= [\mathbf{A}, \mathbf{C}]\mathbf{B} + \mathbf{A}[\mathbf{B}, \mathbf{C}] \end{aligned} \tag{20.2.9c}$$

Using (20.2.9a) we can commute arbitrary powers to get something that resembles binomial expansions.

$$\begin{aligned} \mathbf{a}\mathbf{a}^{\dagger n} &= n\mathbf{a}^{\dagger n-1} + \mathbf{a}^{\dagger n}\mathbf{a} \\ \mathbf{a}^2\mathbf{a}^{\dagger n} &= n\mathbf{a}\mathbf{a}^{\dagger n-1} + \mathbf{a}\mathbf{a}^{\dagger n}\mathbf{a} \\ &= n(n-1)\mathbf{a}^{\dagger n-2} + n\mathbf{a}^{\dagger n-1}\mathbf{a} + n\mathbf{a}^{\dagger n-1}\mathbf{a} + \mathbf{a}^{\dagger n}\mathbf{a}^2 \\ &= n(n-1)\mathbf{a}^{\dagger n-2} + 2n\mathbf{a}^{\dagger n-1}\mathbf{a} + \mathbf{a}^{\dagger n}\mathbf{a}^2 \\ \mathbf{a}^3\mathbf{a}^{\dagger n} &= n(n-1)\mathbf{a}\mathbf{a}^{\dagger n-2} + 2n\mathbf{a}\mathbf{a}^{\dagger n-1}\mathbf{a} + \mathbf{a}\mathbf{a}^{\dagger n}\mathbf{a}^2 \\ &= n(n-1)(n-2)\mathbf{a}^{\dagger n-3} + n(n-1)\mathbf{a}^{\dagger n-2}\mathbf{a} + 2n(n-1)\mathbf{a}^{\dagger n-2}\mathbf{a} + 2n\mathbf{a}^{\dagger n-1}\mathbf{a}^2 + n\mathbf{a}^{\dagger n-1}\mathbf{a}^2 + \mathbf{a}^{\dagger n}\mathbf{a}^3 \\ &= n(n-1)(n-2)\mathbf{a}^{\dagger n-3} + 3n(n-1)\mathbf{a}^{\dagger n-2}\mathbf{a} + 3n\mathbf{a}^{\dagger n-1}\mathbf{a}^2 + \mathbf{a}^{\dagger n}\mathbf{a}^3 \end{aligned}$$

Using binomial coefficients $\binom{m}{r} = \frac{m!}{r!(m-r)!}$ this becomes a formula for any power $m=..3,4..$

$$\mathbf{a}^3\mathbf{a}^{\dagger n} = \binom{3}{0} \frac{n!}{(n-3)!} \mathbf{a}^{\dagger n-3} + \binom{3}{1} \frac{n!}{(n-2)!} \mathbf{a}^{\dagger n-2}\mathbf{a} + \binom{3}{2} \frac{n!}{(n-1)!} \mathbf{a}^{\dagger n-1}\mathbf{a}^2 + \binom{3}{3} \frac{n!}{(n-0)!} \mathbf{a}^{\dagger n}\mathbf{a}^3$$

The general $\mathbf{a}.. \mathbf{a}^\dagger$ to $\mathbf{a}^\dagger.. \mathbf{a}$ *power shuffle formula* is the result we want.

$$\mathbf{a}^m\mathbf{a}^{\dagger n} = \sum_{r=0}^m \binom{m}{r} \frac{n!}{(n-m+r)!} \mathbf{a}^{\dagger n-m+r} \mathbf{a}^r = \sum_{r=0}^m \frac{m!}{r!(m-r)!} \frac{n!}{(n-m+r)!} \mathbf{a}^{\dagger n-m+r} \mathbf{a}^r \tag{20.2.10a}$$

Normalization requires a special case of this formula with $m=n$.

$$\mathbf{a}^n\mathbf{a}^{\dagger n} = \sum_{r=0}^n \binom{n}{r} \frac{n!}{r!} \mathbf{a}^{\dagger r} \mathbf{a}^r = n! \left(\mathbf{1} + n\mathbf{a}^\dagger\mathbf{a} + \frac{n(n-1)}{2! \cdot 2!} \mathbf{a}^{\dagger 2}\mathbf{a}^2 + \frac{n(n-1)(n-3)}{3! \cdot 3!} \mathbf{a}^{\dagger 3}\mathbf{a}^3 + \dots \right) \tag{20.2.10b}$$

(1) Normalization and ladder operations

To create quantum states $|n\rangle$ with n greater than 0 or 1, it is necessary to derive the normalization constant as a function of n for a state obtained by applying the \mathbf{a}^\dagger operator n -times.

$$|n\rangle = \frac{\mathbf{a}^{\dagger n}|0\rangle}{const.}, \quad \text{where: } 1 = \langle n|n\rangle = \frac{\langle 0|\mathbf{a}^n\mathbf{a}^{\dagger n}|0\rangle}{(const.)^2} = n! \frac{\langle 0|\mathbf{1}+n\mathbf{a}^\dagger\mathbf{a}+\dots|0\rangle}{(const.)^2} = \frac{n!}{(const.)^2}.$$

The result is root-factorial normalization:
$$|n\rangle = \frac{\mathbf{a}^{\dagger n}|0\rangle}{\sqrt{n!}} \quad (20.2.11)$$

Note that for n equal to 0 or 1, the normalization is unity. (Yes, it is conventional to define $0! = 1 = 1!$) Clearly, we need to generalize the $n = 0$ or 1 creation and destruction formulas (20.2.5) to higher n -quanta.

Applying a creation operator \mathbf{a}^\dagger to an n -quantum state (20.10.11) gives the following.

$$\mathbf{a}^\dagger|n\rangle = \frac{\mathbf{a}^{\dagger n+1}|0\rangle}{\sqrt{n!}} = \sqrt{n+1} \frac{\mathbf{a}^{\dagger n+1}|0\rangle}{\sqrt{(n+1)!}} \quad (20.2.12a)$$

Applying a destruction operator \mathbf{a} to an n -quantum state using (20.2.10) gives the following.

$$\mathbf{a}|n\rangle = \frac{\mathbf{a}\mathbf{a}^{\dagger n}|0\rangle}{\sqrt{n!}} = \frac{(n\mathbf{a}^{\dagger n-1} + \mathbf{a}^{\dagger n}\mathbf{a})|0\rangle}{\sqrt{n!}} = \sqrt{n} \frac{\mathbf{a}^{\dagger n-1}|0\rangle}{\sqrt{(n-1)!}} \quad (20.2.12b)$$

These can be summarized by the following oscillator ladder relations.

$$\mathbf{a}^\dagger|n\rangle = \sqrt{n+1}|n+1\rangle \quad (20.10.13a) \quad \mathbf{a}|n\rangle = \sqrt{n}|n-1\rangle \quad (20.2.13b)$$

A mnemonic rule: Always put the larger of the two quanta under the radical factor for either case. The creation and destruction operators are represented in the $\{|0\rangle, |1\rangle, |2\rangle, \dots\}$ basis by semi-infinite matrices.

$$\langle \mathbf{a}^\dagger \rangle = \begin{pmatrix} \cdot & & & & & \\ 1 & \cdot & & & & \\ & \sqrt{2} & \cdot & & & \\ & & \sqrt{3} & \cdot & & \\ & & & \sqrt{4} & \cdot & \\ & & & & \ddots & \ddots \end{pmatrix} \quad (20.2.13c) \quad \langle \mathbf{a} \rangle = \begin{pmatrix} \cdot & 1 & & & & \\ & \cdot & \sqrt{2} & & & \\ & & \cdot & \sqrt{3} & & \\ & & & \cdot & \sqrt{4} & \\ & & & & \cdot & \ddots \\ & & & & & \ddots \end{pmatrix} \quad (20.2.13d)$$

(2) Number operator

The Hamiltonian (20.2.4) contains the operator $\hbar\omega \mathbf{a}^\dagger\mathbf{a}$ plus the zero-point energy $\frac{1}{2}\hbar\omega$. It is important to understand the operator $\mathbf{a}^\dagger\mathbf{a}$. Its effect on a quantum state follows using (20.2.10).

$$\mathbf{a}^\dagger\mathbf{a}|n\rangle = \frac{\mathbf{a}^\dagger\mathbf{a}\mathbf{a}^{\dagger n}|0\rangle}{\sqrt{n!}} = n \frac{\mathbf{a}^\dagger\mathbf{a}^{\dagger n-1}|0\rangle}{\sqrt{n!}} = n \frac{\mathbf{a}^{\dagger n}|0\rangle}{\sqrt{n!}} = n|n\rangle \quad (20.2.14)$$

It counts quanta and hence it is called the *number operator* $\mathbf{a}^\dagger\mathbf{a}$. This is proof that $|n\rangle$ are \mathbf{H} eigenstates.

$$\mathbf{H}|n\rangle = \hbar\omega \mathbf{a}^\dagger\mathbf{a}|n\rangle + \frac{\hbar\omega}{2}\mathbf{1}|n\rangle = (\hbar\omega n + \frac{\hbar\omega}{2})|n\rangle \quad (20.2.15a)$$

$$\langle \mathbf{H} \rangle = \hbar\omega \langle \mathbf{a}^\dagger\mathbf{a} \rangle + \frac{\hbar\omega}{2}\langle \mathbf{1} \rangle = \hbar\omega \begin{pmatrix} 0 & & & & \\ & 1 & & & \\ & & 2 & & \\ & & & 3 & \\ & & & & \ddots \end{pmatrix} + \hbar\omega \begin{pmatrix} 1/2 & & & & \\ & 1/2 & & & \\ & & 1/2 & & \\ & & & 1/2 & \\ & & & & \ddots \end{pmatrix} \quad (20.2.15b)$$

(3) *Expectation values and uncertainty*

The \mathbf{a} -algebra helps to find expectation values of operators besides the Hamiltonian \mathbf{H} . Consider position \mathbf{x} and momentum \mathbf{p} . Solving (20.2.1) gives \mathbf{x} and \mathbf{p} in terms of \mathbf{a} and \mathbf{a}^\dagger .

$$\sqrt{\frac{M\omega}{2\hbar}}\mathbf{x} = \frac{\mathbf{a} + \mathbf{a}^\dagger}{2}, \quad \sqrt{\frac{1}{2\hbar M\omega}}\mathbf{p} = \frac{\mathbf{a} - \mathbf{a}^\dagger}{2i} \quad (20.2.16)$$

The eigenstates expectation values of \mathbf{x} and \mathbf{p} for are zero because $\langle n|\mathbf{a}|n\rangle = 0 = \langle n|\mathbf{a}^\dagger|n\rangle$.

$$\bar{\mathbf{x}}|_n = \langle n|\mathbf{x}|n\rangle = \sqrt{\frac{\hbar}{2M\omega}} \langle n|(\mathbf{a} + \mathbf{a}^\dagger)|n\rangle = 0 \quad (20.2.17a)$$

$$\bar{\mathbf{p}}|_n = \langle n|\mathbf{p}|n\rangle = i\sqrt{\frac{\hbar M\omega}{2}} \langle n|(\mathbf{a}^\dagger - \mathbf{a})|n\rangle = 0 \quad (20.2.17b)$$

The zeros can also be seen to be a result of the symmetry of the potential and its eigenfunctions such as were shown in Fig. 20.2.1. However, the mean squares or \mathbf{x}^2 and \mathbf{p}^2 expectations are non-zero.

$$\overline{\mathbf{x}^2}|_n = \langle n|\mathbf{x}^2|n\rangle = \frac{\hbar}{2M\omega} \langle n|(\mathbf{a} + \mathbf{a}^\dagger)^2|n\rangle \quad (20.2.18a)$$

$$\overline{\mathbf{p}^2}|_n = \langle n|\mathbf{p}^2|n\rangle = i^2 \frac{\hbar M\omega}{2} \langle n|(\mathbf{a}^\dagger - \mathbf{a})^2|n\rangle \quad (20.2.18b)$$

$$= \frac{\hbar}{2M\omega} \langle n|(\mathbf{a}^2 + \mathbf{a}^\dagger\mathbf{a} + \mathbf{a}\mathbf{a}^\dagger + \mathbf{a}^{\dagger 2})|n\rangle \quad (20.2.18a)$$

$$= -\frac{\hbar M\omega}{2} \langle n|(\mathbf{a}^{\dagger 2} - \mathbf{a}^\dagger\mathbf{a} - \mathbf{a}\mathbf{a}^\dagger + \mathbf{a}^2)|n\rangle \quad (20.2.18b)$$

$$= \frac{\hbar}{2M\omega} (2n+1) \quad (20.2.18a)$$

$$= \frac{\hbar M\omega}{2} (2n+1) \quad (20.2.18b)$$

The basic commutation $\mathbf{a}\mathbf{a}^\dagger = \mathbf{a}^\dagger\mathbf{a} + \mathbf{1}$ (20.2.3) and number value (20.2.14) was used. This lets us estimate the mean or expected kinetic and potential energies.

$$\overline{PE}|_n = \frac{1}{2}M\omega^2 \overline{\mathbf{x}^2}|_n = \frac{1}{2}M\omega^2 \frac{\hbar(2n+1)}{2M\omega} \quad (20.2.19a)$$

$$\overline{KE}|_n = \frac{1}{2M} \overline{\mathbf{p}^2}|_n = \frac{1}{2M} \frac{\hbar M\omega}{2} (2n+1) \quad (20.2.19b)$$

$$= \frac{1}{2}\hbar\omega \left(n + \frac{1}{2}\right) \quad (20.2.19a)$$

$$= \frac{1}{2}\hbar\omega \left(n + \frac{1}{2}\right) \quad (20.2.19b)$$

The fact that they are equal is peculiar to the harmonic oscillator's phase space or $X \leftrightarrow P$ symmetry.

Uncertainty or *standard deviation* Δq of a statistical quantity q is its root mean-square difference.

$$(\Delta q)^2 = \overline{(q - \bar{q})^2} \quad \text{or: } \Delta q = \sqrt{\overline{(q - \bar{q})^2}} \quad (20.2.20a)$$

Harmonic oscillator coordinate and momentum uncertainty follow from (20.2.17) and (20.2.18).

$$\Delta x = \sqrt{\overline{\mathbf{x}^2}} = \sqrt{\frac{\hbar(2n+1)}{2M\omega}} \quad (20.2.20b)$$

$$\Delta p = \sqrt{\overline{\mathbf{p}^2}} = \sqrt{\frac{\hbar M\omega(2n+1)}{2}} \quad (20.2.20c)$$

The *Heisenberg uncertainty product* for the n -quantum eigenstate is

$$\Delta x \cdot \Delta p|_n = \sqrt{\overline{\mathbf{x}^2}} \sqrt{\overline{\mathbf{p}^2}}|_n = \sqrt{\frac{\hbar(2n+1)}{2M\omega}} \sqrt{\frac{\hbar M\omega(2n+1)}{2}} = \hbar \left(n + \frac{1}{2}\right) \quad (20.2.20d)$$

The *Heisenberg minimum uncertainty product* occurs for the 0-quantum (ground) eigenstate.

$$\Delta x \cdot \Delta p|_0 = \frac{\hbar}{2} \quad (20.2.20e)$$

(4) Uncertainty approximation for anharmonic spectra

The preceding harmonic oscillator uncertainty relations are the simplest ones we've seen so far. They are a great deal simpler than the Δp or Δx functions for most anharmonic oscillator power-law potentials $V(x) = Ax^P$ with powers other than $P=2$.

While relation (20.2.20d) is only exact for $P=2$ potentials, it may be used to approximate the spectra of other potentials, too. The idea that an n -quantum state occupies $n\hbar$ units of phase space is related to the classical Liouville phase-space-incompressibility theorem and applies to any potential.

The trick is to set *root-mean-square (rms)* values $x = \Delta x$ and $p = \Delta p$ in the Hamiltonian H and minimize $H=E$ with respect to Δx subject to the constraint (20.2.20d) of phase-space-incompressibility.

$$E_v = \text{MIN} \left(\frac{p^2}{2M} + Ax^P = \frac{(\Delta p)^2}{2M} + A(\Delta x)^P \right) \text{ subject to: } \Delta x \cdot \Delta p = x \cdot p = v = (n + \frac{1}{2})\hbar \quad (20.2.21a)$$

By putting $p = \Delta p = v/\Delta x = v/x$ into an energy function and zeroing the x -derivative we find $\Delta x = x_{\min}$.

$$\begin{aligned} \frac{d}{dx} \left(\frac{p^2}{2M} + Ax^P \right) &= \frac{d}{dx} \left(\frac{v^2}{2Mx^2} + Ax^P \right) = \frac{-2v^2}{2Mx^3} + APx^{P-1} = 0 = \frac{-v^2}{M} + APx^{P+2} \\ \Delta x = x_{\min} &= \left(\frac{v^2}{MAP} \right)^{\frac{1}{P+2}}, \quad \Delta p = p_{\min} = \frac{v}{x_{\min}} = v \left(\frac{v^2}{MAP} \right)^{\frac{-1}{P+2}} \end{aligned} \quad (20.2.21b)$$

For the harmonic oscillator PE power $P=2$ and spring constant $A=k/2=1/2M\omega^2$, the values (20.2.21) equal the exact results (20.2.20) and minimum energy subject to constant $\Delta x \Delta p$.

Quantum v -number dependence factors out of the resulting general minimum energy.

$$E_v = \frac{v^2}{2M} \left(\frac{v^2}{MAP} \right)^{\frac{-2}{P+2}} + A \left(\frac{v^2}{MAP} \right)^{\frac{P}{P+2}} = v^{\frac{2P}{P+2}} \left(\frac{1}{2M^{\frac{P}{P+2}} A^{\frac{-2}{P+2}} P^{\frac{-2}{P+2}}} + \frac{1}{M^{\frac{P}{P+2}} A^{\frac{-2}{P+2}} P^{\frac{P}{P+2}}} \right) \quad (20.2.22a)$$

Then the kinetic ($KE = p^2 / 2M$) and the potential ($PE = Ax^P$) parts simplify, too.

$$E_v = v^{\frac{2P}{P+2}} \frac{A^{\frac{2}{P+2}}}{M^{\frac{P}{P+2}}} \left[\frac{1}{2P^{\frac{-2}{P+2}}} + \frac{1}{P^{\frac{P}{P+2}}} \right] = v^{\frac{2P}{P+2}} \frac{A^{\frac{2}{P+2}}}{(MP)^{\frac{P}{P+2}}} \left[\frac{P+2}{2} \right] \quad (20.2.22b)$$

Again, the oscillator parameters $P=2$ and $A=k/2=1/2M\omega^2$ reduce this to the exact energy $E_v = v\omega = \hbar\omega(n+1/2)$.

However, this approximation works pretty well for other power-laws. First, it gives the *Virial ratio* $P:2$ between KE and PE that was derived in (18.3.10). Then a uniform force field (like terrestrial gravity) with $P=1$ has a spectrum shown in Fig. 20.4.2 that goes as $v^{2/3}$. A square-well corresponds to a large power $P \rightarrow \infty$. Then, (20.2.22b) correctly predicts the quantum dependence $v^{2P/P+2}$ approaches v^2 . At the opposite extreme, a Coulomb potential k/r has $P=-1$. According to (20.2.22b), it has an inverse power - v^{-2} -spectrum. As we will see in Chapter 26, this result is exactly true. (Note that (20.2.21) gives the Bohr radius discussed back in (5.4.3a) and the momentum (20.2.21b) agrees with (5.4.3b).)

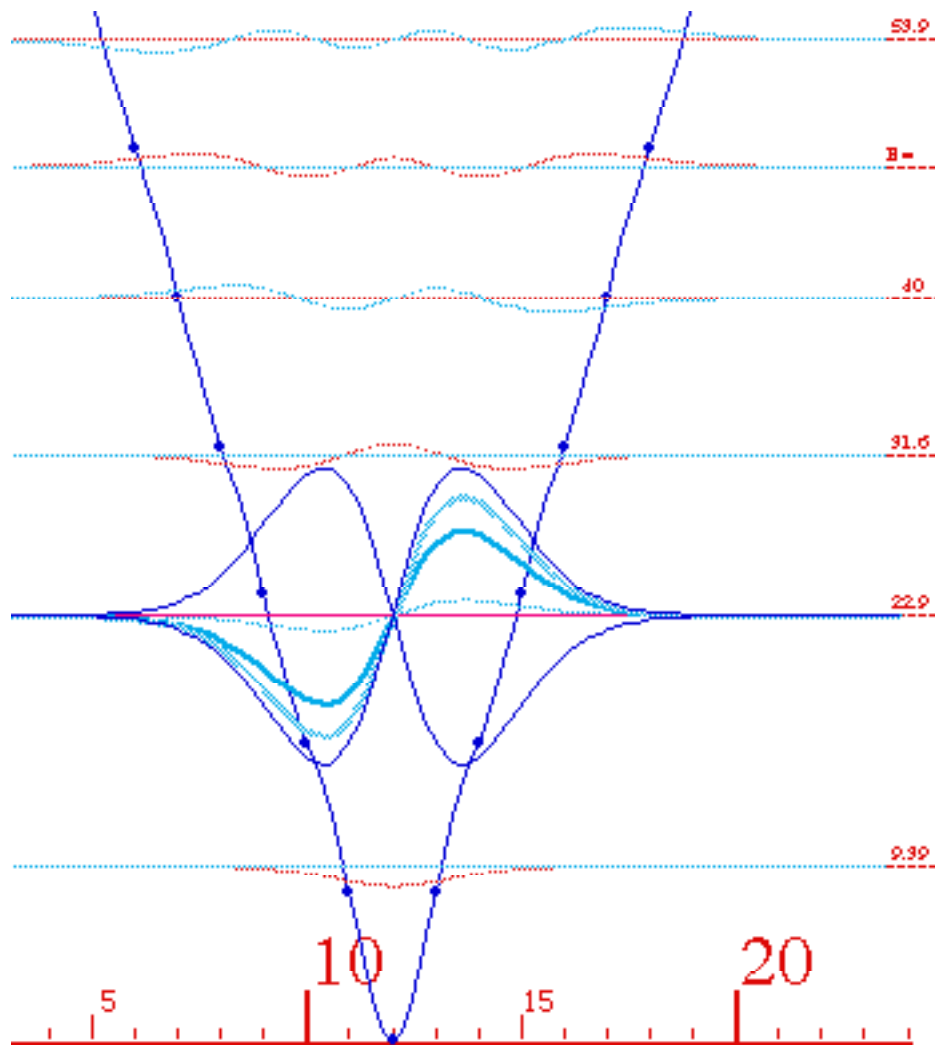


Fig. 20.2.2 First excited state wavefunction of linear potential $V(y)=mg|y|$. ($V=98$ Bu for $N=24$)

A 24-pendulum model in Fig. 20.2.2 provides a wavefunction and energy spectrum for a linear potential $V(x)=V|x|$ and clearly shows the decreasing energy level spacing as energy increases. The linear potential wavefunctions $\psi_{\mu}(x)$ have a superficial resemblance to the corresponding Hermite oscillator wavefunctions shown in Fig. 20.2.1. However, their algebraic properties are quite different. First of all, the zero-point energy is a larger fraction 0.69 of the first transition energy than the 0.5 obtained for the harmonic oscillator. The fraction μ_0 in quantum phase space area $\hbar\omega(n + \mu_0)$ is called *Maslov's index*.

The linear potential wavefunctions are called *Airy functions*. If you keep only odd- n anti-symmetric Airy wavefunctions such as the $\psi_1(x)$ shown and $\psi_3(x), \psi_5(x), \psi_7(x), \dots$ and discard the even- n $\psi_0(x), \psi_2(x), \psi_4(x), \dots$ waves, then you will have a complete set of *bouncing-ball eigensolutions* due to an infinite potential wall at the origin (and symmetry axis) of Fig. 20.2.2. These are discussed in an article by Julio Geo-Benacloche. (AJP September 1999)

(c) High quantum oscillator states

The repeated application of the creation operator to the ground state yields higher and higher quantum numbers and eigenstates and more and more complicated wavefunctions. An example with $n=20$ is shown in Fig. 20.2.3.

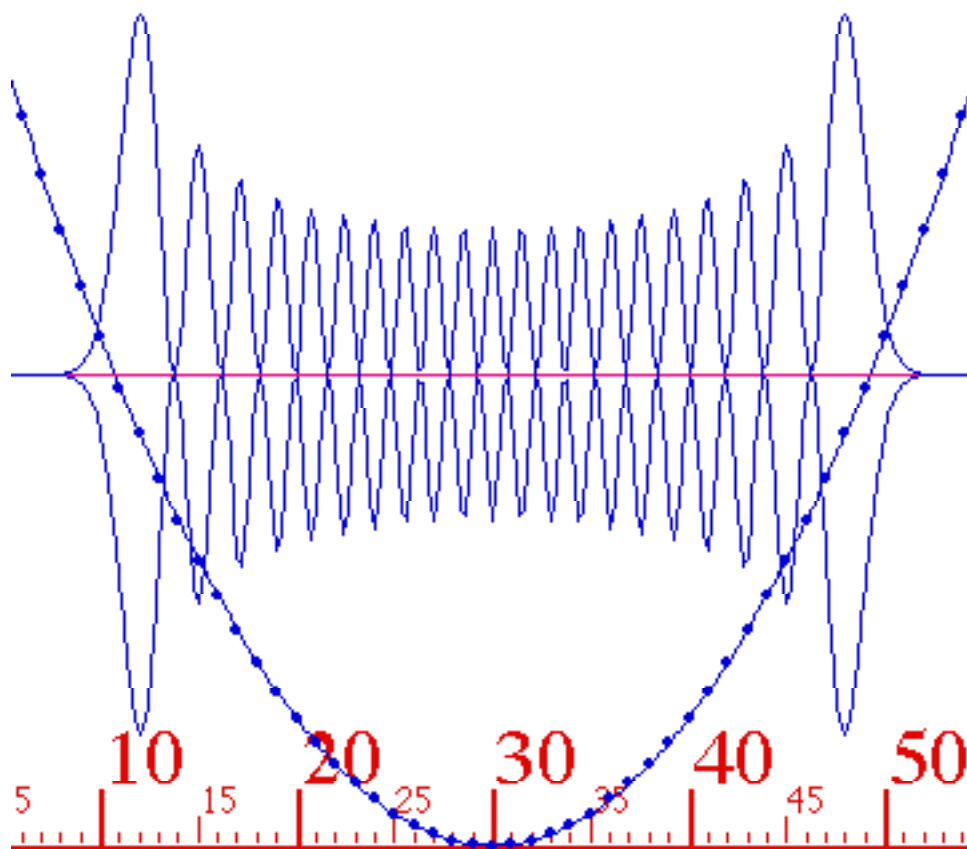


Fig. 20.2.3 $n=20$ probability for harmonic oscillator potential $V(x)=Vx^2$. ($V=100$ Bu for $P=60$)

This is still a long way from a classical energy value of 1 Joule; for a 1 Hz oscillator that would take a quantum number of roughly $n=100,000,000,000,000,000,000,000,000,000=10^{35}$ which is to say the least, beyond the capability of current computers to simulate. (How big would the number P of pendulums be?)

However, even this relatively low quantum excitation is showing some visible classical properties. The envelope of the probability distribution is beginning to look like an inverse cosine function which is the classical probability distribution of a sinusoidally oscillating particle.

20.3 Harmonic Oscillator Dynamics and Coherent States

(a) Oscillator quantum beats

So far, our study of oscillator eigenstates has been lifeless; eigenstates, by themselves, appear to be dead since the absolute square kills Planck phase oscillation ($\Psi_\mu(x,t) = e^{-i\omega_\mu t} \psi_\mu(x)$) of each eigenstate.

$$|\Psi_0(x,t)|^2 = |e^{-i\omega_0 t} \langle x|0\rangle|^2 = |\psi_0(x)|^2, \quad |\Psi_1(x,t)|^2 = |e^{-i\omega_1 t} \langle x|1\rangle|^2 = |\psi_1(x)|^2, \dots \quad (20.3.1)$$

Planck's oscillation of a quantum phasor is observable only relative to another phasor which has a different frequency and when the two phasors can interfere with each other. Then their combined probability distribution wobbles or "beats" at a frequency that is the difference between their Planck rates.

This is how a quantum harmonic oscillator can actually oscillate like a classical pendulum. The simplest example of this is had by mixing the first two eigenstates, the ground and excited states $|0\rangle$ and $|1\rangle$ with wave functions $\psi_0(x) = \langle x|0\rangle$ and $\psi_1(x) = \langle x|1\rangle$ shown in Fig. 20.2.1, gives the following state .

$$|\Psi\rangle = |0\rangle\langle 0|\Psi\rangle + |1\rangle\langle 1|\Psi\rangle = |0\rangle\Psi_0 + |1\rangle\Psi_1 \quad (20.3.2a)$$

Eigenfunctions $\psi_0(x) = \langle x|0\rangle$ and $\psi_1(x) = \langle x|1\rangle$ (shown in Fig. 20.2.1) are mixed to give

$$\Psi(x) = \langle x|\Psi\rangle = \langle x|0\rangle\langle 0|\Psi\rangle + \langle x|1\rangle\langle 1|\Psi\rangle = \psi_0(x)\Psi_0 + \psi_1(x)\Psi_1 \quad (20.3.2b)$$

The greatest oscillation occurs with 50-50 mixing coefficients

$$\Psi_0 = \langle 0|\Psi\rangle = 1/\sqrt{2}, \quad \Psi_1 = \langle 1|\Psi\rangle = 1/\sqrt{2} \quad (20.3.3)$$

The time dependence $\Psi(x,t)$ of the mixed wave is then

$$\Psi(x,t) = \psi_0(x) e^{-i\omega_0 t} \Psi_0 + \psi_1(x) e^{-i\omega_1 t} \Psi_1 = (\psi_0(x) e^{-i\omega_0 t} + \psi_1(x) e^{-i\omega_1 t})/\sqrt{2} \quad (20.3.4)$$

and probability amplitude $|\Psi(x,t)|$ envelope beats back and forth according to

$$\begin{aligned} |\Psi(x,t)| &= \sqrt{\Psi^* \Psi} = \sqrt{\left(e^{-i\omega_0 t} \psi_0(x) + e^{-i\omega_1 t} \psi_1(x) \right)^* \left(e^{-i\omega_0 t} \psi_0(x) + e^{-i\omega_1 t} \psi_1(x) \right) / 2} \\ &= \sqrt{\left(|\psi_0(x)|^2 + |\psi_1(x)|^2 + \psi_0(x)\psi_1(x) \left(e^{i(\omega_1 - \omega_0)t} + e^{-i(\omega_1 - \omega_0)t} \right) \right) / 2} \quad (20.3.5a) \\ &= \sqrt{\left(|\psi_0(x)|^2 + |\psi_1(x)|^2 + 2\psi_0(x)\psi_1(x) \cos(\omega_1 - \omega_0)t \right) / 2} \end{aligned}$$

This oscillation of $\Psi(x,t)$ and $|\Psi(x,t)|$ is shown in Fig. 20.3.1 for a single beat period τ_{beat} . It is strong wherever *wave overlap* $\psi_0(x)\psi_1(x)$ is large and occurs at the angular beat frequency $\omega_1 - \omega_0 = 2\pi/\tau_{beat}$.

The general 2-state quantum probability beat wavefunction is

$$\Psi(x,t)^* \Psi(x,t) = |A_0(x)|^2 + |A_1(x)|^2 + 2|A_0(x)A_1(x)| \cos(\theta_{01}(x) + (\omega_1 - \omega_0)t), \quad (20.3.5b)$$

Here individual mixed-wave amplitudes are $A_0(x) = \psi_0(x)\Psi_0$ and $A_1(x) = \psi_1(x)\Psi_1$ and wave overlap

$$A_0(x)A_1(x) = |A_0(x)A_1(x)| e^{i\theta_{01}(x)} \quad (20.3.5c)$$

may be complex with a phase θ_{01} that varies with x . In (20.3.4) both $A_0(x)$ and $A_1(x)$ are real and $\theta_{01} = 0$.

The beat frequency is the eigenfrequency difference

$$\omega_{beat} = \omega_1 - \omega_0 = \omega, \quad (20.3.5d)$$

which also happens to be the classical oscillator's natural frequency ω . So, this is the first example of a quantum oscillator behaving like a classical oscillator or pendulum.

Frequency ω_{beat} is called a *transition frequency* since it is $(1/\hbar)$ times a *transition energy*

$$\Delta E = E_{1 \leftarrow 0 \text{ transition}} = E_1 - E_0 = \hbar\omega \tag{20.3.6}$$

Here ΔE is the energy difference between the first excited level $E_1 = \hbar\omega_1$ and ground level $E_0 = \hbar\omega_0$. However, for a harmonic oscillator all neighboring pairs of levels have the same transition frequency ω . Furthermore, all pairs of levels will beat at a frequency that is an integral harmonic of ω .

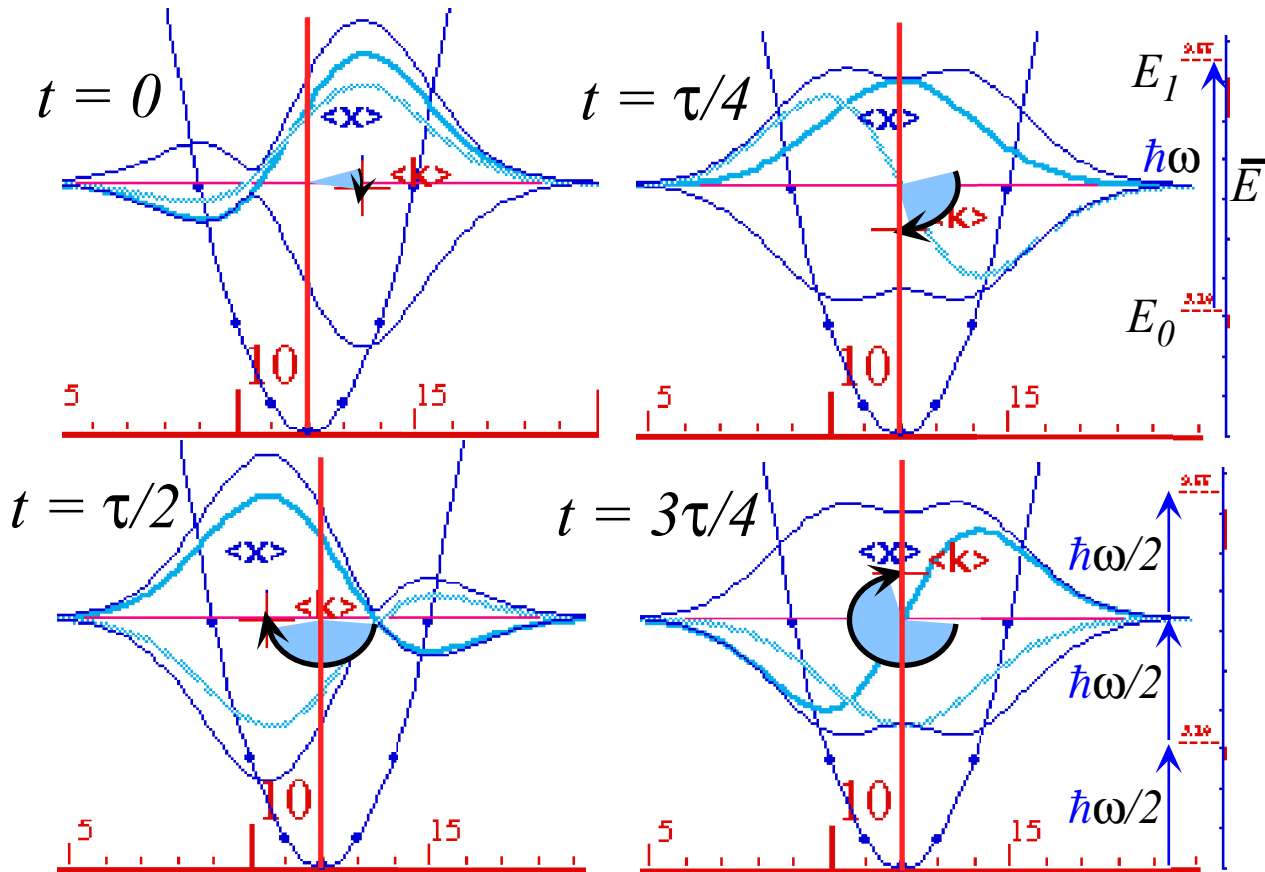


Fig. 20.3.1 Beat oscillation for mixed 01-state of harmonic oscillator showing x and k expectation.

(1) Energy expectation value

The energy expectation value or mean energy was given in Sec. 12.1(c) as the matrix sum (12.1.8) over energy eigenvalues E_n times the probability $|\Psi_n|^2$ for each of the eigenstates.

$$\begin{aligned} \bar{E} &= \langle \Psi | \mathbf{H} | \Psi \rangle = \langle 0 | \mathbf{H} | 0 \rangle \langle 0 | \Psi \rangle^2 + \langle 1 | \mathbf{H} | 1 \rangle \langle 1 | \Psi \rangle^2 + \dots \\ &= E_0 |\Psi_0|^2 + E_1 |\Psi_1|^2 + \dots \end{aligned} \tag{20.3.7a}$$

For a 50-50 combination example (20.4.3) pictured in Fig. 20.3.1 the expected or mean energy is $\hbar\omega$, too.

$$\bar{E} = E_0 \cdot 1/2 + E_1 \cdot 1/2 = (\hbar\omega/2) \cdot 1/2 + (3\hbar\omega/2) \cdot 1/2 = \hbar\omega \tag{20.3.7b}$$

(Mean $(E_0+E_1)/2$ of oscillator E -values E_0 and E_1 just happens to equal their transition energy E_0-E_1 .)

(2) Position expectation values

The position expectation involves a double matrix sum over eigenstates since the \mathbf{x} -operator is not diagonal in the energy basis. The Ch. 12 equation (12.1.11) treats the general case.

$$\bar{x} |\Psi\rangle = \langle \Psi | \mathbf{x} | \Psi \rangle = \sum_{m=1}^{\infty} \sum_{n=1}^{\infty} \langle \Psi | m \rangle \langle m | \mathbf{x} | n \rangle \langle n | \Psi \rangle \quad (20.3.8a)$$

Here the *dipole matrix elements* $\langle m | \mathbf{x} | n \rangle$ are easily derived using **a**-algebra. Generalizing (20.2.17a) gives

$$\begin{aligned} \langle m | \mathbf{x} | n \rangle &= \sqrt{\frac{\hbar}{2M\omega}} \langle m | (\mathbf{a} + \mathbf{a}^\dagger) | n \rangle = \sqrt{\frac{\hbar}{2M\omega}} \left(\sqrt{n} \langle m | n-1 \rangle + \sqrt{n+1} \langle m | n+1 \rangle \right) \\ &= \left(x_0 / \sqrt{2} \right) \left(\sqrt{n} \delta_{m,n-1} + \sqrt{n+1} \delta_{m,n+1} \right) \end{aligned} \quad (20.3.8b)$$

where x_0 is the *zero-point classical turning point* x_0 is where $E_0 = 1/2 M \omega^2 x_0^2 = \hbar \omega / 2$.

$$x_0 = [\hbar / M \omega]^{1/2} \quad (20.3.8c)$$

The off-diagonal **x**-matrix means the **x**-expectation value is not constant for a general state.

$$|\Psi(t)\rangle = |0\rangle e^{-i\omega_0 t} \Psi_0 + |1\rangle e^{-i\omega_1 t} \Psi_1 + \dots \quad (20.3.9)$$

The matrix form of (20.3.8) is, perhaps, easier to compute and more revealing.

$$\begin{aligned} \langle \mathbf{x} \rangle &= \bar{x} |\Psi(t)\rangle = \langle \Psi(t) | \mathbf{x} | \Psi(t) \rangle \\ &= \sqrt{\frac{\hbar}{2M\omega}} \begin{pmatrix} \Psi_0^*(t) & \Psi_1^*(t) & \Psi_2^*(t) & \dots \end{pmatrix} \begin{pmatrix} \cdot & \sqrt{1} & \cdot & \dots \\ \sqrt{1} & \cdot & \sqrt{2} & \dots \\ \cdot & \sqrt{2} & \cdot & \sqrt{3} \\ \vdots & \vdots & \sqrt{3} & \ddots \end{pmatrix} \begin{pmatrix} \Psi_0(t) \\ \Psi_1(t) \\ \Psi_2(t) \\ \vdots \end{pmatrix} \\ &= \left(x_0 / \sqrt{2} \right) \begin{pmatrix} \Psi_0^* e^{i\omega_0 t} & \Psi_1^* e^{i\omega_1 t} & \Psi_2^* e^{i\omega_2 t} & \dots \end{pmatrix} \begin{pmatrix} \cdot & \sqrt{1} & \cdot & \dots \\ \sqrt{1} & \cdot & \sqrt{2} & \dots \\ \cdot & \sqrt{2} & \cdot & \sqrt{3} \\ \vdots & \vdots & \sqrt{3} & \ddots \end{pmatrix} \begin{pmatrix} \Psi_0 e^{-i\omega_0 t} \\ \Psi_1 e^{-i\omega_1 t} \\ \Psi_2 e^{-i\omega_2 t} \\ \vdots \end{pmatrix} \\ &= \left(x_0 / \sqrt{2} \right) \begin{pmatrix} \Psi_0^* e^{i\omega_0 t} & \Psi_1^* e^{i\omega_1 t} & \Psi_2^* e^{i\omega_2 t} & \dots \end{pmatrix} \begin{pmatrix} \sqrt{1} \Psi_1 e^{-i\omega_1 t} \\ \sqrt{1} \Psi_0 e^{-i\omega_0 t} + \sqrt{2} \Psi_2 e^{-i\omega_2 t} \\ \sqrt{2} \Psi_1 e^{-i\omega_1 t} + \sqrt{3} \Psi_3 e^{-i\omega_3 t} \\ \vdots \end{pmatrix} \end{aligned} \quad (20.3.10a)$$

If only the first two levels have non-zero amplitude then $\langle x \rangle$ beats at frequency $\omega_{10} = \omega_1 - \omega_0$.

$$\begin{aligned} \langle \mathbf{x} \rangle &= \bar{x} |\Psi(t)\rangle = \left(x_0 / \sqrt{2} \right) \left(\Psi_0^* e^{i\omega_0 t} \sqrt{1} \Psi_1 e^{-i\omega_1 t} + \Psi_1^* e^{i\omega_1 t} \sqrt{1} \Psi_0 e^{-i\omega_0 t} \right) \\ &= \left(x_0 / \sqrt{2} \right) |\Psi_1^* \Psi_0| \left(e^{i(\omega_{10} t + \theta_{10})} + e^{-i(\omega_{10} t + \theta_{10})} \right) \text{ where } : \omega_{10} = \omega_1 - \omega_0 \end{aligned} \quad (20.3.10b)$$

The *amplitude overlap product* is $\Psi_1^* \Psi_0 = |\Psi_1^* \Psi_0| e^{i\theta_{10}}$ (20.3.10c)

This product is $(1/\sqrt{2})(1/\sqrt{2}) = 1/2$ for a 50-50 combination state (20.3.3) giving the following x -oscillation.

$$\langle \mathbf{x}(t) \rangle = \bar{x} |\Psi(t)\rangle = \left(x_0 / \sqrt{2} \right) \cos(\omega_1 - \omega_0)t = \left(x_{0I} / 2 \right) \cos \omega t \quad (20.3.10d)$$

Oscillation amplitude $\langle x \rangle$ is $\sqrt{I/2}$ of x_0 or $1/2$ of the classical turning point x_{0I} at mean energy $\bar{E} = \hbar \omega$ of a 50-50 combination of E_0 and E_1 states given by (20.3.7b). x_{0I} is also the dipole matrix element $\langle 0 | \mathbf{x} | 1 \rangle$.

The range of expectation $\langle x \rangle$ is plotted numerically with the expectation $\langle k \rangle$ of momentum in Fig. 20.3.1. It is larger than the 18% achieved by poor prisoner M in the square well $\langle x \rangle$ of (12.1.15). This is because the harmonic oscillator is a "softer" prison than an infinite square well, and it allows a significant fraction of the low- n waves to evanesce into walls. The widening potential at higher E increases their uncertainty range Δx , but high- n waves meet steeper walls with more momentum. So, the fraction of evanescent wave goes down as n goes up as seen in the $n=20$ example of Fig. 20.2.3.

(3) Momentum expectation values

For a 50-50 combination state (20.3.3) the mean or expected momentum is

$$\langle p(t) \rangle = \bar{p} |\Psi(t)\rangle = -\left(M\omega x_0 / \sqrt{2} \right) \sin(\omega_1 - \omega_0)t = (p_{0I} / 2) \sin \omega t \quad (20.3.11)$$

(The derivation is left as an exercise.) The expected momentum $\langle p \rangle$ or Fourier transform wavevector component $\langle k \rangle$ is plotted vertically versus $\langle x \rangle$ for four $1/4$ -periods of the oscillator in Fig. 20.3.1. The resulting path resembles a classical phase space ellipse, or if $\langle p \rangle$ is rescaled by $M\omega$, a phasor circle.

This shows some essential classical dynamics of the oscillator being reproduced by a 50-50 mixing of the lowest two quantum states, $|0\rangle$ and $|1\rangle$, of the quantum oscillator. Uneven mixtures 40-60, 30-70, and so forth, will oscillate on similar phase paths but with reduced amplitude according to the value of the overlap product (20.3.10c). However, even the maximum amplitude achieved with a 50-50 mixture is still only a fraction of the corresponding classical oscillation of the same energy. This fraction gradually increases for mixtures of quantum states $|n\rangle$ and $|n+1\rangle$ for larger and larger n . Again, this is related to the decreasing fraction of the evanescent parts of higher quantum states. Now we see ways to involve many eigenstates in making more effective or "coherent" wave packet dynamics.

(b) Oscillator coherent states ("Shoved" and "kicked" states)

Most who study quantum mechanics have a desire to see classical manifestations of classical dynamics in quantum systems. The harmonic oscillator is one of few systems that can indulge our desire for a return to our classical birthplace. The oscillator has a nearly perfect classical-imitation-state having an almost child-like simplicity. This state is called a harmonic oscillator *coherent state*.

There is hardly a child (or healthy adult) alive who, when seeing a pendulum, spring and mass, or other oscillator, can resist the urge to swing it or ring it. The more gentle of us might just pull it off center and release it, while a more impatient provocateur might just kick it. A true physicist will only be satisfied after repeatedly dealing the poor oscillator both kinds of punishment. Here we consider quantum operators that perform these child-like acts on wave functions and quantum states in general, and we will see how such actions affect oscillators in particular.

The usual coherent state is the result of applying such operations to an oscillator ground state $|0\rangle$, but more general sorts of states are possible as we will see. Quantum states have infinitely more freedom and variety than classical states, but now we just want it to reproduce a tiny piece of a classical world.

Coherent states are made by translation and boost (shove and kick) operators just like the ones discussed in Chapter 17.1(d). The Geoppert-Mayer-Snyder-Richards gauge transformation (17.1.16b) is the boost or "kick" operator derived in (20.3.20) below. But, first we derive the "shove" operator.

(1) Translation operators and generators: (A "shove")

Suppose there exists an operator $\mathbf{T}(a)$ which does nothing more than translate x -wavefunctions.

$$\mathbf{T}(a) \cdot \psi(x) = \psi(x-a) = \langle x | \mathbf{T}(a) | \psi \rangle = \langle x-a | \psi \rangle \quad (20.3.12a)$$

Such an operator is called a *translation operator* $\mathbf{T}(a)$ (Good name, don't you think?) Its effect is to move the function a units to the right (positively). (Or, its dual moves the x -space a units negatively to the left.)

$$\langle x | \mathbf{T}(a) = \langle x-a |, \text{ or: } \mathbf{T}^\dagger(a) | x \rangle = | x-a \rangle, \text{ or since } \mathbf{T}^\dagger(a) = \mathbf{T}(-a): \mathbf{T}(a) | x \rangle = | x+a \rangle. \quad (20.3.12b)$$

For very small translations $a \rightarrow da$ such an operation becomes nearly the identity operation $\mathbf{1}$ with a small add-on operator $\mathbf{G}da$ which is linear in, or proportional to, the tiny (infinitesimal) translation δa .

$$\mathbf{T}(\delta a) = \mathbf{1} + \mathbf{G}\delta a \quad (20.3.13a)$$

The tiny-translation operator is called an *infinitesimal translation operator* $\mathbf{T}(da)$ and the add-on operator is called a *generator* \mathbf{G} of translations. If $\mathbf{T}(a)$ is a continuous function of a then the generator is the first-derivative part of a Taylor series.

$$\mathbf{G} = \left. \frac{\partial \mathbf{T}}{\partial a} \right|_{a=0} \quad (20.3.13b)$$

Tiny translations on an arbitrary continuous function $\psi(x)$ gives a single-term Taylor series, too.

$$\mathbf{T}(da) \cdot \psi(x) = \psi(x - da) = \psi(x) - \frac{\partial}{\partial x} \psi(x) da \quad (20.3.14a)$$

Comparing this to the effect of (20.3.13) gives

$$\mathbf{T}(da) \cdot \psi(x) = (\mathbf{1} + \mathbf{G}da) \cdot \psi(x) = \psi(x) + \mathbf{G} \cdot \psi(x) da \quad (20.3.14b)$$

Solving (20.3.13b) and (20.3.14) yields an abstract operator exponential expression for finite $\mathbf{T}(a)$,

$$\mathbf{T}(a) = \mathbf{T}(0) \cdot e^{a\mathbf{G}} = e^{a\mathbf{G}} \quad (20.3.15a)$$

and a coordinate x -space representation of the generator \mathbf{G} ,

$$\mathbf{G} \cdot \psi(x) = -\frac{\partial}{\partial x} \psi(x) = \langle x | \mathbf{G} | \psi \rangle \quad (20.3.15b)$$

and the x -representation of the finite translation of a function.

$$\begin{aligned} \mathbf{T}(a) \cdot \psi(x) &= e^{a\mathbf{G}} \cdot \psi(x) = e^{-a \frac{\partial}{\partial x}} \cdot \psi(x) \\ &= \psi(x) - a \frac{\partial \psi(x)}{\partial x} + \frac{a^2}{2!} \frac{\partial^2 \psi(x)}{\partial x^2} - \frac{a^3}{2!} \frac{\partial^3 \psi(x)}{\partial x^3} + \dots \end{aligned} \quad (20.3.15c)$$

Note the relation between the translation generator \mathbf{G} and the momentum operator $\mathbf{p} \rightarrow \frac{\hbar}{i} \frac{\partial}{\partial x} = -i\hbar \frac{\partial}{\partial x}$

$$\mathbf{G} = -\frac{i}{\hbar} \mathbf{p} \quad (20.3.15d)$$

In terms of \mathbf{a} -operators the finite translation has a useful form.

$$\mathbf{T}(a) = e^{-i\mathbf{a}\mathbf{p}/\hbar} = e^{a(\mathbf{a}^\dagger - \mathbf{a})\sqrt{M\omega/2\hbar}} \quad (20.3.15e)$$

To check \pm signs of a $\mathbf{T}(a)$ operator try it out on a plane-wave function using the DeBroglie relation $p = \hbar k$.

$$\mathbf{T}(a) e^{ikx} = e^{-i\mathbf{a}\mathbf{p}/\hbar} e^{ikx} = e^{-iak} e^{ikx} = e^{ik(x-a)} \quad (20.3.16)$$

(2) Boost operators and generators: (A "kick")

There also exists an operator $\mathbf{B}(b)$ which "translates" momentum p -wavefunctions.

$$\mathbf{B}(b) \cdot \psi(p) = \psi(p-b) = \langle x | \mathbf{B}(b) | \psi \rangle = \langle p-b | \psi \rangle \quad (20.3.17a)$$

Such an operator is called a *boost operator* $\mathbf{B}(b)$ and it increases the momentum of any ket-state by b units. (Or, its dual moves the p -space b units negatively or to the left.)

$$\langle p | \mathbf{B}(b) = \langle p-b |, \text{ or: } \mathbf{B}^\dagger(b) | p \rangle = | p-b \rangle, \text{ or: } \mathbf{B}(b) | p \rangle = | p+b \rangle. \quad (20.3.17b)$$

For very small boosts $b \rightarrow db$ such an operation becomes nearly the identity operation $\mathbf{1}$ with a small add-on operator $\mathbf{K}db$ linear in, or proportional to, the tiny (infinitesimal) boost db .

$$\mathbf{B}(db) = \mathbf{1} + \mathbf{K}db \quad (20.3.18a)$$

If $\mathbf{B}(b)$ is a continuous function of b then $\mathbf{K}db$ is the first- derivative part of a Taylor series.

$$\mathbf{K} = \left. \frac{\partial \mathbf{B}}{\partial b} \right|_{b=0} \quad (20.3.18b)$$

Tiny boosts of a momentum function $\psi(p)$ give a single-term Taylor series.

$$\mathbf{B}(db) \cdot \psi(p) = \psi(p - db) = \psi(p) - \frac{\partial}{\partial p} \psi(p) db \quad (20.3.19a)$$

Comparing this to the effect of (20.3.18) gives

$$\mathbf{B}(db) \cdot \psi(p) = (\mathbf{1} + \mathbf{K}db) \cdot \psi(p) = \psi(p) + \mathbf{K} \cdot \psi(p) db \quad (20.3.19b)$$

Solving (20.3.18b) and (20.3.19) yields an abstract operator exponential expression for finite $\mathbf{B}(b)$,

$$\mathbf{B}(b) = \mathbf{B}(0) \cdot e^{b\mathbf{K}} = e^{b\mathbf{K}} \quad (20.3.20a)$$

and a momentum p -space representation of the boost generator \mathbf{K} ,

$$\mathbf{K} \cdot \psi(p) = -\frac{\partial}{\partial p} \psi(p) = \langle p | \mathbf{K} | \psi \rangle \quad (20.3.20b)$$

and the p -representation of the finite boost.

$$\begin{aligned} \mathbf{B}(b) \cdot \psi(p) &= e^{b\mathbf{K}} \cdot \psi(p) = e^{-b \frac{\partial}{\partial p}} \cdot \psi(p) \\ &= \psi(p) - b \frac{\partial \psi(p)}{\partial p} + \frac{b^2}{2!} \frac{\partial^2 \psi(p)}{\partial p^2} - \frac{b^3}{2!} \frac{\partial^3 \psi(p)}{\partial p^3} + \dots \end{aligned} \quad (20.3.20c)$$

Note a relation between the boost generator \mathbf{K} and the position operator $\mathbf{x} \rightarrow \hbar i \frac{\partial}{\partial p} = i \frac{\partial}{\partial k}$

$$\mathbf{K} = \frac{i}{\hbar} \mathbf{x} \rightarrow -\frac{\partial}{\partial p} = \frac{-1}{\hbar} \frac{\partial}{\partial k} \quad (20.3.20d)$$

In terms of \mathbf{a} -operators the finite boost has a form analogous to the form (20.3.15e) for $\mathbf{T}(a)$.

$$\mathbf{B}(b) = e^{ib\mathbf{x}/\hbar} = e^{ib(\mathbf{a}^\dagger + \mathbf{a})/\sqrt{2\hbar M\omega}} \quad (20.3.20e)$$

To check \pm signs of a $\mathbf{B}(b)$ operator try it out on a plane-wave function using the deBroglie relation $p = \hbar k$.

$$\mathbf{B}(b) e^{ikx} = e^{ib\mathbf{x}/\hbar} e^{ikx} = e^{ibx/\hbar} e^{ikx} = e^{i(k+b/\hbar)x} \quad (20.3.21)$$

(3) Applying boost-translation combinations

The $\mathbf{T}(a)$ and $\mathbf{B}(b)$ operations do not commute. The question arises: "Which should come first?" Again, neither and both seems a fair settlement! A *combined boost-translation operation* is defined.

$$\mathbf{C}(a,b) = e^{i(b\mathbf{x}-a\mathbf{p})/\hbar} \quad (20.3.22)$$

This choice is like a Darboux rotation operator $e^{-i\Omega t/\hbar}$. Euler operations, on the other hand, consist of three factors $e^{-i\mathbf{J}_z\alpha/\hbar}e^{-i\mathbf{J}_y\beta/\hbar}e^{-i\mathbf{J}_z\gamma/\hbar}$ in a special order. These operators are related in Appendix. 10.A.

The $\mathbf{C}(a,b)$ combination is easier to disentangle, however, using the following operator identity.

$$e^{\mathbf{A}+\mathbf{B}} = e^{\mathbf{A}}e^{\mathbf{B}}e^{-[\mathbf{A},\mathbf{B}]/2} = e^{\mathbf{B}}e^{\mathbf{A}}e^{[\mathbf{A},\mathbf{B}]/2}, \text{ where: } [\mathbf{A},[\mathbf{A},\mathbf{B}]] = \mathbf{0} = [\mathbf{B},[\mathbf{A},\mathbf{B}]] \quad (20.3.23)$$

This is known as the *Baker-Campbell-Hausdorff identity* and is left as an exercise. Since $[\mathbf{x},\mathbf{p}] = i\hbar\mathbf{1}$, the double commutations $[[\mathbf{x},\mathbf{p}],\mathbf{x}]$ and $[[\mathbf{x},\mathbf{p}],\mathbf{p}]$ are zero as required and $\mathbf{C}(a,b)$ factors either way.

$$\begin{aligned} \mathbf{C}(a,b) &= e^{i(b\mathbf{x}-a\mathbf{p})/\hbar} = e^{ib\mathbf{x}/\hbar}e^{-ia\mathbf{p}/\hbar}e^{-ab[\mathbf{x},\mathbf{p}]/2\hbar^2} = e^{ib\mathbf{x}/\hbar}e^{-ia\mathbf{p}/\hbar}e^{-iab/2\hbar} \\ &= \mathbf{B}(b)\mathbf{T}(a)e^{-iab/2\hbar} = \mathbf{T}(a)\mathbf{B}(b)e^{iab/2\hbar} \end{aligned} \quad (20.3.24a)$$

Reordering only affects the overall phase. The same applies to an \mathbf{a} -operator expression for $\mathbf{C}(a,b)$.

$$\begin{aligned} \mathbf{C}(a,b) &= e^{i(b\mathbf{x}-a\mathbf{p})/\hbar} = e^{ib(\mathbf{a}^\dagger + \mathbf{a})/\sqrt{2\hbar M\omega} + a(\mathbf{a}^\dagger - \mathbf{a})\sqrt{M\omega/2\hbar}} \\ &= e^{\alpha\mathbf{a}^\dagger - \alpha^*\mathbf{a}} = e^{-|\alpha|^2/2}e^{\alpha\mathbf{a}^\dagger}e^{-\alpha^*\mathbf{a}} = e^{|\alpha|^2/2}e^{-\alpha^*\mathbf{a}}e^{\alpha\mathbf{a}^\dagger} \end{aligned} \quad (20.3.24b)$$

Here the complex *phasor-space position coordinate* $\alpha(a,b)$ is defined by

$$\alpha(a,b) = a\sqrt{M\omega/2\hbar} + ib/\sqrt{2\hbar M\omega} = \left[a + i\frac{b}{M\omega} \right] \sqrt{M\omega/2\hbar}. \quad (20.3.24c)$$

Applying the combination operator $\mathbf{C}(x_0,p_0)$ to the ground state $|0\rangle$ simply picks up the ground state Gaussian and plunks it down at phase space position (x_0,p_0) with an overall factor $e^{-|\alpha|^2}$. This is called a *coherent wavepacket state* $|\alpha(x_0,p_0)\rangle$. It turns out to have expected position x_0 and momentum p_0 .

$$\begin{aligned} |\alpha_0(x_0,p_0)\rangle &= \mathbf{C}(x_0,p_0)|0\rangle = e^{i(x_0\mathbf{x}-p_0\mathbf{p})/\hbar}|0\rangle \\ &= e^{-|\alpha_0|^2/2}e^{\alpha_0\mathbf{a}^\dagger}e^{-\alpha_0^*\mathbf{a}}|0\rangle \\ &= e^{-|\alpha_0|^2/2}e^{\alpha_0\mathbf{a}^\dagger}|0\rangle \\ &= e^{-|\alpha_0|^2/2} \sum_{n=0}^{\infty} \frac{(\alpha_0\mathbf{a}^\dagger)^n}{n!}|0\rangle/n! \\ &= e^{-|\alpha_0|^2/2} \sum_{n=0}^{\infty} \frac{(\alpha_0)^n}{\sqrt{n!}}|n\rangle, \text{ where: } |n\rangle = \frac{\mathbf{a}^{\dagger n}|0\rangle}{\sqrt{n!}} \end{aligned} \quad (20.3.25a)$$

What's neat about a coherent $|\alpha(x_0,p_0)\rangle$ state is that it is an eigenvector of the destruction operator.

$$\begin{aligned} \mathbf{a}|\alpha_0(x_0,p_0)\rangle &= e^{-|\alpha_0|^2/2} \sum_{n=0}^{\infty} \frac{(\alpha_0)^n}{\sqrt{n!}} \mathbf{a}|n\rangle = e^{-|\alpha_0|^2/2} \sum_{n=0}^{\infty} \frac{(\alpha_0)^n}{\sqrt{n!}} \sqrt{n}|n-1\rangle \\ &= \alpha_0|\alpha_0(x_0,p_0)\rangle \end{aligned} \quad (20.3.25b)$$

And the left-pointing coherent bra is an eigenvector of the creation operator. (*Quelle apropos!*)

$$\langle\alpha_0(x_0,p_0)|\mathbf{a}^\dagger = \langle\alpha_0(x_0,p_0)|\alpha_0^* \quad (20.3.25c)$$

This makes calculation of position and momentum expectation operators quite easy.

$$\begin{aligned}\langle \alpha_0(x_0, p_0) | \mathbf{x} | \alpha_0(x_0, p_0) \rangle &= \sqrt{\frac{\hbar}{2M\omega}} \langle \alpha_0(x_0, p_0) | (\mathbf{a} + \mathbf{a}^\dagger) | \alpha_0(x_0, p_0) \rangle \\ &= \sqrt{\frac{\hbar}{2M\omega}} (\alpha_0 + \alpha_0^*) = x_0\end{aligned}\quad (20.3.25d)$$

$$\begin{aligned}\langle \alpha_0(x_0, p_0) | \mathbf{p} | \alpha_0(x_0, p_0) \rangle &= i\sqrt{\frac{M\omega\hbar}{2}} \langle \alpha_0(x_0, p_0) | (\mathbf{a}^\dagger - \mathbf{a}) | \alpha_0(x_0, p_0) \rangle \\ &= i\sqrt{\frac{M\omega\hbar}{2}} (\alpha_0^* - \alpha_0) = p_0\end{aligned}\quad (20.3.25e)$$

The expected position and momentum is, well, exactly what we would expect classically.

(4) Time evolution of coherent states

Time evolution is calculated using the time evolution operator whose general form is

$$\mathbf{U}(t, 0) = e^{-i\mathbf{H}t/\hbar}, \quad (20.3.26)$$

according to (2.8.10e). Oscillator eigenstate time evolution is simply determined by harmonic phases.

$$\mathbf{U}(t, 0) | n \rangle = e^{-i\mathbf{H}t/\hbar} | n \rangle = e^{-i(n+1/2)\omega t} | n \rangle \quad (20.3.27)$$

The coherent state evolution uses this result.

$$\begin{aligned}\mathbf{U}(t, 0) | \alpha_0(x_0, p_0) \rangle &= e^{-|\alpha_0|^2/2} \sum_{n=0}^{\infty} \frac{(\alpha_0)^n}{\sqrt{n!}} \mathbf{U}(t, 0) | n \rangle = e^{-|\alpha_0|^2/2} \sum_{n=0}^{\infty} \frac{(\alpha_0)^n}{\sqrt{n!}} e^{-i(n+1/2)\omega t} | n \rangle \\ &= e^{-i\omega t/2} e^{-|\alpha_0|^2/2} \sum_{n=0}^{\infty} \frac{(\alpha_0 e^{-i\omega t})^n}{\sqrt{n!}} | n \rangle\end{aligned}$$

This simplifies to a variable coherent state

$$\mathbf{U}(t, 0) | \alpha_0(x_0, p_0) \rangle = e^{-i\omega t/2} | \alpha_t(x_t, p_t) \rangle \quad (20.3.28)$$

with a time dependent phasor coordinate (20.3.24c)

$$\begin{aligned}\alpha_t(x_t, p_t) &= e^{-i\omega t} \alpha_0(x_0, p_0) \\ \left[x_t + i \frac{p_t}{M\omega} \right] &= e^{-i\omega t} \left[x_0 + i \frac{p_0}{M\omega} \right],\end{aligned}\quad (20.3.29a)$$

whose real and imaginary parts (the expected x_t and $p_t/M\omega$) go clockwise around the phasor circle.

$$\begin{aligned}x_t &= x_0 \cos \omega t + \frac{p_0}{M\omega} \sin \omega t \\ \frac{p_t}{M\omega} &= -x_0 \sin \omega t + \frac{p_0}{M\omega} \cos \omega t\end{aligned}\quad (20.3.29b)$$

The (x_t, p_t) mimic perfectly a classical oscillator. Evolution of $|\alpha_t(x_t, p_t)\rangle$ is shown in Fig. 20.3.2.

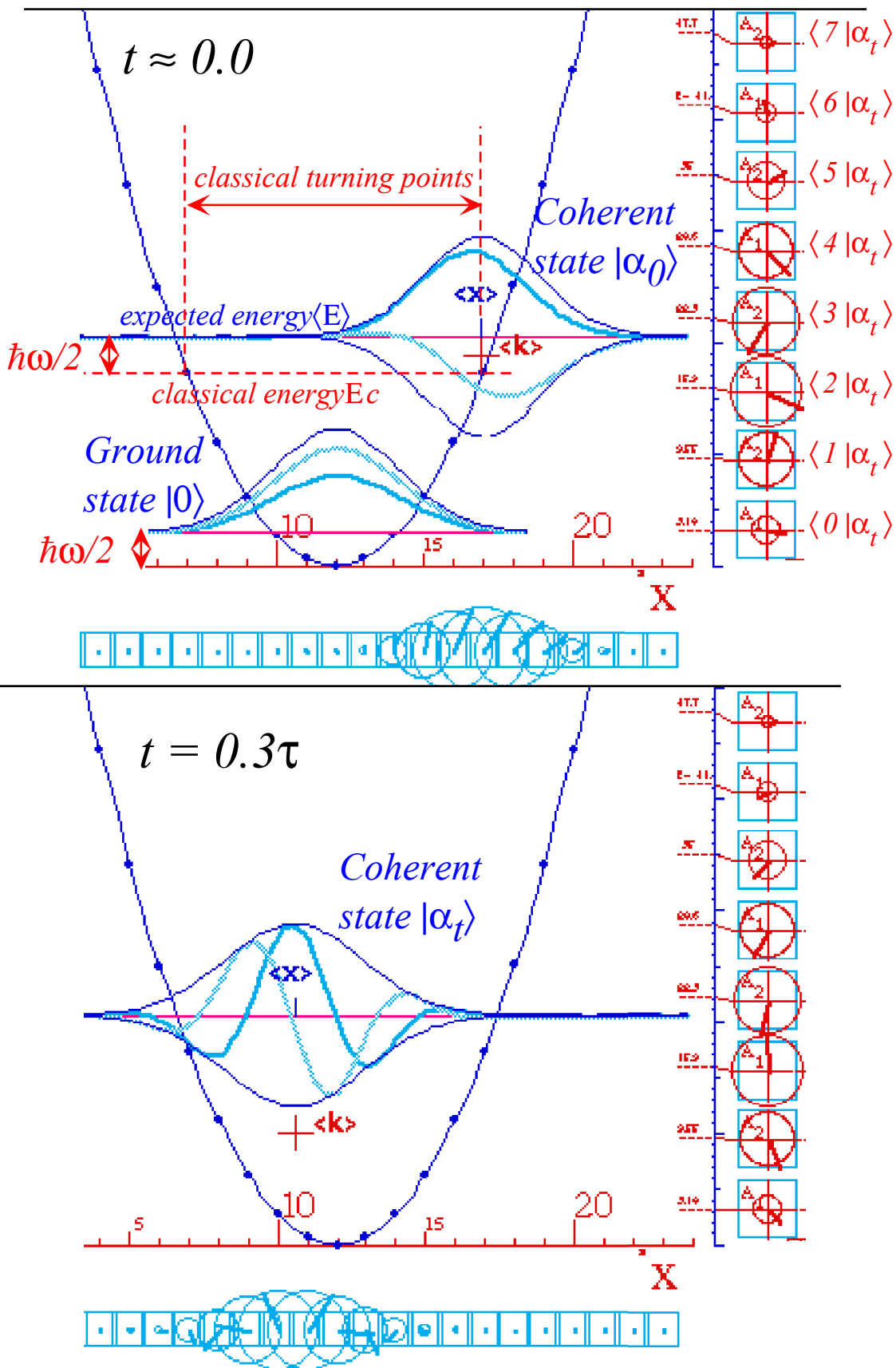


Fig. 20.3.2 Coherent state oscillation for harmonic oscillator showing E , x and k expectation.

At last, it appears that the goal of recovering perfect classical correspondence of a quantum system has been achieved! Well, almost. There are still some issues that we will discuss shortly. But, at least Fig. 20.3.2 is a big improvement over the wobbly wave beating that appeared in Fig. 20.3.1. The coherent wave envelope $\langle x|\psi\rangle = \langle x|\alpha_t(x_t, p_t)\rangle$ and the $\langle x\rangle$ expectation march rigidly in lock step from one side of the well to the other and back again without the envelope distorting even the slightest from the Gaussian shape of the ground state wave. Recall that the $\langle x\rangle$ expectation of the wave in Fig. 20.3.1 only beats itself half way to the classical turning point corresponding to its expected energy.

Closer examination of Fig. 20.3.2 reveals that the coherent wave also fails to reach the classical turning points corresponding to its expected energy. Its expected quantum energy is

$$\begin{aligned}\langle E\rangle\bigg|_{\alpha_0} &= \langle \alpha_0(x_0, p_0) | H | \alpha_0(x_0, p_0) \rangle = \langle \alpha_0(x_0, p_0) | \left(\hbar\omega \mathbf{a}^\dagger \mathbf{a} + \frac{\hbar\omega}{2} \mathbf{1} \right) | \alpha_0(x_0, p_0) \rangle \\ &= \hbar\omega \alpha_0^* \alpha_0 + \frac{\hbar\omega}{2}\end{aligned}\quad (20.3.30a)$$

This has two parts. The first term is the classical energy using the phasor coordinate (20.3.24c).

$$\begin{aligned}E_{classical} &= \hbar\omega \alpha_0^* \alpha_0 = \hbar\omega \left| \left[x_0 + i \frac{p_0}{M\omega} \right] \sqrt{M\omega / 2\hbar} \right|^2 \\ &= \frac{1}{2} M\omega x_0^2 + \frac{p_0^2}{2M}\end{aligned}\quad (20.3.30b)$$

The second term is the zero-point energy E_0 that is part of the quantum result.

$$\begin{aligned}\langle E\rangle\bigg|_{\alpha_0} &= E_{classical} + E_0 = \hbar\omega \alpha_0^* \alpha_0 + \frac{\hbar\omega}{2} \\ &= \frac{1}{2} M\omega x_0^2 + \frac{p_0^2}{2M} + \frac{\hbar\omega}{2}\end{aligned}\quad (20.3.30c)$$

Fig. 20.3.2 shows both the quantum expectation and classical energy levels. It is seen that the expectation values oscillate between the intersections of the classical energy ($E_{classical}$) level with the potential $V(x) = 1/2M\omega x^2$ parabola. The classical level lies $\hbar\omega/2$ below the true total energy (20.3.30c) of the coherent wave state. The turning points associated with the true quantum energy are not reached by the x -expectation value. So quantum mechanics gets the last word even in this, a nearly perfect of example of classical correspondence. And, well that it should.

The distribution of quantum eigenstates needed to make a coherent wave are given by (20.3.25c).

$$\langle n | \alpha_0(x_0, p_0) \rangle = e^{-|\alpha_0|^2/2} \frac{(\alpha_0)^n}{\sqrt{n!}}, \quad \left| \langle n | \alpha_0(x_0, p_0) \rangle \right|^2 = e^{-|\alpha_0|^2} \frac{|\alpha_0|^{2n}}{n!} \quad (20.3.31)$$

This $a^{2n} e^{-a^2}/n!$ probability distribution is called a *Poissonian distribution*. The corresponding amplitude distribution is evident in the varying size of eigenphasors on the extreme right hand side of Fig. 20.3.2.

The peak and mean of the distribution occurs near the expected energy levels. (See exercises.)

(c) Classical and quantum dynamics of wavepackets

The coherent state wavefunction follows from its abstract state definition (20.3.25a). To get the coordinate wavefunction we just clothe (20.3.25a) with an $\langle x|$ -bra.

$$\begin{aligned}\langle x|\alpha_0(x_0, p_0)\rangle &= \langle x|\mathbf{C}(x_0, p_0)|0\rangle = \langle x|e^{i(x_0\mathbf{x}-p_0\mathbf{p})/\hbar}|0\rangle \\ &= e^{-|\alpha_0|^2/2} \sum_{n=0}^{\infty} \frac{(\alpha_0)^n}{\sqrt{n!}} \langle x|n\rangle\end{aligned}\quad (20.3.32)$$

Starting with (20.3.24a) the first line uses boost function (20.3.20e) and translation axiom (20.3.12).

$$\begin{aligned}\langle x|\alpha_0(x_0, p_0)\rangle &= \langle x|\mathbf{C}(x_0, p_0)|0\rangle = \langle x|\mathbf{B}(p_0)\mathbf{T}(x_0)|0\rangle e^{-ix_0 p_0/2\hbar} \\ &= \langle x|e^{ip_0\mathbf{x}/\hbar}\mathbf{T}(x_0)|0\rangle e^{-ix_0 p_0/2\hbar} \\ &= e^{ip_0 x/\hbar} \langle x|\mathbf{T}(x_0)|0\rangle e^{-ix_0 p_0/2\hbar} \\ &= e^{ip_0 x/\hbar} \langle x-x_0|0\rangle e^{-ix_0 p_0/2\hbar}\end{aligned}\quad (20.3.33)$$

Let us change Dirac notation back to $\Psi(x)$ -notation using ground state wavefunction from (20.2.7).

$$\langle x|\Psi_0\rangle = \Psi_0(x) = e^{-M\omega x^2/2\hbar} (M\omega/\pi\hbar)^{1/4} \quad (20.3.34a)$$

Rearrangement turns the coherent wave into a *complex Gaussian wavepacket* $e^{-A(z-\alpha)^2}$.

$$\begin{aligned}\Psi_{\alpha_0}(x) &= \langle x|\alpha_0(x_0, p_0)\rangle = e^{ip_0 x/\hbar} e^{-M\omega(x-x_0)^2/2\hbar} e^{-ix_0 p_0/2\hbar} \left(\frac{M\omega}{\pi\hbar}\right)^{1/4} \\ &= e^{ip_0 x_0/2\hbar} e^{-M\omega(x-x_0)^2/2\hbar + ip_0(x-x_0)/\hbar} \left(\frac{M\omega}{\pi\hbar}\right)^{1/4}\end{aligned}\quad (20.3.34b)$$

The peak of the complex Gaussian $\langle x|\alpha_0\rangle$ is located in the complex z -plane or phasor space at $z = \alpha_t$

$$\alpha_t(x_t, p_t) = e^{-i\omega t} \alpha_0(x_0, p_0) = \left[x_t + i \frac{p_t}{M\omega} \right] = e^{-i\omega t} \left[x_0 + i \frac{p_0}{M\omega} \right], \quad (20.3.34c)$$

according to (20.3.29). Its time behavior is obtained from (20.3.28).

$$\Psi_{\alpha_t}(x) = \langle x|\alpha_t(x_t, p_t)\rangle = e^{ip_t x_t/2\hbar - i\omega t/2\hbar} \left[e^{-M\omega(x-x_t)^2/2\hbar + ip_t(x-x_t)/\hbar} \left(\frac{M\omega}{\pi\hbar}\right)^{1/4} \right] \quad (20.3.34d)$$

The phase factor outside the complex Gaussian in the braces ([]) is known as the *semi-classical action phase* or *eikonal phase factor*. Its theory has a wonderful history. We give a brief sketch of parts of the theory. We first discussed action and phase back in Section 5.3(a).

(1) Classical action and phase

Dirac and Feynman are generally credited with fully realizing the significance and utility of the classical action, but many of the creators of quantum mechanics beginning with Bohr, Einstein, Keller, Jordan, Wentzels, Kramers, Born (of the *JWKB* method) and others have developed the ideas which continue to grow in modern physics.

The beginnings of these ideas go back even to Newton who started the classical mechanics which Lagrange, Legendre, Poincare, Hamilton, and Jacobi developed to such a high level that they almost discovered quantum theory using logical deduction alone. (Or, so it might appear using 20-20 hindsight!) There are four or five related classical developments of classical mechanics which foreshadow quantum theory and experienced a later renaissance.

These are, in order of their appearance, the *Lagrangian function* $L=T-V$ which for the oscillator is

$$L = T - V = \frac{M\dot{x}^2}{2} - \frac{M\omega^2 x^2}{2} = \frac{p^2}{2M} - \frac{M\omega^2 x^2}{2}, \quad (20.3.35a)$$

the *Hamiltonian function* $H=T+V$ which for the oscillator has the form (preferred format first)

$$H = T + V = \frac{p^2}{2M} + \frac{M\omega^2 x^2}{2} = \frac{M\dot{x}^2}{2} + \frac{M\omega^2 x^2}{2}, \quad (20.3.35b)$$

and the *Poincare invariant* dS or *Legendre transformation generator* relation between H and L

$$dS = L dt = p dx - H dt, \quad (20.3.35c)$$

whose integral is the *Hamilton's Principle action integral* S_p

$$S_p = \int dS = \int L dt = \int p dx - \int H dt, \quad (20.3.35d)$$

which includes *Hamilton's Characteristic action integral* S_H also known as "*reduced*" *action*

$$S_H = \int p dx, \quad (20.3.35e)$$

The word "*Principle*" (not "Principal") may be capitalized since it refers to *Hamilton's Minimum Principle*, that is, that S_p is minimum for classical paths. So is the word "*Characteristic*" since it refers to the *Method of Characteristics* used to solve partial differential wave equations by integrating along their ray trajectories. The partial differential equations being solved in those days were (among others) the *Hamilton Jacobi equations* which follow directly from (20.3.35c)

$$dS = L dt = \frac{\partial S}{\partial x} dx + \frac{\partial S}{\partial t} dt, \quad (20.3.35f)$$

where:

$$p = \frac{\partial S}{\partial x}, \quad H = -\frac{\partial S}{\partial t} \quad (20.3.35g)$$

determine *S-eikonal* wavefronts normal to the classical momentum. ($\mathbf{p} = \nabla S$ in 2 or 3-dimensions.)

Dirac and Feynman developed the idea that the quantum wave function correspond to the S -wavefronts and that a wavefunction such as (20.3.34d) has the form

$$\Psi = e^{iS/\hbar} \phi = e^{i\int L dt/\hbar} \phi. \quad (20.3.36)$$

It certainly works well when both p and $H=E$ are constant since then (20.3.35d) reduces to the form

$$S_p / \hbar = (p x - H t) / \hbar = k x - \omega t, \quad (20.3.37)$$

of the relativistically invariant plane wave phase angle of the plane wave $e^{i(kx-\omega t)}$.

However, the idea applies to the oscillator wavefunction and many other problems as well. For the oscillator the reduced action comes out as follows.

$$\begin{aligned} S_H &= \int_0^t p_t dx_t = \int_0^t \sqrt{2M \left(E_c - \frac{M\omega^2}{2} x_t^2 \right)} dx_t = S_p + E_c t \\ &= \frac{x_t p_t}{2} \Big|_0^t + \frac{E_c}{\omega} \arcsin \left(\frac{M\omega}{\sqrt{2ME_c}} x_t \right) \Big|_0^t = \frac{x_t p_t - x_0 p_0}{2} + E_c t \end{aligned} \quad (20.3.38a)$$

So, (20.3.36) is consistent with the oscillator wavepacket (20.3.34d)

$$\Psi = e^{iS/\hbar} \phi = e^{i(x_t p_t - x_0 p_0)/2\hbar - i\omega t/2} \phi, \tag{20.3.38b}$$

if the zero-point energy difference (20.3.30c) between classical and quantum-expectation energies is accounted for.

(2) *Quantum generating functions*

The coherent wavepacket with zero momentum ($p_0=0$) from (20.3.32) and (20.3.34b) is

$$\Psi_{x_0}(x) = e^{-M\omega|x_0|^2/4\hbar} \sum_{n=0}^{\infty} \left(\frac{M\omega}{2\hbar}\right)^{n/2} \frac{(x_0)^n}{\sqrt{n!}} \psi_n(x) = e^{-M\omega(x-x_0)^2/2\hbar} \left(\frac{M\omega}{\pi\hbar}\right)^{1/4} \tag{20.3.39}$$

This yields *eigenwave generating functions*.

$$\sum_{n=0}^{\infty} \left(\frac{M\omega}{2\hbar}\right)^{n/2} \frac{(x_0)^n}{\sqrt{n!}} \psi_n(x) = e^{-\frac{M\omega x^2}{2\hbar}} e^{-\frac{M\omega}{2\hbar} \left(\frac{x_0^2}{2} - 2xx_0\right)} \left(\frac{M\omega}{\pi\hbar}\right)^{1/4} \tag{20.3.40a}$$

We redefine ψ_n and write coordinate x in units y of zero-point classical turning point. ($x_0^{CTP} = [\hbar/M\omega]^{1/2}$)

$$\psi_n(x) = \left(\frac{\pi\hbar}{M\omega}\right)^{1/4} \frac{2^{n/2} H_n(y) e^{-y^2/2}}{\sqrt{n!}} \quad \text{and: } x = \sqrt{\frac{\hbar}{M\omega}} y, \quad x_0 = \sqrt{\frac{\hbar}{M\omega}} y_0 \tag{20.3.40c}$$

This simplifies the generating expansion.

$$\sum_{n=0}^{\infty} \frac{(y_0)^n}{n!} H_n(y) = H_0(y) + y_0 H_1(y) + \frac{y_0^2}{2!} H_2(y) + \dots = e^{-(y_0^2/4 - yy_0)} \tag{20.3.40b}$$

(20.3.40b) gives successive *Hermite polynomials* $H_n(y)$ which multiply the Gaussian $e^{-y^2/2}$.

$$\begin{aligned} H_0(y) &= e^{-\frac{y_0^2}{4} + yy_0} \Big|_{y_0=0} = 1, & H_1(y) &= \frac{d}{dy_0} e^{-\frac{y_0^2}{4} + yy_0} \Big|_{y_0=0} = y \\ H_2(y) &= \frac{d^2}{dy_0^2} e^{-\frac{y_0^2}{4} + yy_0} \Big|_{y_0=0} = y^2 - \frac{1}{2}, & H_3(y) &= \frac{d^3}{dy_0^3} e^{-\frac{y_0^2}{4} + yy_0} \Big|_{y_0=0} = y^3 - \frac{3}{2}y \end{aligned} \tag{20.3.40d}$$

In many texts, the Hermite polynomials $H_n(y)$ are defined as the above multiplied by 2^n . (Let: $y_0 \rightarrow 2y_0$.)

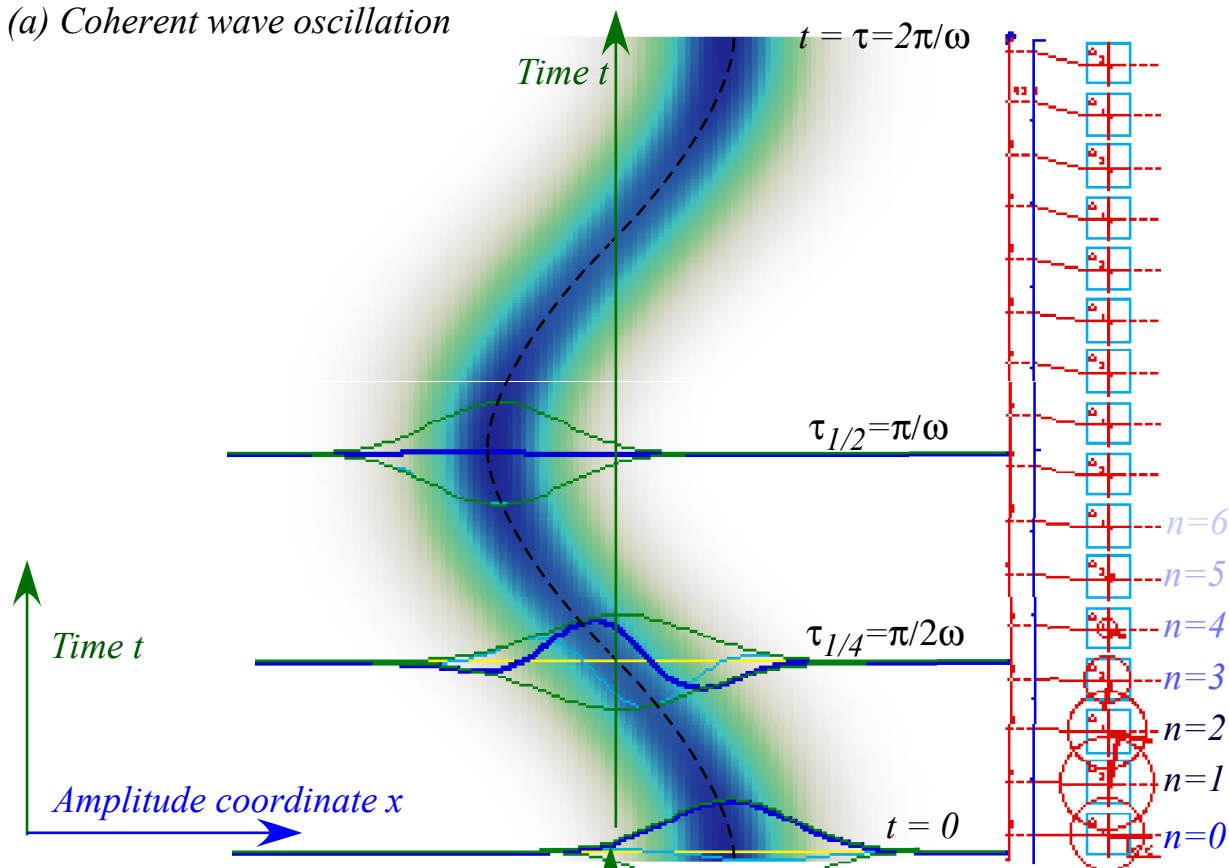
When using that convention, move the 2^n -factor of (20.3.40c) down to the denominator.

(d) Shaped packet states (“Squeezed” states)

Coherent state motion in Fig. 20.3.3(a) results if a ground state (or “vacuum” state) Gaussian wave function e^{-y^2/Δ^2} a translated by $e^{-ia\mathbf{p}} = e^{-a\partial/\partial y}$ or boosted by $e^{ib\mathbf{x}} = e^{iby}$. We may generalize this to include exponentials of polynomials of generators $-i\mathbf{p}$ and $i\mathbf{x}$. Perhaps, the simplest is the squared or quadratic generator $(i\mathbf{x})^2 = -y^2$ in an operator $e^{-s\mathbf{x}^2} = e^{-sy^2}$ that gives a state called a *squeezed state* whose wave function $\psi_s(y) = e^{-sy^2} e^{-y^2/\Delta^2} = e^{-y^2/\Delta'^2}$ is a Gaussian whose width Δ is altered to $\Delta' = 1/\sqrt{s+1/\Delta^2}$, that is, either *expanded*, if squeezing parameter s is negative, or else *squeezed* if s is positive.

The time behavior of such a squeezed wave is shown in Fig. 20.3.3(b). As expected it returns to its “natural” width, but then overshoots to become an expanded Gaussian. The result is a “breathing” motion of expansion and squeezing at *twice* natural frequency ω . (This is called “squeezed vacuum” oscillation.)

(a) Coherent wave oscillation



(b) Squeezed ground state (“Squeezed vacuum” oscillation)

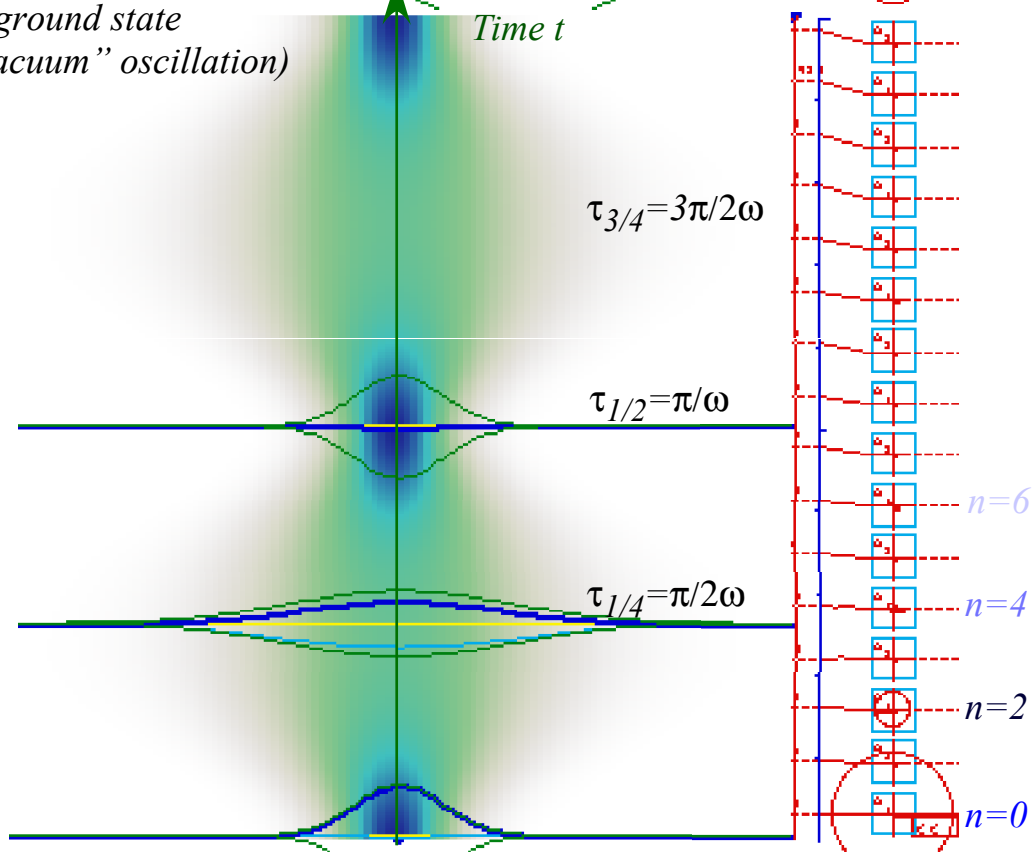


Fig. 20.3.3 (a) Elementary coherent wave. (b) Elementary squeezed ground state wave

Notice that the squeezed vacuum “breathing” is symmetric since it involves only even quantum states $n=0, 2, 4, \dots$ in its $|n\rangle$ expansion. This accounts for its double-frequency (2ω) of oscillation that starts with a fraction $f=0.5$ of zero-point uncertainty $\Delta x_0 = \sqrt{\hbar/2M\omega}$, “inhales” and expands to a maximum value $\Delta x_0/f = 2 \cdot \Delta x_0$ in a quarter period $\tau_{1/4} = \frac{1}{4}(2\pi/\omega)$, then “exhales” back to the minimum value $f \cdot \Delta x_0 = 0.5 \cdot \Delta x_0$ at half period $\tau_{1/2}$, and takes another breath between $\tau_{1/2}$ and τ in Fig. 20.3.3(b).

Compare this to the elementary coherent oscillation in Fig. 20.3.3(a) that combines both odd and even states $n=0, 1, 2, 3, 4, \dots$ in its $|n\rangle$ expansion (20.3.25), and so its center of intensity $\langle \mathbf{x} \rangle = \bar{x}$ oscillates at the fundamental frequency ω , in fact, it follows a classical $\bar{x} = x_0 \cos \omega t$ time trajectory clearly visible in the figure and consistent with (20.3.29b) in the case that initial expected momentum is zero ($p_0 = 0$).

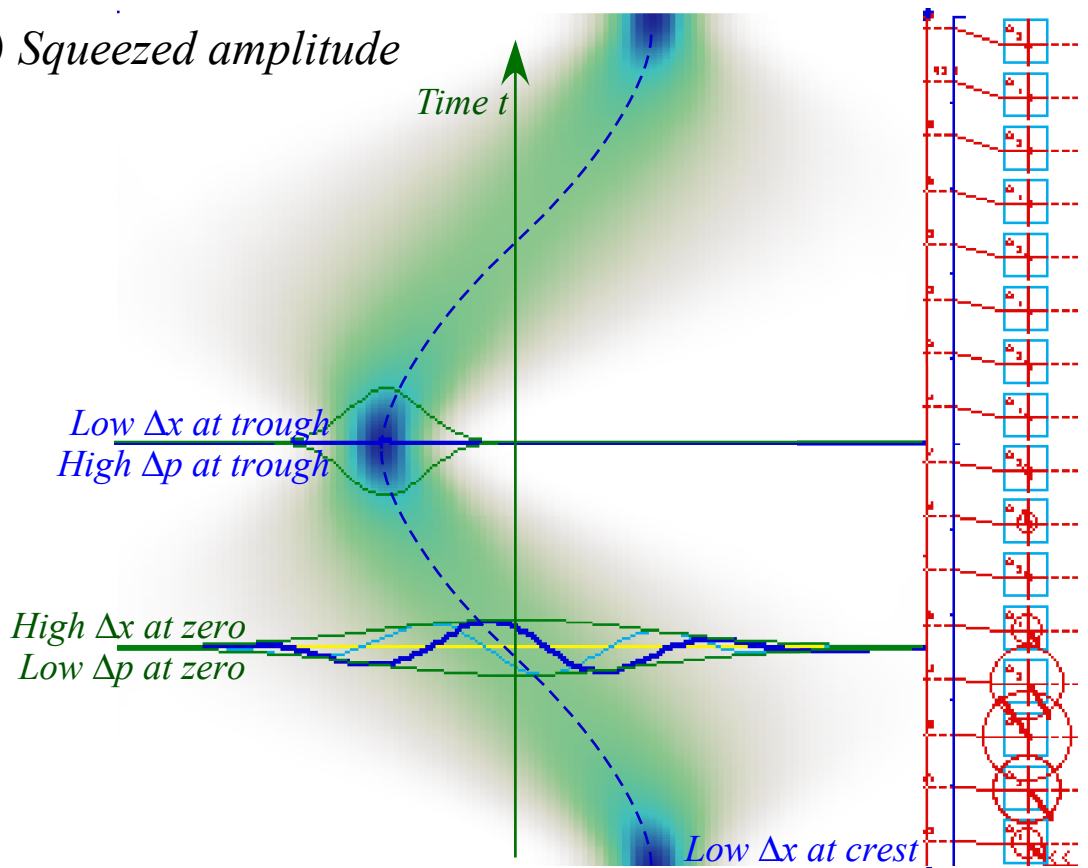
By combining the elementary coherent $\langle \mathbf{x} \rangle$ oscillation in Fig. 20.3.3(a) with the coherent $\langle \mathbf{x}^2 \rangle$ “breathing” oscillation in Fig. 20.3.3(b) it is possible to sharpen the precision of either amplitude or phase of a coherent oscillation. If we simply combine the two distributions in Fig. 20.3.3(a-b), then a squeezed amplitude wave results with sharpened uncertainty at each of the $\frac{1}{4}$ -period times of maximum (or minimum) amplitude as shown in Fig. 20.3.4(a). The price we pay for more precise or *certain* amplitude position is more *uncertain* momentum, and this translates into more uncertain location at the times when the amplitude crosses the zero point. That is, more *certain amplitude* implies more *uncertain phase*.

To have a more *certain phase* we need to adjust zero-crossing time to coincide with moments of x-inhalation as shown in Fig. 20.3.4(b), but this gives a state with more *uncertain amplitude*. It should not be surprising that phase and amplitude behave like conjugate variables of position and momentum. Phase angle Φ and amplitude A obey a generalized Heisenberg uncertainty relation analogous to (20.2.20d-e).

$$\Delta\Phi \cdot \Delta A \geq \frac{\hbar}{2A}$$

Since the product $c = A \cdot \Phi$ is the circumferential arc length orthogonal to the radial amplitude distance A , this relation is really identical to (20.2.20e) and to one for angular momentum to be derived later. Note that angular uncertainty is inversely proportional to the product $A \cdot \Delta A$. This is responsible for the tremendous phase precision of high-amplitude lasers.

(a) Squeezed amplitude



(b) Squeezed phase

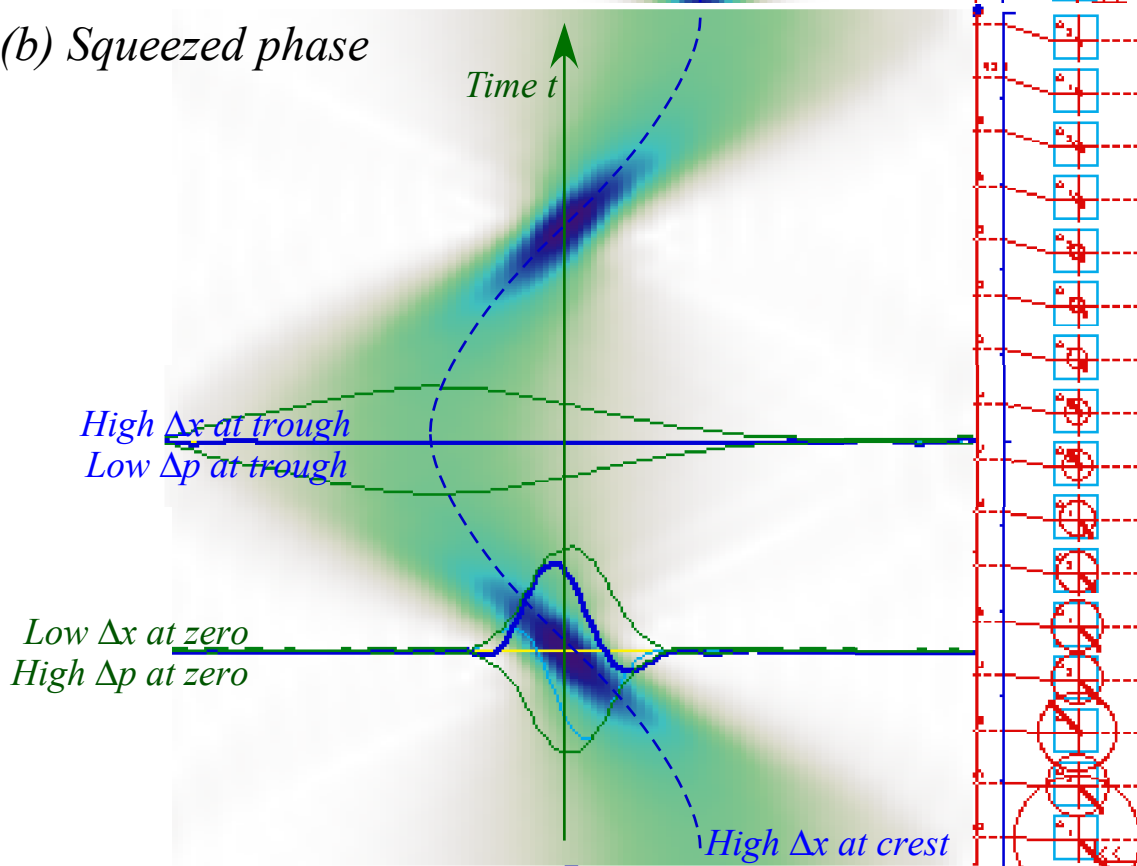


Fig. 20.3.4 (a) Squeezed amplitude. (b) Squeezed phase zeros.

Problems for Chapter 20

Uncertain Quantum Viriality

1. First: verify equations (20.2.21) to (20.2.22).

(a) With: $H = \mathbf{p}^2/2M + V(\mathbf{x})$. show that $[H, \mathbf{x}] = \hbar \mathbf{p}/Mi$.

(b) With: $H|j\rangle = \hbar\omega_j|j\rangle$ and $\Omega_{j1} = \omega_j - \omega_1$ show that $\langle j | \mathbf{p} | 1 \rangle = Mi \Omega_{j1} \langle j | \mathbf{x} | 1 \rangle$.

(c) Use (a-b) to show $\langle k | \mathbf{x} \mathbf{p} | k \rangle = \hbar i/2 = -\langle k | \mathbf{p} \mathbf{x} | k \rangle$ for any eigenstate $|\Psi\rangle = |k\rangle$.

(d) Show: $\partial/\partial t \langle k | \mathbf{x} \mathbf{p} | k \rangle = 0 = i/\hbar \langle k | [H, \mathbf{x} \mathbf{p}] | k \rangle$.

(e) Compare uncertainty calculation for Coulomb ($P=-1$) potential to the Bohr radius and Δp in (5.4.3).

(f) For $V(x) = Ax^P$ show that: $\langle k | KE | k \rangle = \langle k | \mathbf{p}^2/2M | k \rangle = \langle k | PE | k \rangle P/2$ (A virial theorem)

(g) Derive energy spectrum and the KE/PE ratio for a hyper-power Hamiltonian $\mathbf{p}^Q/2M + Ax^P$.

The Beats Go On

2. Consider quantum beats between saturated (50-50) pairs of harmonic oscillator states.

(a) Derive expected momentum \bar{p} as a function of time for a 50-50 combination state of the ground $|0\rangle$ and first excited state $|1\rangle$. Compare to the expected position. Does $m\dot{\bar{x}} = \bar{p}$?

(b) Derive the expected position-squared $\langle x^2 \rangle$ and momentum-squared $\langle p^2 \rangle$ for the same combination state as (a). Discuss their relations.

(c) Derive the expected position and momentum as a function of time for a 50-50 combination state of the ground $|0\rangle$ and second excited state $|2\rangle$. Compare. Does $m\dot{\bar{x}} = \bar{p}$?

Coherent Deviation

3. Here we consider the mean and standard deviation (20.2.20a) or "width" of coherent state distributions for physical quantities.

(a) Derive a (simple) formula for the coherent state norm $\langle \alpha | \alpha \rangle$.

(b) Derive formulas for the position-squared and momentum-squared expectation values in a coherent state $|\alpha\rangle$.

(c) Use (b) to derive the standard deviation of position and momentum distributions.

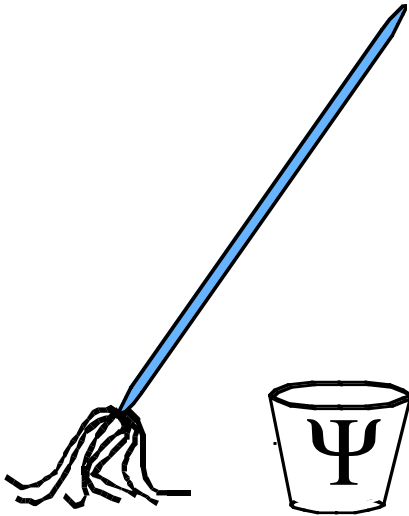
(d) Derive a formula for the mean value \bar{n} of n in the Poisson distribution (20.3.25b).

(d) Approximate a formula for the width of the Poisson distribution around mean value \bar{n} .

Coherent Derivation

4. Use the coherent wave generating function to derive analytic formula for oscillator eigenfunctions $\langle x | n \rangle$ and write out the first three. Derive the momentum wavefunctions $\langle p | n \rangle$, too. (Should be an easy symmetry task.)

Unit 7 Quantum Oscillators



QM for AMOP

Chapter 21

Two-Dimensional

Oscillator States and Dynamics

W. G. Harter

Using the 1D-harmonic oscillator algebra from the preceding Chapter 20, the 2D oscillator quantum mechanics is developed. Much of the theory applies to 3D, 4D, and higher dimensional oscillators, as well. Quantum em fields treated in Chapter 22 begin with many-D oscillators, one dimension for each em-mode. However, the main objective of this Chapter 21 is to give the quantum version of the classical ABCD oscillator analogy to quantum spin-1/2, polarization, and other $U(2)$ systems discussed in Chapter 10. This sets the stage for a powerful development, due to Schwinger, of the quantum theory of angular momentum in Chapter 23.

CHAPTER 21. 2D-HARMONIC OSCILLATOR STATES AND DYNAMICS1

21.1 Two-Dimensional Harmonic Oscillator Hamiltonians and Bases.....1

(a) 2D-Oscillator basics1

 (1) Hamiltonians and operators1

 (2) Commutation relations: Bosons and Fermions.....1

(b) Two-dimensional (or 2-particle) base states3

(c) Two-dimensional (or 2-particle) matrix operators.....5

(d) 2D-Oscillator eigensolutions7

 (1) Fundamental eigenstates7

 (2) $U(2) \supset C_2^A$ eigenstates and wavefunctions10

 (3) $U(2) \supset C_2^A$ oscillator wavefunctions.....11

21.2 2D Oscillator Symmetry, Spin, and Wavefunctions.....15

(a) Angular momentum eigenstates: C_2^C symmetry15

 (1) Angular momentum labeling: Fundamental base states $\{|\uparrow\rangle, |\downarrow\rangle\}$ 16

 (2) 3-Vector base states ($\nu=2$) or ($j=1$).....19

(b) Polar coordinates: C_2^C symmetry variable separation.....22

21.3 N-Dimensional Oscillator Levels25

(a) Pascal triangle and $U(N)$ degeneracy25

Problems for Chapter 2128

Chapter 21. 2D-Harmonic Oscillator States and Dynamics

21.1 Two-Dimensional Harmonic Oscillator Hamiltonians and Bases

So far, most wavefunctions have been one-dimensional . The classical waves in the "Hall of Mirrors" wave-guide and its cavity described in Sec. 6.3 are one exception. Now we extend the oscillator theory of the preceding Chapter 20 to an oscillator system of two (or more) dimensions.

(a) 2D-Oscillator basics

As far as symmetry algebra goes it is a big jump to go from a 1D oscillator Hamiltonian with a $U(1)$ phase space (The 1-D phase space has two real dimensions (x,p) or one complex dimension $\alpha=x+ip$) to a 2D oscillator with a $U(2)$ phase space. The 2-D oscillator phase space has four real *phase space* dimensions (x_1, p_1, x_2, p_2) or two complex *phasor* dimensions $(\alpha_1 =x_1+ip_1, \alpha_2 =x_2+ip_2)$.

To help understand the physics and mathematics of this formidable system it helps to appeal to the analogy in Sec. 10.1 between a two-dimensional classical oscillator and a two state quantum system. The $U(2)$ catalog in Fig. 10.4.2 showed three archetypes of 2-state Hamiltonians labeled $A, B,$ and C each corresponding to different values of parameters $A, B, C,$ and D that give different symmetry and physics. The goal here is to solve (and more importantly, understand) the eigensolutions of the quantum version of the $A, B,$ and C type oscillators and how their solutions are derived as symmetry varies.

(1) Hamiltonians and operators

The first step is easy. We rewrite a classical 2-D Hamiltonian (10.1.3a) with a thick-tip pen!

$$\mathbf{H} = \frac{A}{2}(\mathbf{p}_1^2 + \mathbf{x}_1^2) + B(\mathbf{x}_1\mathbf{x}_2 + \mathbf{p}_1\mathbf{p}_2) + C(\mathbf{x}_1\mathbf{p}_2 - \mathbf{x}_2\mathbf{p}_1) + \frac{D}{2}(\mathbf{p}_2^2 + \mathbf{x}_2^2) \quad (21.1.1)$$

The second step is not so hard either. The symmetric form lets us relate each \mathbf{x} and \mathbf{p} to creation and destruction operators as in (20.2.1) and (20.2.16). (Here the pesky \sqrt{M} and \hbar factors are absorbed in $A, B, C,$ and D .) Each oscillator dimension has a set of operators. First, the number-1 oscillator is set up.

$$\mathbf{a}_1 = (\mathbf{x}_1 + i \mathbf{p}_1)/\sqrt{2} \qquad \mathbf{a}_1^\dagger = (\mathbf{x}_1 - i \mathbf{p}_1)/\sqrt{2} \qquad (21.1.2a)$$

$$\mathbf{x}_1 = (\mathbf{a}_1^\dagger + \mathbf{a}_1)/\sqrt{2} \qquad \mathbf{p}_1 = i(\mathbf{a}_1^\dagger - \mathbf{a}_1)/\sqrt{2} \qquad (21.1.2b)$$

Then, the number-2 oscillator gets the same treatment.

$$\mathbf{a}_2 = (\mathbf{x}_2 + i \mathbf{p}_2)/\sqrt{2} \qquad \mathbf{a}_2^\dagger = (\mathbf{x}_2 - i \mathbf{p}_2)/\sqrt{2} \qquad (21.1.2c)$$

$$\mathbf{x}_2 = (\mathbf{a}_2^\dagger + \mathbf{a}_2)/\sqrt{2} \qquad \mathbf{p}_2 = i(\mathbf{a}_2^\dagger - \mathbf{a}_2)/\sqrt{2} \qquad (21.1.2d)$$

(2) Commutation relations: Bosons and Fermions

The next step involves a little thinking about what sort of commutation relations these operators should obey. It helps to think about what a 2-D oscillator model would model in the real world. Perhaps, the thing that comes to mind is a particle in a 2-D harmonic potential as was shown in Fig. 10.1.2. As

explained in Appendix 10.A-B, this is also a model for optical polarization described in $(x, y) = (x_1, x_2)$ space or a charged particle in a very cold magnetic or optical trap.

However, as shown by Fig. 10.1.1 a-b, a 2D oscillator is also a model for two 1D oscillators that may or may not be coupled to each other. In other words, a 2D oscillator could be a two-particle system with particle-1 and particle-2 each having a separate 1D coordinate x_1 , and x_2 , respectively.

Different dimensions for any system are orthogonal and independent. Either can be transformed without affecting the other. For this reason we will demand *inter-dimensional commutivity*.

$$[\mathbf{x}_1, \mathbf{p}_2] = \mathbf{0} = [\mathbf{x}_2, \mathbf{p}_1], \quad [\mathbf{a}_1, \mathbf{a}_2^\dagger] = \mathbf{0} = [\mathbf{a}_2, \mathbf{a}_1^\dagger] \quad (21.1.3)$$

All number-1 operators commute with all number-2 operators, but the operator commutation relations within the number-1 space or within the number-2 space remain the same as they were for a 1D-oscillator.

$$[\mathbf{a}_1, \mathbf{a}_1^\dagger] = \mathbf{1}, \quad [\mathbf{a}_2, \mathbf{a}_2^\dagger] = \mathbf{1} \quad (21.1.4)$$

The commutation relations are summarized for all N -dimensional oscillator problems as follows.

$$\begin{aligned} [\mathbf{a}_m, \mathbf{a}_n] &= \mathbf{a}_m \mathbf{a}_n - \mathbf{a}_n \mathbf{a}_m, & [\mathbf{a}_m, \mathbf{a}_n^\dagger] &= \mathbf{a}_m \mathbf{a}_n^\dagger - \mathbf{a}_n^\dagger \mathbf{a}_m, & [\mathbf{a}_m^\dagger, \mathbf{a}_n^\dagger] &= \mathbf{a}_m^\dagger \mathbf{a}_n^\dagger - \mathbf{a}_n^\dagger \mathbf{a}_m^\dagger, \\ &= \mathbf{0} & &= \delta_{mn} \mathbf{1} & &= \mathbf{0}. \end{aligned} \quad \begin{array}{l} (21.1.5a) \\ (21.1.5b) \\ (21.1.5c) \end{array}$$

These are the \mathbf{a} -operator equivalent of the orthonormality axiom-2 first given in Chapter 2.

Orthonormality and unit-scale relations (21.1.2) make it easy to find an \mathbf{a} -operator expression for the 2D Hamiltonian (21.1.1).

$$\begin{aligned} \mathbf{H} &= H_{11}(\mathbf{a}_1^\dagger \mathbf{a}_1 + \mathbf{1}/2) + H_{12} \mathbf{a}_1^\dagger \mathbf{a}_2 &= A(\mathbf{a}_1^\dagger \mathbf{a}_1 + \mathbf{1}/2) + (B - iC) \mathbf{a}_1^\dagger \mathbf{a}_2 \\ &+ H_{21} \mathbf{a}_2^\dagger \mathbf{a}_1 + H_{22}(\mathbf{a}_2^\dagger \mathbf{a}_2 + \mathbf{1}/2) &+ (B + iC) \mathbf{a}_2^\dagger \mathbf{a}_1 + D(\mathbf{a}_2^\dagger \mathbf{a}_2 + \mathbf{1}/2) \end{aligned} \quad (21.1.6)$$

This expression was written on two lines in order to emphasize that the 2D quantum oscillator operator \mathbf{H} has the form of the 2-state $ABCD$ Hamiltonian \mathbf{H} matrix (10.1.1b) used in Chapter 10.

$$\mathbf{H} = \begin{pmatrix} H_{11} & H_{12} \\ H_{21} & H_{22} \end{pmatrix} = \begin{pmatrix} A & B - iC \\ B + iC & D \end{pmatrix} \quad (21.1.6b)$$

The ket-bras $|m\rangle\langle n|$ used in the latter are replaced by symmetrized $\mathbf{a}_m^\dagger \mathbf{a}_n$ operators. Both serve as elementary "place-holder" operators for the Hamiltonian components H_{mn} or parameters A , $B \pm iC$, and D .

$$|m\rangle\langle n| \rightarrow (\mathbf{a}_m^\dagger \mathbf{a}_n + \mathbf{a}_n \mathbf{a}_m^\dagger) / 2 = \mathbf{a}_m^\dagger \mathbf{a}_n + \delta_{m,n} \mathbf{1}/2 \quad (21.1.7)$$

The commutivity embodied in (21.1.5) is commonly known as *Bose symmetry* after Bose who first described the permutational symmetry of photons. The $(\mathbf{a}_m, \mathbf{a}_n^\dagger)$ operators are called *Boson operators* and the quanta or "particles" they create and destroy are known as *Bosons*.

Each time \mathbf{a}_m^\dagger is used to raise quantum number of mode- m of an electromagnetic resonator (like the "Hall of Mirrors" cavity) it is equivalent to creating a new *photon*. If \mathbf{a}_m^\dagger is used to raise the quantum number of mode- m of a molecule we can say we're creating a new *vibron*. Just put the suffix "-on" onto whatever your favorite oscillator motion is called and you have a cute name for your favorite Boson.

There exists an opposite kind of particle, the *Fermion* named after Enrico Fermi who is credited with describing the permutational anti-symmetry of electrons and nucleons. The creation-destruction operators for Fermions are defined in quite the opposite way using *anti-commutators* $\{A,B\} = AB+BA$.

$$\begin{aligned} \{c_m, c_n\} &= c_m c_n + c_n c_m, & \{c_m, c_n^\dagger\} &= c_m c_n^\dagger + c_n^\dagger c_m, & \{c_m^\dagger, c_n^\dagger\} &= c_m^\dagger c_n^\dagger + c_n^\dagger c_m^\dagger, \\ &= \mathbf{0} & &= \delta_{mn} \mathbf{1} & &= \mathbf{0}. \end{aligned} \tag{21.1.8a} \tag{21.1.8b} \tag{21.1.8c}$$

The general two-dimensional Fermion Hamiltonian has ket-bras $|m\rangle\langle n|$ replaced by anti-symmetrized $c_m^\dagger c_n$ operators.

$$|m\rangle\langle n| \rightarrow (c_m^\dagger c_n - c_n^\dagger c_m) / 2 = c_m^\dagger c_n - \delta_{m,n} \mathbf{1} / 2 \tag{21.1.7}$$

Fermi operators have a rigid birth-control policy; they are allowed only one Fermion or else, none at all. Creating two Fermions of the same type is punished by death. This is because $x=-x$ implies $x=0$.

$$c_m^\dagger c_m^\dagger |0\rangle = -c_m^\dagger c_m^\dagger |0\rangle = \mathbf{0} \tag{21.1.8}$$

No two indistinguishable Fermions can occupy the same state. This is called the *Pauli exclusion principle*. Quantum numbers of $n=0$ and $n=1$ are the only allowed eigenvalues of the number operator.

$$c_m^\dagger c_m |0\rangle = \mathbf{0}, \quad c_m^\dagger c_m |1\rangle = |1\rangle, \quad c_m^\dagger c_m |n\rangle = \mathbf{0} \text{ for: } n>1 \tag{21.1.9}$$

(b) Two-dimensional (or 2-particle) base states

A state for a particle moving in two-dimensions (or two one-dimensional particles) is described using "*ket-kets*" $|n_1\rangle|n_2\rangle$ which are outer products of the kets for each single dimension. The dual description is done similarly using "*bra-bras*" $\langle n_2|\langle n_1| = (|n_1\rangle|n_2\rangle)^\dagger$ which are outer products of the bras. This applies to all types of states $|\Psi_1\rangle|\Psi_2\rangle$ whether they are eigenstates $|n_1\rangle|n_2\rangle$, position states $|x_1\rangle|x_2\rangle$ and $\langle x_2|\langle x_1|$, coherent states $|\alpha_1\rangle|\alpha_2\rangle$ and $\langle \alpha_2|\langle \alpha_1|$, or whatever.

The scalar product is defined so that the two kinds of particles or dimensions will somehow "find" each other and completely ignore the presence of the other kind(s).

$$\langle x_2|\langle x_1|\Psi_1\rangle|\Psi_2\rangle = \langle x_1|\Psi_1\rangle\langle x_2|\Psi_2\rangle \tag{21.1.10a}$$

This allows the probability axiom-1 to give the correct probability for, say, finding particle-1 at x_1 and particle-2 at x_2 , if state $|\Psi_1\rangle|\Psi_2\rangle$ is forced to choose between all x_1 and x_2 . Such a probability is a product

$$|\langle x_1, x_2|\Psi_1, \Psi_2\rangle|^2 = |\langle x_2|\langle x_1|\Psi_1\rangle|\Psi_2\rangle|^2 = |\langle x_1|\Psi_1\rangle|^2 |\langle x_2|\Psi_2\rangle|^2 \tag{21.1.10b}$$

of the individual probabilities $|\langle x_1|\Psi_1\rangle|^2$ and $|\langle x_2|\Psi_2\rangle|^2$ according to standard probability theory. The shorthand big-bra-big-ket notation $\langle x_1, x_2|\Psi_1, \Psi_2\rangle$ for two-dimensional amplitudes $\langle x_2|\langle x_1|\Psi_1\rangle|\Psi_2\rangle$ is commonly used. Note the 1-2 ordering for both the big-bras and big-kets in the shorthand notation.

To gain a better understanding of the bra-bra and ket-ket structure we will ask the perennial modern question: "How would these structures be stored in a computer program?" The usual answer is in product arrays of some kind. Here we will sketch these objects.

We begin with an elementary ket basis for each dimension or particle type-1 and type-2.

$$\begin{array}{ccc}
 \text{Type-1} & & \text{Type-2} & & \dots \\
 |0_1\rangle = \begin{pmatrix} 1 \\ 0 \\ 0 \\ \vdots \end{pmatrix}, |1_1\rangle = \begin{pmatrix} 0 \\ 1 \\ 0 \\ \vdots \end{pmatrix}, |2_1\rangle = \begin{pmatrix} 0 \\ 0 \\ 1 \\ \vdots \end{pmatrix}, \dots & & |0_2\rangle = \begin{pmatrix} 1 \\ 0 \\ 0 \\ \vdots \end{pmatrix}, |1_2\rangle = \begin{pmatrix} 0 \\ 1 \\ 0 \\ \vdots \end{pmatrix}, |2_2\rangle = \begin{pmatrix} 0 \\ 0 \\ 1 \\ \vdots \end{pmatrix}, \dots & & (21.1.11a)
 \end{array}$$

Then Cartesian or outer products are constructed for all states that might have non-zero amplitudes. And, therein lies a conflict between standard analysis and a finite computer. Each ket in (21.1.11) above is a column of ∞ -dimensional and we are about to construct an ∞^2 number of things each of dimension ∞^2 . A computer cannot handle a single ∞ -dimensional ket let alone their outer products.

This is why the finite analysis of Sec. 7.3 is advocated. Constructing sets of adjustable finite sized model systems for each dimension systematizes state counting. Convergence is achieved by orderly upgrades in the number of model "pendulums." Outer products shown below are finite arrays indexed by oscillator quantum labels 0, 1, 2,...(0-based indexing is the default mode in languages such as C++.)

$$|0_1\rangle|0_2\rangle = \begin{pmatrix} 1 \\ 0 \\ 0 \\ \vdots \\ \bar{0} \\ 0 \\ 0 \\ \vdots \\ \bar{0} \\ 0 \\ 0 \\ \vdots \end{pmatrix} = \begin{pmatrix} 1 \\ 0 \\ 0 \\ \vdots \end{pmatrix} \begin{pmatrix} 1 \\ 0 \\ 0 \\ \vdots \end{pmatrix}, |0_1\rangle|1_2\rangle = \begin{pmatrix} 1 \\ 0 \\ 0 \\ \vdots \end{pmatrix} \begin{pmatrix} 0 \\ 1 \\ 0 \\ \vdots \end{pmatrix} = \begin{pmatrix} 0 \\ 1 \\ 0 \\ 0 \\ \vdots \\ \bar{0} \\ 0 \\ 0 \\ \vdots \end{pmatrix}, \dots |1_1\rangle|0_2\rangle = \begin{pmatrix} 0 \\ 1 \\ 0 \\ \vdots \end{pmatrix} \begin{pmatrix} 1 \\ 0 \\ 0 \\ \vdots \end{pmatrix} = \begin{pmatrix} 0 \\ 0 \\ 1 \\ 0 \\ \vdots \\ \bar{0} \\ 0 \\ 0 \\ \vdots \end{pmatrix}, \dots |1_1\rangle|2_2\rangle = \begin{pmatrix} 0 \\ 1 \\ 0 \\ \vdots \end{pmatrix} \begin{pmatrix} 0 \\ 0 \\ 1 \\ \vdots \end{pmatrix} = \begin{pmatrix} 0 \\ 0 \\ 0 \\ 1 \\ \vdots \\ \bar{0} \\ 0 \\ 0 \\ \vdots \end{pmatrix}, (21.1.12a)$$

A 2-wave state product has a lexicographic (00, 01, 02, ...10, 11, 12,..., 20, 21, 22, ...) array indexing.

$$|\Psi_1\rangle|\Psi_2\rangle = \begin{pmatrix} \langle 0|\Psi_1\rangle \\ \langle 1|\Psi_1\rangle \\ \langle 2|\Psi_1\rangle \\ \vdots \end{pmatrix} \otimes \begin{pmatrix} \langle 0|\Psi_2\rangle \\ \langle 1|\Psi_2\rangle \\ \langle 2|\Psi_2\rangle \\ \vdots \end{pmatrix} = \begin{pmatrix} \langle 0|\Psi_1\rangle\langle 0|\Psi_2\rangle \\ \langle 0|\Psi_1\rangle\langle 1|\Psi_2\rangle \\ \langle 0|\Psi_1\rangle\langle 2|\Psi_2\rangle \\ \vdots \\ \langle 1|\Psi_1\rangle\langle 0|\Psi_2\rangle \\ \langle 1|\Psi_1\rangle\langle 1|\Psi_2\rangle \\ \langle 1|\Psi_1\rangle\langle 2|\Psi_2\rangle \\ \vdots \\ \langle 2|\Psi_1\rangle\langle 0|\Psi_2\rangle \\ \langle 2|\Psi_1\rangle\langle 1|\Psi_2\rangle \\ \langle 2|\Psi_1\rangle\langle 2|\Psi_2\rangle \\ \vdots \end{pmatrix} = \begin{pmatrix} \langle 0,0_2|\Psi_1\Psi_2\rangle \\ \langle 0,1_2|\Psi_1\Psi_2\rangle \\ \langle 0,2_2|\Psi_1\Psi_2\rangle \\ \vdots \\ \langle 1,0_2|\Psi_1\Psi_2\rangle \\ \langle 1,1_2|\Psi_1\Psi_2\rangle \\ \langle 1,2_2|\Psi_1\Psi_2\rangle \\ \vdots \\ \langle 2,0_2|\Psi_1\Psi_2\rangle \\ \langle 2,1_2|\Psi_1\Psi_2\rangle \\ \langle 2,2_2|\Psi_1\Psi_2\rangle \\ \vdots \end{pmatrix} \quad (21.1.12b)$$

The same indexing is used for the general 2-particle or 2-dimensional state $|\Psi\rangle$.

$$|\Psi\rangle = \begin{pmatrix} \langle 0_1 0_2 | \Psi \rangle \\ \langle 0_1 1_2 | \Psi \rangle \\ \langle 0_1 2_2 | \Psi \rangle \\ \vdots \\ \langle 1_1 0_2 | \Psi \rangle \\ \langle 1_1 1_2 | \Psi \rangle \\ \langle 1_1 2_2 | \Psi \rangle \\ \vdots \\ \langle 2_1 0_2 | \Psi \rangle \\ \langle 2_1 1_2 | \Psi \rangle \\ \langle 2_1 2_2 | \Psi \rangle \\ \vdots \end{pmatrix} = \begin{pmatrix} \Psi_{00} \\ \Psi_{01} \\ \Psi_{02} \\ \vdots \\ \Psi_{10} \\ \Psi_{11} \\ \Psi_{12} \\ \vdots \\ \Psi_{20} \\ \Psi_{21} \\ \Psi_{22} \\ \vdots \end{pmatrix} \tag{21.1.12c}$$

A word of caution: Do *NOT* assume that a general two-particle state $|\Psi\rangle$ can be written as a single outer product $|\Psi_1\rangle|\Psi_2\rangle$ (or even rarer, as $|\Psi_1\rangle|\Psi_1\rangle$) of two single-particle states $|\Psi_1\rangle$ and $|\Psi_2\rangle$. This would be as unusual as having a general matrix operator \mathbf{M} be a single nilpotent operator $|1\rangle\langle 2|$ or idempotent $|1\rangle\langle 1|$, both of which are singular, that is, have zero determinant. Rather, a general matrix \mathbf{M} is a full combination

$$\mathbf{M} = \sum_m \sum_n M_{m,n} |m\rangle\langle n|$$

of all possible ket-bra elementary operator products $|m\rangle\langle n|$. So, also, is a general state like (21.1.11) a combination of all possible ket-ket products $|x_1\rangle|x_2\rangle$ made from whichever basis is currently being used.

$$|\Psi\rangle = \sum_m \sum_n \Psi_{m,n} |m\rangle|n\rangle \tag{21.1.12d}$$

(c) Two-dimensional (or 2-particle) matrix operators

When a two-dimensional operator acts on a two-dimensional state, each dimension or particle type-1 or type-2 operator "finds" its corresponding type in the state and goes to work on it while ignoring the other type(s). For creation and destruction operations defined in (20.2.13b) the following happens.

$$\begin{aligned} \mathbf{a}_1^\dagger |n_1 n_2\rangle &= \mathbf{a}_1^\dagger |n_1\rangle |n_2\rangle = \sqrt{n_1+1} |n_1+1 n_2\rangle & , & & \mathbf{a}_2^\dagger |n_1 n_2\rangle &= |n_1\rangle \mathbf{a}_2^\dagger |n_2\rangle = \sqrt{n_2+1} |n_1 n_2+1\rangle \\ \mathbf{a}_1 |n_1 n_2\rangle &= \mathbf{a}_1 |n_1\rangle |n_2\rangle = \sqrt{n_1} |n_1-1 n_2\rangle & , & & \mathbf{a}_2 |n_1 n_2\rangle &= |n_1\rangle \mathbf{a}_2 |n_2\rangle = \sqrt{n_2} |n_1 n_2-1\rangle \end{aligned} \tag{21.1.13a} \tag{21.1.13b}$$

This is consistent with the following general definition of the 2D oscillator base state.

$$|n_1 n_2\rangle = \frac{(\mathbf{a}_1^\dagger)^{n_1} (\mathbf{a}_2^\dagger)^{n_2}}{\sqrt{n_1! n_2!}} |0 0\rangle \tag{21.1.14}$$

The $\mathbf{a}_m^\dagger \mathbf{a}_n$ combinations in the *ABCD* Hamiltonian \mathbf{H} in (21.1.6) have fairly simple matrix elements.

$$\begin{aligned} \mathbf{a}_1^\dagger \mathbf{a}_1 |n_1 n_2\rangle &= n_1 |n_1 n_2\rangle & , & & \mathbf{a}_1^\dagger \mathbf{a}_2 |n_1 n_2\rangle &= \sqrt{n_1+1} \sqrt{n_2} |n_1+1 n_2-1\rangle \\ \mathbf{a}_2^\dagger \mathbf{a}_1 |n_1 n_2\rangle &= \sqrt{n_1} \sqrt{n_2+1} |n_1-1 n_2+1\rangle & , & & \mathbf{a}_2^\dagger \mathbf{a}_2 |n_1 n_2\rangle &= n_2 |n_1 n_2\rangle \end{aligned} \tag{21.1.15a}$$

Part of the matrix representation of \mathbf{H} in creation basis (21.1.14) is shown below.

$$\langle \mathbf{H} \rangle = A(\mathbf{1}/2) + D(\mathbf{1}/2) +$$

	$ 00\rangle$	$ 01\rangle$	$ 02\rangle$...	$ 10\rangle$	$ 11\rangle$	$ 12\rangle$...	$ 20\rangle$	$ 21\rangle$	$ 22\rangle$...
$\langle 00 $	0		
$\langle 01 $		D		...	$B+iC$
$\langle 02 $			$2D$...		$\sqrt{2}(B+iC)$
\vdots	\vdots	\vdots	\vdots	\ddots	\vdots	\vdots	\vdots	\ddots				...
$\langle 10 $.	$B-iC$...	A		
$\langle 11 $.	$\sqrt{2}(B-iC)$...		$A+D$...	$\sqrt{2}(B+iC)$
$\langle 12 $					$A+2D$...		$\sqrt{4}(B+iC)$
\vdots	\vdots	\vdots	\vdots	\ddots	\vdots	\vdots	\vdots	\ddots	\vdots	\vdots	\vdots	\ddots
$\langle 20 $.	$\sqrt{2}(B-iC)$...	$2A$...
$\langle 21 $.	$\sqrt{4}(B-iC)$...		$2A+D$...
$\langle 22 $									$2A+2D$...
\vdots	\vdots	\vdots	\vdots	\ddots	\vdots	\vdots	\vdots	\ddots	\vdots	\vdots	\vdots	\ddots

(21.1.15b)

The eigenstates and eigenvalues for this monster matrix will solve the general quantum 2D harmonic oscillator problem. A little rearrangement of rows and columns brings the matrix to a block-diagonal form in which base states $|n_1\rangle|n_2\rangle$ with the same *total quantum number* $v = n_1 + n_2$ are adjacent.

$$\langle \mathbf{H} \rangle = A(\mathbf{1}/2) + D(\mathbf{1}/2) +$$

	$ 00\rangle$	$ 01\rangle$	$ 10\rangle$	$ 02\rangle$	$ 11\rangle$	$ 20\rangle$	$ 03\rangle$	$ 12\rangle$	$ 21\rangle$	$ 30\rangle$...
$\langle 00 $	0										
$\langle 01 $		D	$B+iC$								
$\langle 10 $		$B-iC$	A								
$\langle 02 $				$2D$	$\sqrt{2}(B+iC)$						
$\langle 11 $				$\sqrt{2}(B-iC)$	$A+D$	$\sqrt{2}(B+iC)$					
$\langle 20 $				$\sqrt{2}(B-iC)$		$2A$					
$\langle 03 $							$3D$	$\sqrt{3}(B+iC)$			
$\langle 12 $							$\sqrt{3}(B-iC)$	$A+2D$	$\sqrt{4}(B+iC)$		
$\langle 21 $							$\sqrt{4}(B-iC)$	$2A+D$	$\sqrt{3}(B+iC)$		
$\langle 30 $								$\sqrt{3}(B-iC)$	$3A$		
\vdots	\vdots	\vdots	\vdots	\vdots	\vdots	\vdots	\vdots	\vdots	\vdots	\vdots	\vdots

(21.1.15c)

Note the 2-by-2 sub-space $|n_1 n_2\rangle = \{|01\rangle, |10\rangle\}$ with total quantum number $v=1$. It supports a matrix that is identical to the original 2-by-2 Hamiltonian (21.1.6b). (Except, it is up side down and has the zero-point unit matrix added.) A sub-space with unit total quantum number is called the *fundamental* ($v=1$) vibrational sub-space. Similarity of classical and ($v=1$) quantum matrices means the fundamental quantum eigenvectors are the same as the classical A , B , AB or C normal mode vectors discussed in Sec. 10.2(a, b, c) and Sec. 10.3(a-b). This leads to analytical solutions to all quantum matrices (21.1.15c).

(d) 2D-Oscillator eigensolutions

The analogy between classical 2D-oscillators and a 2-state quantum systems was developed in Sec. 10.5 and solved by special unitary ($SU(2)$) or rotation ($R(3)$) group algebra in Appendices 10.A-B. These solutions lead to solutions for the quantum 2D-oscillator Hamiltonian given above in (21.1.15c-d).

(1) Fundamental eigenstates

The first step is to diagonalize the fundamental 2-by-2 matrix given in (21.1.15c-d).

$$\langle \mathbf{H} \rangle_{\nu=1}^{Fundamental} = \begin{array}{c|cc} n_1, n_2 & |1,0\rangle & |0,1\rangle \\ \hline \langle 1,0| & A & B-iC \\ \langle 0,1| & B+iC & D \end{array} + \frac{A+D}{2} \mathbf{1} \quad (21.1.16)$$

Here we have turned the matrix right-side-up so it matches the Hamiltonian solved in (10.5.10). (A choice of "Little-Endian" indexing (... 10, 01, ...20, 11, 21...) instead of "Big-Endian" indexing (...01, 10, ...02, 1...) reorders the states to match.) The eigensolution (10.5.10) uses the Hamilton decomposition coefficients to define a rotation-crank angular rate vector Ω

$$\Omega = (\Omega_X, \Omega_Y, \Omega_Z) = (2B, 2C, A-D) = (\Omega_B, \Omega_C, \Omega_A), \quad (21.1.17)$$

and the average overall phase rate (including zero-point term $(A+D)/2$) is

$$\Omega_0 = A+D. \quad (21.1.18)$$

This gives \mathbf{H} as follows

$$\begin{pmatrix} A & B-iC \\ B+iC & D \end{pmatrix} + \frac{A+D}{2} \mathbf{1} = (A+D) \begin{pmatrix} 1 & 0 \\ 0 & 1 \end{pmatrix} + 2B \begin{pmatrix} 0 & 1 \\ 1 & 0 \end{pmatrix} \frac{1}{2} + 2C \begin{pmatrix} 0 & -i \\ i & 0 \end{pmatrix} \frac{1}{2} + (A-D) \begin{pmatrix} 1 & 0 \\ 0 & -1 \end{pmatrix} \frac{1}{2}$$

in terms of Jordan-Pauli spin operators. (21.1.19)

$$\begin{aligned} \mathbf{H} &= \Omega_0 \mathbf{1} + \Omega \cdot \vec{\mathbf{S}} = \Omega_0 \mathbf{1} + \Omega_B \mathbf{S}_B + \Omega_C \mathbf{S}_C + \Omega_A \mathbf{S}_A \quad (ABC \text{ Optical vector notation}) \\ &= \Omega_0 \mathbf{1} + \Omega_X \mathbf{S}_X + \Omega_Y \mathbf{S}_Y + \Omega_Z \mathbf{S}_Z \quad (XYZ \text{ Electron spin notation}) \end{aligned}$$

The frequency eigenvalues ω_{\pm} of $\mathbf{H} - \Omega_0 \mathbf{1}/2$ and *fundamental transition frequency* $\Omega = \omega_+ - \omega_-$ are

$$\begin{aligned} \omega_{\pm} &= \frac{\Omega_0 \pm \Omega}{2} = \frac{A+D \pm \sqrt{(2B)^2 + (2C)^2 + (A-D)^2}}{2} \\ &= \frac{A+D}{2} \pm \sqrt{\left(\frac{A-D}{2}\right)^2 + B^2 + C^2} \end{aligned} \quad (21.1.20a)$$

Ω "points out" eigenvectors whose spin vectors \mathbf{S} align or anti-align with the Ω -vector of \mathbf{H} . The polar angles of the \mathbf{S} -vector are Euler angles (α, β) in Fig. 10.5.8. Equating (α, β) in an Euler state (10.A.1a) to polar angles (φ, ϑ) of the $+\Omega$ -vector (or polar angles $(\varphi, \vartheta \pm \pi)$ of the $-\Omega$ -vector) gives \mathbf{H} eigenvectors.

$$|\omega_+\rangle = \begin{pmatrix} e^{-i\varphi/2} \cos \frac{\vartheta}{2} \\ e^{i\varphi/2} \sin \frac{\vartheta}{2} \end{pmatrix}, \quad |\omega_-\rangle = \begin{pmatrix} -e^{-i\varphi/2} \sin \frac{\vartheta}{2} \\ e^{i\varphi/2} \cos \frac{\vartheta}{2} \end{pmatrix} \quad \text{where: } \begin{cases} \cos \vartheta = \frac{A-D}{\Omega} \\ \tan \varphi = \frac{C}{B} \end{cases} \quad (21.1.20b)$$

The ket eigenvectors are being expressed in terms of $\{|10\rangle, |01\rangle\}$ bases.

$$|\omega_+\rangle = e^{-i\varphi/2} \left(\cos \frac{\vartheta}{2} |10\rangle + e^{i\varphi} \sin \frac{\vartheta}{2} |01\rangle \right), \quad |\omega_-\rangle = e^{-i\varphi/2} \left(-\sin \frac{\vartheta}{2} |10\rangle + e^{i\varphi} \cos \frac{\vartheta}{2} |01\rangle \right) \quad (21.1.20c)$$

More important for the general solution, are the *eigen-creation operators* \mathbf{a}_+^\dagger and \mathbf{a}_-^\dagger defined by

$$\mathbf{a}_+^\dagger = e^{-i\varphi/2} \left(\cos \frac{\vartheta}{2} \mathbf{a}_1^\dagger + e^{i\varphi} \sin \frac{\vartheta}{2} \mathbf{a}_2^\dagger \right), \quad \mathbf{a}_-^\dagger = e^{-i\varphi/2} \left(-\sin \frac{\vartheta}{2} \mathbf{a}_1^\dagger + e^{i\varphi} \cos \frac{\vartheta}{2} \mathbf{a}_2^\dagger \right) \quad (21.1.20d)$$

The \mathbf{a}_\pm^\dagger create \mathbf{H} eigenstates (21.1.20c) directly from the ground state.

$$\mathbf{a}_+^\dagger |0\rangle = |\omega_+\rangle, \quad \mathbf{a}_-^\dagger |0\rangle = |\omega_-\rangle \quad (21.1.20e)$$

In terms of the eigen- \mathbf{a}_\pm^\dagger operators, the Hamiltonian has zero off-diagonal components ($B=0=C$) and is reduced to (at worst) an A -type (Asymmetric Diagonal) or C_2^A -symmetric operator described in Sec. 10.2(a). But, if the eigenvalues are degenerate ($\omega_+ = \omega_-$) then \mathbf{H} is a fully $SU(2)$ symmetric unit 2-by-2 Hamiltonian like the case where ($B=0=C$) and ($A=D$).

Setting ($B=0=C$) and ($A=\omega_+$) and ($D=\omega_-$) in (21.1.15c) gives diagonal block matrices.

$$\langle \mathbf{H} \rangle = A(\mathbf{1}/2) + D(\mathbf{1}/2) +$$

	$ 00\rangle$	$ 01\rangle$	$ 10\rangle$	$ 02\rangle$	$ 11\rangle$	$ 20\rangle$	$ 03\rangle$	$ 12\rangle$	$ 21\rangle$	$ 30\rangle$...
$\langle 00 $	0										
$\langle 01 $		ω_-									
$\langle 10 $			ω_+								
$\langle 02 $				$2\omega_-$							
$\langle 11 $					$\omega_+ + \omega_-$						
$\langle 20 $						$2\omega_+$					
$\langle 03 $							$3\omega_-$				
$\langle 12 $								$\omega_+ + 2\omega_-$			
$\langle 21 $									$2\omega_+ + \omega_-$		
$\langle 30 $										$3\omega_+$	
\vdots											

(21.1.21)

The eigenvalue splitting pattern shown in Fig. 21.1.1 is a function of the fundamental splitting frequency.

$$\omega_+ - \omega_- = \Omega = \sqrt{(2B)^2 + (2C)^2 + (A - D)^2} = A - D \quad (21.1.22)$$

For $SU(2)$ symmetry ($\Omega=0$) the spectrum reduces to perfect harmonically spaced levels of eigen-frequency $\omega = \nu + I$ and degeneracy $\nu + I = 1, 2, 3, 4, \dots$ for each total quantum number $\nu = 0, 1, 2, 3, \dots$, respectively. As will be shown later, this is precisely analogous to the spin angular momentum quantum *multiplet* levels of total angular momentum quantum numbers $j = 0, 1/2, 1, 3/2, \dots$. In fact, each degenerate level corresponds to a different irep of $SU(2)$ and the integral $j = 0, 1, 2, \dots$ correspond to ireps of the related rotation group $R(3)$ in three dimensions. What we have here is a very powerful way to understand and derive the quantum theory of angular momentum.

As the splitting frequency increases each multiplet splits entirely since the symmetry is reduced to a commutative $C_2^{A,B,orC}$ subgroup of $SU(2)$ that does not require degeneracy. Every level differs from the nearest neighbor in its multiplet by the same transition frequency Ω . So no matter what the value of the

parameters $\{A, B, C, D\}$, this model maintains its harmonic spectrum to some extent. However, at rational values of the ratio Ω/ω , there will occur a varying number of degeneracies between levels split off from different multiplets and some interesting effects in the classical and quantum dynamics.

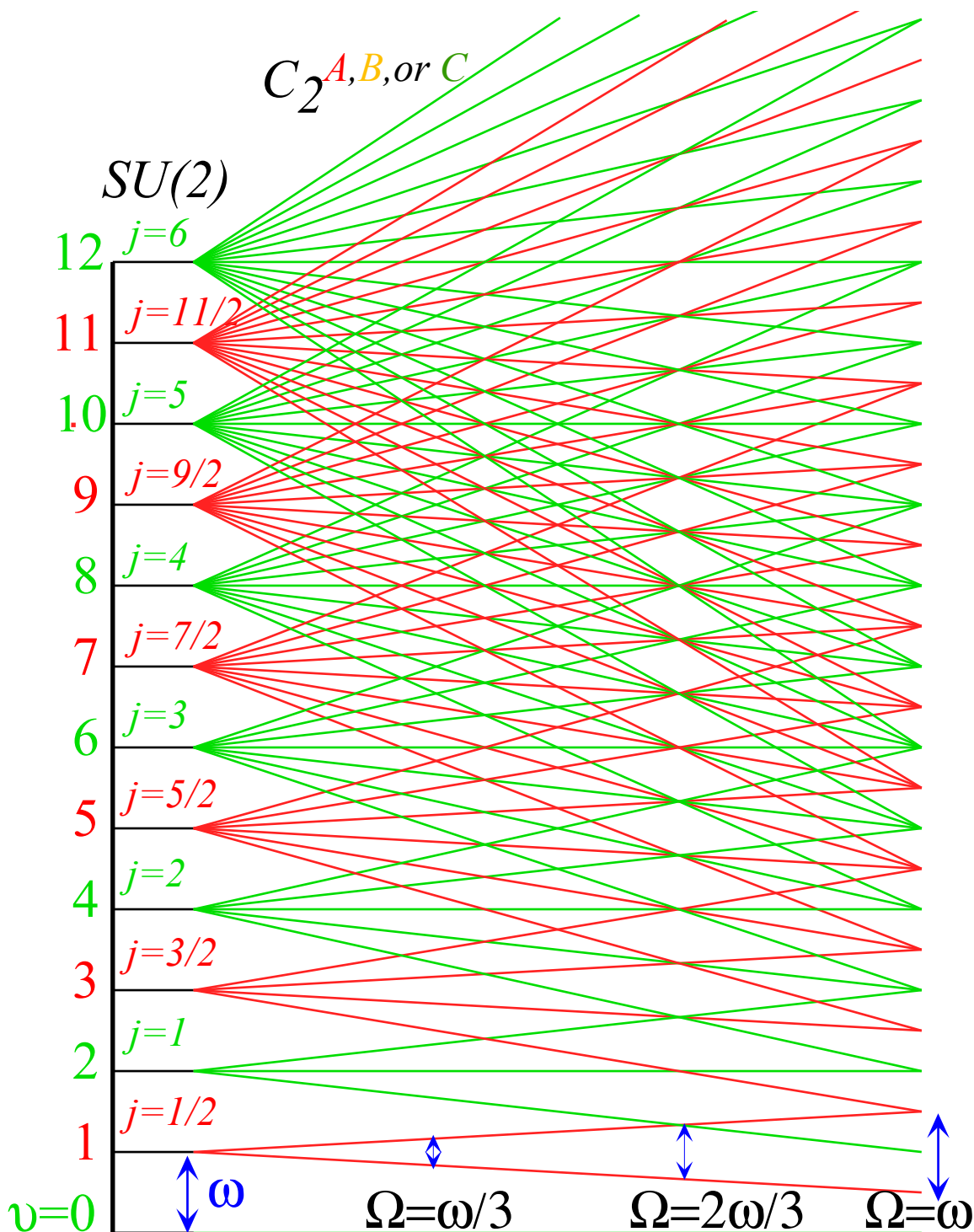


Fig. 21.1.1 Two-Dimensional harmonic oscillator levels with $SU(2)$ degeneracy and C_2 splitting.

(2) $U(2) \supset C_2^A$ eigenstates and wavefunctions

The simplest examples of 2D oscillator eigensolutions are found for the type- A or *Asymmetric Diagonal* Hamiltonian \mathbf{H} in (21.1.1) for which only the parameters A and D are non-zero. ($B=0=C$)

$$\mathbf{H}^A = \frac{A}{2}(\mathbf{p}_1^2 + \mathbf{x}_1^2) + \frac{D}{2}(\mathbf{p}_2^2 + \mathbf{x}_2^2) \quad (21.1.23)$$

In terms of \mathbf{a} -operators, \mathbf{H} in (21.1.6) reduces to sums of number operators $\mathbf{a}_m^\dagger \mathbf{a}_m$ or unit operator $\mathbf{1}$.

$$\mathbf{H}^A = A(\mathbf{a}_1^\dagger \mathbf{a}_1 + \mathbf{1}/2) + D(\mathbf{a}_2^\dagger \mathbf{a}_2 + \mathbf{1}/2) \quad (21.1.24)$$

Then the \mathbf{H} matrix (21.1.15) is diagonal, and the eigenvalues are simple combinations of quanta n_1 and n_2 .

$$\begin{aligned} \varepsilon_{n_1 n_2}^A &= A\left(n_1 + \frac{1}{2}\right) + D\left(n_2 + \frac{1}{2}\right) = \frac{A+D}{2}(n_1 + n_2 + 1) + \frac{A-D}{2}(n_1 - n_2) \\ &= \Omega_0(n_1 + n_2 + 1) + \frac{\Omega}{2}(n_1 - n_2) = \Omega_0(v+1) + \Omega m \end{aligned} \quad (21.1.25a)$$

Here *total quantum number* v and half-difference or *asymmetry quantum number* m

$$v = n_1 + n_2 \quad , \quad m = \frac{n_1 - n_2}{2} \quad (21.1.25b)$$

multiply the *fundamental frequency* $\Omega_0 = \omega$ and *splitting 1/2-beat frequency* Ω as seen in Fig. 21.1.2.

$$\omega = \Omega_0 = \frac{A+D}{2} \quad , \quad \Omega = \frac{A-D}{2} \quad (21.1.25c)$$

The eigenstates for the asymmetric-diagonal \mathbf{H}^A Hamiltonian are just the base states from (21.1.14).

$$|n_1 n_2\rangle = \frac{(\mathbf{a}_1^\dagger)^{n_1} (\mathbf{a}_2^\dagger)^{n_2}}{\sqrt{n_1! n_2!}} |0 0\rangle \quad (21.1.26)$$

The eigenstates belong to the symmetry C_2^A first discussed in Sec. 10.2(a) and listed near the left hand side of Fig. 10.4.2. The two x_1 and x_2 fundamental normal mode classical vibrations associated with this symmetry are shown in Fig. 10.2.1. If these two motions have the same frequency ($A=D$) then the symmetry is much higher, indeed. The ($A=D$)-case has the full $U(2)$ symmetry that a 2D oscillator can have as indicated on the extreme left hand side of Fig. 10.4.2. The $U(2)$ -symmetric Hamiltonian

$$\mathbf{H}^{U(2)} = E(\mathbf{a}_1^\dagger \mathbf{a}_1 + \mathbf{a}_2^\dagger \mathbf{a}_2 + \mathbf{1}) \quad \text{where: } A = E = D \quad (21.1.27a)$$

has the same eigenvalues as a 1D harmonic oscillator with the zero-point increased from 1/2 to 1.

$$\varepsilon_{n_1 n_2}^{U(2)} = \Omega_0(n_1 + n_2 + 1) = \omega(v+1) \quad (u = 0, 1, 2, 3, \dots) \quad (21.1.27b)$$

However, the degeneracy of the v -th level is equal to the total quantum number v as was shown in Fig. 21.1.2 on the extreme left hand side where the splitting frequency Ω is zero.

The redux of the 1D spectrum in a C_2^A -symmetric two-dimensional system is not surprising if you consider the two-pendulum analogy in Fig. 10.1.1 with equal pendulums or in Fig. 10.2.3 with the coupling spring removed. The result is two independent pendulums. The only effect of having two of them is that the energy level degeneracy and zero-point goes up, but they're just 1D levels.

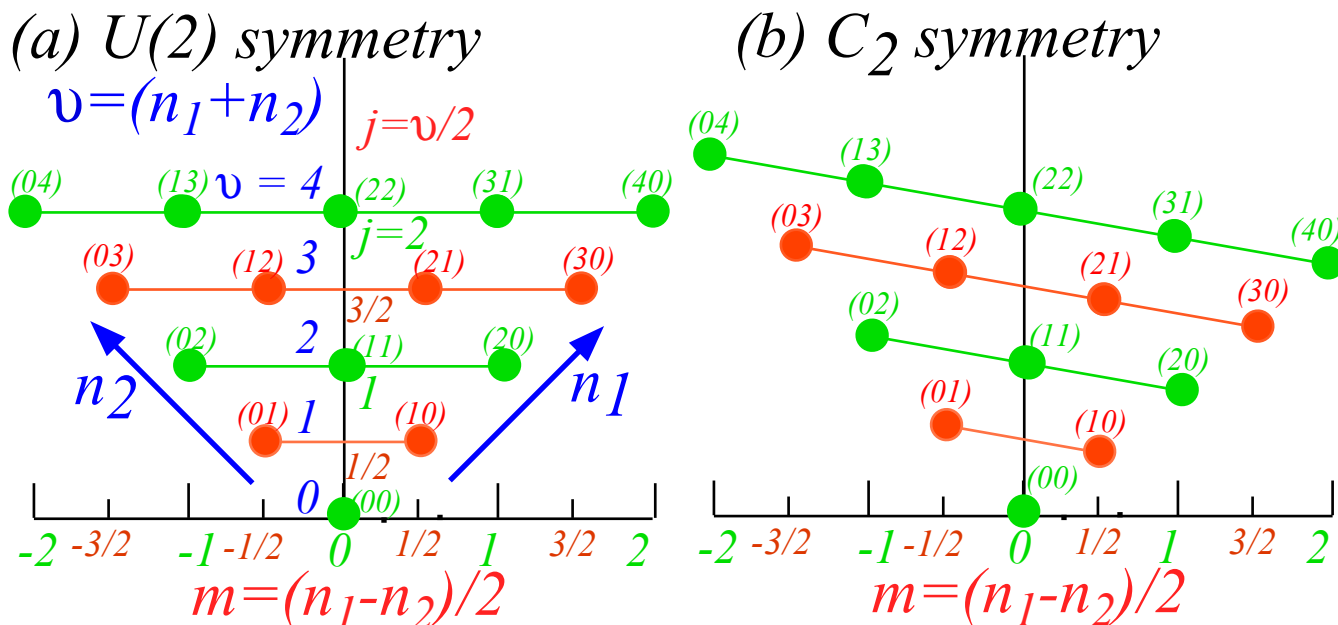


Fig. 21.1.2 Two-Dimensional harmonic oscillator quanta with (a)U(2) degeneracy and (b) C₂ splitting.

A sketch of the energy-quantum-number relation (21.1.27) is shown in Fig. 21.1.2. With U(2) symmetry ($\Omega=0$), the degenerate energy values lie along a horizontal line. The states $|n_1, n_2\rangle$ with larger n_1 appear proportionally farther to the right while those with larger n_2 sit to the left. As Ω becomes non-zero the lines tip in proportion to Ω and the reduction of U(2) to a C₂ symmetry shows up in the splitting of the degenerate levels. The splitting seen in Fig. 21.1.1 is a vertical projection of the tipped points in Fig. 21.1.2 with the n_1 vibrations assumed to be slower ($A < D$) so they lose frequency in proportion to n_1 while the faster n_2 states gain in proportion to their quantum n_2 -values.

(3) U(2) \supset C₂^A oscillator wavefunctions

A two-dimensional oscillator eigenfunction is a simple product of two one-dimensional functions.

$$\langle x_1 x_2 | n_1 n_2 \rangle = \langle x_1 | n_1 \rangle \langle x_2 | n_2 \rangle$$

For example, the ground state eigenfunction $\langle x_1 x_2 | 00 \rangle$ follows from (20.2.7c) with scale $M\omega/\hbar=1$.

$$\psi_{00}(x_1, x_2) = \langle x_1 | 0 \rangle \langle x_2 | 0 \rangle = \frac{e^{-x_1^2/2}}{(\pi)^{1/4}} \frac{e^{-x_2^2/2}}{(\pi)^{1/4}} = \frac{e^{-(x_1^2+x_2^2)/2}}{(\pi)^{1/2}} \tag{21.1.28}$$

This ($v=0$) Gaussian is plotted in Fig. 21.1.3, and the ($v=1$) excited state wave doublet in Fig. 21.1.3.

$$\psi_{10}(x_1, x_2) = \frac{\sqrt{2}x_1 e^{-(x_1^2+x_2^2)/2}}{(\pi)^{1/2}}, \quad \psi_{01}(x_1, x_2) = \frac{\sqrt{2}x_2 e^{-(x_1^2+x_2^2)/2}}{(\pi)^{1/2}} \tag{21.1.29}$$

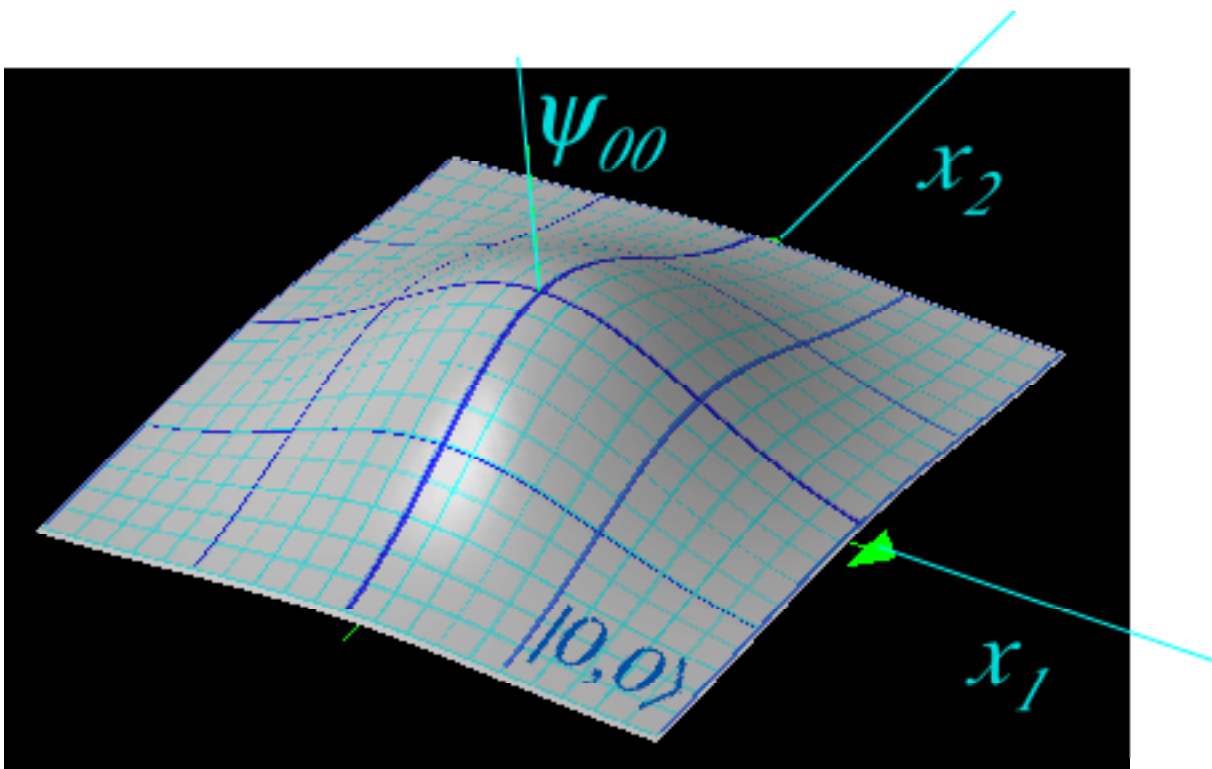


Fig. 21.1.3 2-D harmonic oscillator ground state wave function $\Psi_{00}(x_1, x_2)$

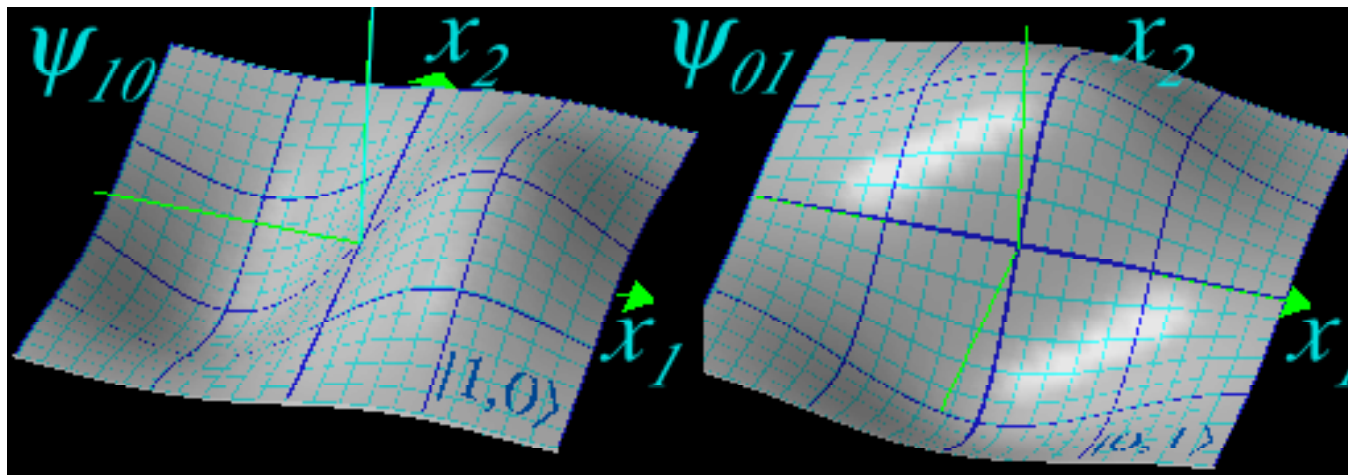


Fig. 21.1.4 2-D harmonic oscillator first excited state wave functions: $\Psi_{10}(x_1, x_2)$ and $\Psi_{01}(x_1, x_2)$.

The two components of the doublet are related by a 90° rotation in the (x_1, x_2) -plane. Here, we are looking at the real part of waves that each have their usual complex time factor $e^{-i\varepsilon_n t/\hbar}$ which in this case is a different frequency $\omega_{n_1, n_2} = \varepsilon_{n_1, n_2}/\hbar$ given by (21.1.25a) for each, in general. So these pictures represent snapshots of standing waves that oscillate up and down just like their 1D ancestors in Fig. 20.2.1.

However, their probability distributions shown below in Fig. 21.1.5 are motionless as must be any distribution for a pure-energy eigenstate. The squared wavefunctions are greater than zero everywhere and falls off more rapidly for large x .

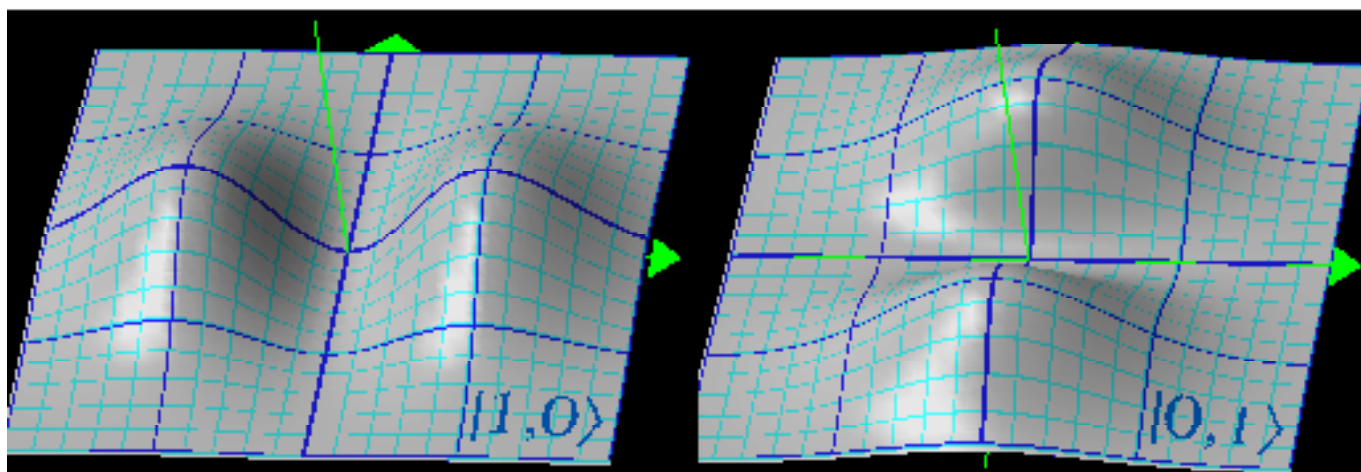
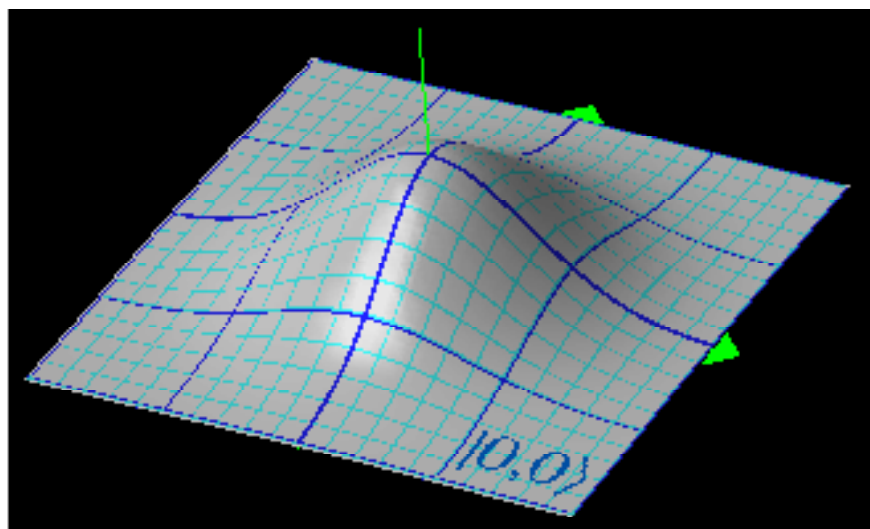


Fig. 21.1.5 2-D oscillator probability distributions: $|\Psi_{00}(x_1,x_2)|^2$, $|\Psi_{10}(x_1,x_2)|^2$, and $|\Psi_{01}(x_1,x_2)|^2$.

Combination wave functions, on the other hand, have moving probability distributions if their component states have different eigenfrequencies. Consider for example, the 50-50 combination of the first two excited states $|10\rangle$ and $|01\rangle$ whose probability distributions are shown for three different times in Fig. 21.1.6. The result is the quantum version of the classical beats shown in Fig. 10.2.2 for uncoupled oscillators and in Fig. 10.2.5 and Fig. 10.2.6 for coupled bilaterally symmetric oscillators.

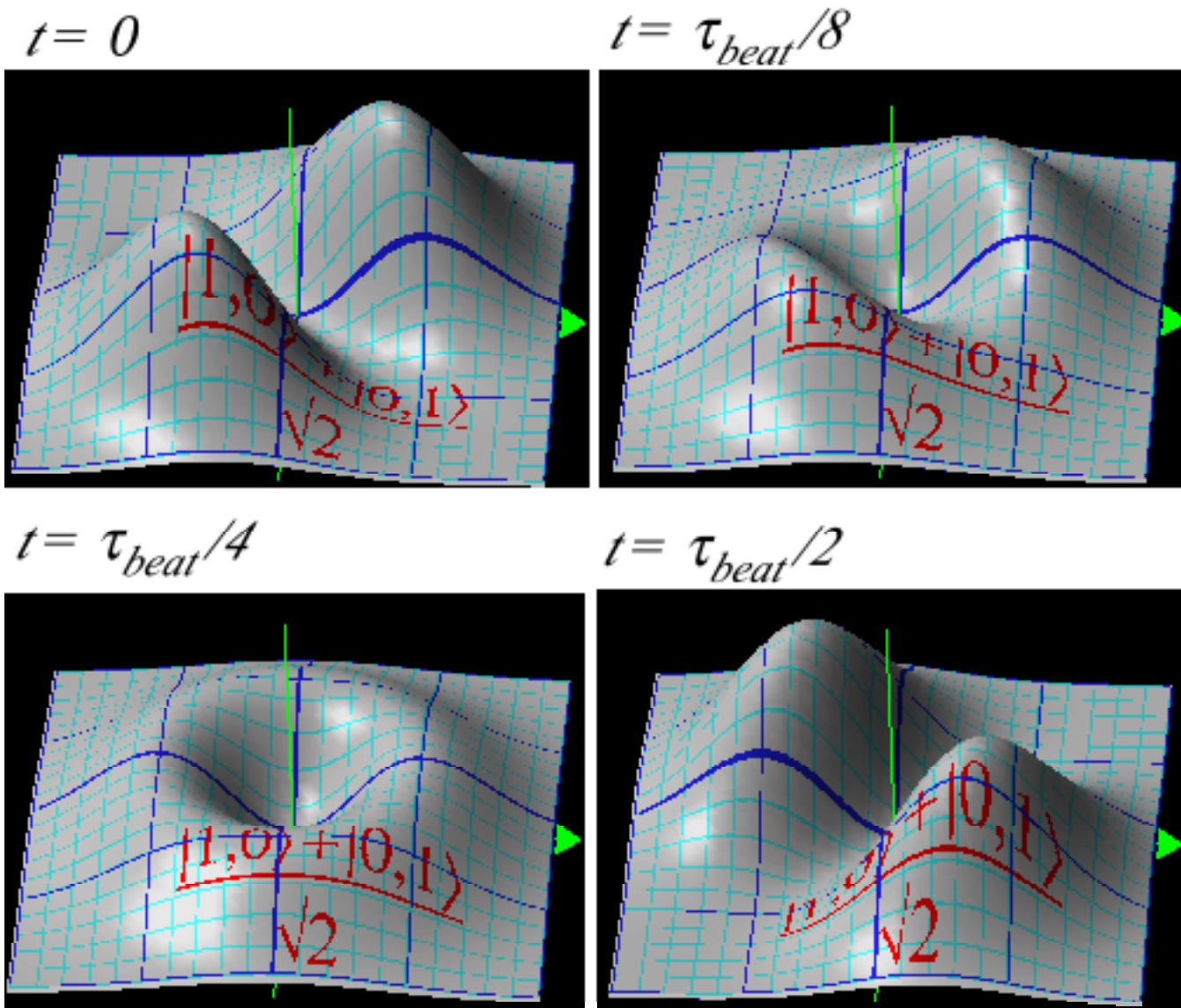


Fig. 21.1.6 2-D oscillator probability distributions: $| e^{-i\omega_{10} t/\hbar} \Psi_{10}(x_1, x_2) + e^{-i\omega_{01} t/\hbar} \Psi_{01}(x_1, x_2) |^2$.

The time-dependent wavefunction plotted in Fig. 21.1.6 oscillates with beat period $\tau_{beat} = 2\pi/(\omega_{10} - \omega_{01})$.

$$\begin{aligned} \Psi(x_1, x_2, t) &= \frac{1}{2} \left| \psi_{10}(x_1, x_2) e^{-i\omega_{10}t} + \psi_{01}(x_1, x_2) e^{-i\omega_{01}t} \right|^2 e^{-(x_1^2 + x_2^2)} = \frac{e^{-(x_1^2 + x_2^2)}}{2\pi} \left| \sqrt{2} x_1 e^{-i\omega_{10}t} + \sqrt{2} x_1 e^{-i\omega_{01}t} \right|^2 \\ &= \frac{e^{-(x_1^2 + x_2^2)}}{\pi} (x_1^2 + x_2^2 + 2x_1 x_2 \cos(\omega_{10} - \omega_{01})t) = \frac{e^{-(x_1^2 + x_2^2)}}{\pi} \begin{cases} |x_1 + x_2|^2 & \text{for: } t=0 \\ x_1^2 + x_2^2 & \text{for: } t=\tau_{beat}/4 \\ |x_1 - x_2|^2 & \text{for: } t=\tau_{beat}/2 \end{cases} \quad (21.1.30) \end{aligned}$$

At one quarter of beat period ($\tau_{beat}/4$) a circular distribution appears. It is equivalent to the 1/4-wave circular polarization motion shown in the classical model by Fig. 10.2.6(a). The pictures above will apply exactly to a *B*-type oscillator if they are all rotated by 45° in the (x_1, x_2) -plane.

21.2 2D Oscillator Symmetry, Spin, and Wavefunctions

For a given cranking frequency Ω , the eigenvalues shown in Fig. 21.1.1 are the same no matter what values we choose for the parameters $\{A, B, C, D\}$. However, the eigenvectors or states depend acutely on parameter values as do the underlying symmetries and physics.

The Abelian symmetry analysis in Chapter 8-9 uses C_6 symmetry to dictate a fixed set of eigenvectors, but their eigenvalues depend on the values of six **H**-parameters. However, for non-Abelian D_3 or D_6 symmetry analysis in Chapter 15, both eigenvalues and eigenvectors may vary with the **H**-parameters and the eigenstates may have a range of different local symmetry subgroups and correspondingly different physics. Different choices for local symmetry subgroups or *Maximal Sets of Commuting Observables (MSOCO)* such as in Fig. 15.2.1, gives different types of symmetry states and wave dynamics. So it is with $U(2)$ symmetry that is an infinite non-Abelian group. Its subgroups correspond to a range of different eigensolutions.

For the $U(2)$ model, all parameters $\{A, B, C, D\}$ have basically the same eigenvalues for a given Ω as shown in Fig. 21.1.1, but the eigenvectors or eigenstates will vary according to which $U(2)$ subgroups C_2^A (*Asymmetric diagonal*), C_2^B (*Bilateral*), C_2^{AB} (*Mixed AB*), C_2^C (*Circular*), or C_1^{ABCD} (*Elliptical*) listed in the $U(2)$ catalog of Fig. 10.4.2 are the Abelian sub-group symmetries of the **H**-Hamiltonian. The classical two-dimensional-oscillator and analogous quantum two-state eigenstates for these symmetries are compared in Sections 10.2(a), 10.2(b), 10.3(a-b), 10.2(c), and 10.4(a-b), respectively. Now we compare the corresponding quantum two-dimensional-oscillators having these symmetries. Of these, C_2^C (*Circular*) is most useful for understanding quantum angular momentum.

(a) Angular momentum eigenstates: C_2^C symmetry

Consider having the C -parameter be non-zero. ($A=D, B=0, C \neq 0$.) According to Sec. 2.9(c) this corresponds to physics with " C -ness", that is, chirality, circular polarization, current states, Coriolis splitting, cyclotron resonance, and anything resembling moving waves with definite right or left-handed momenta. From (21.1.1) with $A=D, B=0, C \neq 0$, we have

$$\mathbf{H}^C = \frac{A}{2}(\mathbf{p}_1^2 + \mathbf{x}_1^2 + \mathbf{p}_2^2 + \mathbf{x}_2^2) + C(\mathbf{x}_1\mathbf{p}_2 - \mathbf{x}_2\mathbf{p}_1) \quad (21.2.1a)$$

Note that \mathbf{H}^C contains a term that is C -times the two-dimensional *angular momentum operator* \mathbf{l}_3 .

$$\mathbf{l}_3 = \mathbf{x}_1\mathbf{p}_2 - \mathbf{x}_2\mathbf{p}_1 \quad (21.2.1b)$$

A pure- C Hamiltonian \mathbf{H}^C with $A=D$ belongs to C_2^C subgroup of $SU(2)$ and conserves *angular momentum* \mathbf{l}_3 which becomes a key observable and quantum label. In terms of **a**-operators, \mathbf{H}^C is.

$$\mathbf{H}^C = A(\mathbf{a}_1^\dagger\mathbf{a}_1 + \mathbf{a}_2^\dagger\mathbf{a}_2 + \mathbf{1}) + iC(\mathbf{a}_2^\dagger\mathbf{a}_1 - \mathbf{a}_1^\dagger\mathbf{a}_2) \quad (21.2.2)$$

From (21.1.22) it appears that the eigenvalues will be the same as (21.1.25) but with $\Omega = 2C$. This will be shown below when the eigenstates are derived. The fundamental representation (21.1.16) of \mathbf{H}^C is

$$\langle \mathbf{H}^C \rangle_{v=1}^{Fundamental} = \begin{array}{c|cc} n_1, n_2 & |1,0\rangle & |0,1\rangle \\ \hline \langle 1,0| & A & -iC \\ \langle 0,1| & +iC & A \end{array} + A\mathbf{1} \quad (21.2.3)$$

\mathbf{H}^C commutes with a complex reflection σ_C and a real continuous rotation $\mathbf{R}[\phi]$ generated by σ_C .

$$s_C = \begin{pmatrix} 0 & -i \\ i & 0 \end{pmatrix}, \quad \mathbf{R}[\phi] = \begin{pmatrix} \cos \phi & -\sin \phi \\ \sin \phi & \cos \phi \end{pmatrix} = e^{-i\phi s_C} \quad (21.2.4)$$

This means \mathbf{H}^C is "smooth" or perfectly circular. It does not have any potential valleys or "bumps" which change angular momentum and require standing-or-galloping-wave eigenstates. So its eigenwaves (like those of a Ring Laser) have no nodes or antinodes and are of the form $e^{\pm im\phi} = (x_1 \pm ix_2)^m$ for which the probability distribution is perfectly circular in the complex phasor plane. Their complex continuous circularity provides some more mnemonic reasons to use the letter " C " to designate such a symmetry.

The complex C -symmetry $(x_1 \pm ix_2)$ -states differ from the real standing wave $(x_1$ and $x_2)$ states of C_2^A symmetry or $(x_1 \pm x_2)$ states of C_2^B symmetry described in Sec. 10.2(a) through Sec. 10.3(b). We started by basing our oscillator theory on linear $(x_1$ and $x_2)$ states of C_2^A . The A -axis bases will need to be moved to the chiral C -axis of Fig. 10.5.6 using, for example, a 90° rotation around the B -axis. This will be done shortly.

(1) *Angular momentum labeling: Fundamental base states $\{|\uparrow\rangle, |\downarrow\rangle\}$*

First, let us re-label and "rename" the lowest five $U(2)$ base sets as follows.

$$\left. \begin{array}{l} \left. \begin{array}{l} j=0 \quad \left| \begin{smallmatrix} 0 \\ 0 \end{smallmatrix} \right\rangle = |00\rangle \quad \text{"scalar"} \\ \hline j = \frac{1}{2} \quad \left| \begin{smallmatrix} 1/2 \\ 1/2 \end{smallmatrix} \right\rangle = |10\rangle = |\uparrow\rangle \\ \quad \quad \left| \begin{smallmatrix} 1/2 \\ -1/2 \end{smallmatrix} \right\rangle = |01\rangle = |\downarrow\rangle \\ \hline \left| \begin{smallmatrix} 1 \\ 1 \end{smallmatrix} \right\rangle = |20\rangle \\ j=1 \quad \left| \begin{smallmatrix} 1 \\ 0 \end{smallmatrix} \right\rangle = |11\rangle \quad \text{"3-vector"} \\ \quad \quad \left| \begin{smallmatrix} 1 \\ -1 \end{smallmatrix} \right\rangle = |02\rangle \\ \hline \left| \begin{smallmatrix} 3/2 \\ 1/2 \end{smallmatrix} \right\rangle = |30\rangle \\ j = \frac{3}{2} \quad \left| \begin{smallmatrix} 3/2 \\ 1/2 \end{smallmatrix} \right\rangle = |21\rangle \\ \quad \quad \left| \begin{smallmatrix} 3/2 \\ -1/2 \end{smallmatrix} \right\rangle = |12\rangle \\ \quad \quad \left| \begin{smallmatrix} 3/2 \\ -3/2 \end{smallmatrix} \right\rangle = |03\rangle \\ \hline \left| \begin{smallmatrix} 2 \\ 2 \end{smallmatrix} \right\rangle = |40\rangle \\ \left| \begin{smallmatrix} 2 \\ 1 \end{smallmatrix} \right\rangle = |31\rangle \\ j=2 \quad \left| \begin{smallmatrix} 2 \\ 0 \end{smallmatrix} \right\rangle = |22\rangle \quad \text{"tensor"} \\ \quad \quad \left| \begin{smallmatrix} 2 \\ -1 \end{smallmatrix} \right\rangle = |13\rangle \\ \quad \quad \left| \begin{smallmatrix} 2 \\ -2 \end{smallmatrix} \right\rangle = |04\rangle \\ \hline \vdots \end{array} \right\} \left. \begin{array}{l} j = \frac{v}{2} = \frac{n_1 + n_2}{2} \\ m = \frac{n_1 - n_2}{2} \end{array} \right\} \begin{array}{l} n_1 = j + m = 2v + m \\ n_2 = j - m = 2v - m \end{array} \quad (21.2.5)$$

Famous examples of chiral spin objects include electrons, nucleons, neutrinos, and other particles of total spin $j=1/2$ units of \hbar . If we choose the fundamental $U(2)$ bases states $\{|1\rangle,|2\rangle\}$ to be *spin-up* $|\uparrow\rangle$ and *spin-dn* $|\downarrow\rangle$ then the quantum theory of angular momentum is mathematically identical to an analysis $U(2)$ oscillator states. Each number-1 boson counts for one-half \hbar -unit of angular momentum $m = +1/2$ while each number-2 boson counts for minus one-half \hbar -unit of angular momentum $m = -1/2$ along the C -axis or Z -axis.

$U(2)$ levels from Fig. 21.1.1 are separated and labeled according to angular momentum notation in Fig. 21.2.1. *Odd-ν* and half-integral $j= 1/2, 3/2,..$ levels are sketched on the left-hand side while the *even-ν* and integral $j= 0, 1, 2,..$ levels are sketched on the right-hand side. Common names "*spinor*", "*vector*" and "*tensor*" are applied to multiplets $j=1/2, 1,$ and $2,$ respectively. The half-integral- j side is generally associated with the group $U(2)$ that works on complex 2-dimensional "*spinor*" space, while the integral- j side (which belongs to $U(2)$, too) is generally associated with real 3-dimensional $R(3)$ rotations in optical ABC -space or in a real XYZ -space, not entirely different from the one in which we live.

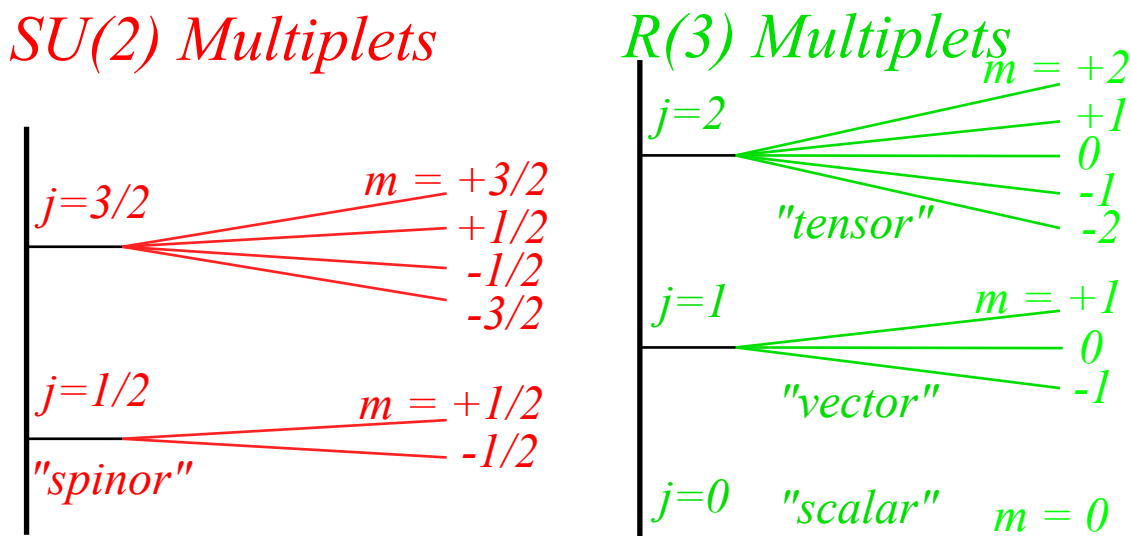


Fig. 21.2.1 $SU(2)$ and $R(3)$ angular momentum levels labeled by j and m .

A C -Hamiltonian is diagonalized by a $\Theta=90^\circ$ rotation around the X or B -axis which takes a spin vector \mathbf{S} on the Z or A -axis down to the Y or C -axis. X -rotations have polar angles $[\varphi = 0^\circ, \vartheta = 90^\circ]$. Putting these angles into a Darboux rotation matrix (2.10.15d) gives

$$\langle \mathbf{R}_B(90^\circ) \rangle = \langle \mathbf{R}[\varphi = 0^\circ, \vartheta = 90^\circ, \Theta = 90^\circ] \rangle = \begin{pmatrix} 1 & -i \\ \sqrt{2} & \sqrt{2} \\ -i & 1 \\ \sqrt{2} & \sqrt{2} \end{pmatrix} = \begin{pmatrix} \langle R|x_1 \rangle & \langle R|x_2 \rangle \\ \langle L|x_1 \rangle & \langle L|x_2 \rangle \end{pmatrix} \quad (21.2.6a)$$

This is a transformation between linear optical polarization states $\{|x_1\rangle,|x_2\rangle\}$ and states of circular right-or-left-polarization $\{|R\rangle,|L\rangle\}$ or electronic states of spin-up-or-dn $\{|\uparrow\rangle=|+1/2\rangle,|\downarrow\rangle=|-1/2\rangle\}$

$$\begin{aligned}
 |R\rangle = |\uparrow\rangle &= \begin{vmatrix} 1/2 \\ +1/2 \end{vmatrix} = \frac{|x_1\rangle + i|x_2\rangle}{\sqrt{2}}, & |L\rangle = |\downarrow\rangle &= \begin{vmatrix} 1/2 \\ -1/2 \end{vmatrix} = \frac{i|x_1\rangle + |x_2\rangle}{\sqrt{2}}, \\
 \langle R| = \langle\uparrow| &= \begin{vmatrix} 1/2 \\ +1/2 \end{vmatrix} = \frac{\langle x_1| - i\langle x_2|}{\sqrt{2}}, & \langle L| = \langle\downarrow| &= \begin{vmatrix} 1/2 \\ -1/2 \end{vmatrix} = \frac{-i\langle x_1| + \langle x_2|}{\sqrt{2}}.
 \end{aligned}
 \tag{21.2.6b}$$

This must also be the transformation between the corresponding sets of $\{\mathbf{a}_1^\dagger, \mathbf{a}_2^\dagger\}$ and $\{\mathbf{a}^\dagger_\uparrow, \mathbf{a}^\dagger_\downarrow\}$ operators which create the base states $\{|x_1\rangle = \mathbf{a}_1^\dagger|0\rangle, |x_2\rangle = \mathbf{a}_2^\dagger|0\rangle\}$ and $\{|\uparrow\rangle = \mathbf{a}^\dagger_\uparrow|0\rangle, |\downarrow\rangle = \mathbf{a}^\dagger_\downarrow|0\rangle\}$.

$$\begin{aligned}
 \mathbf{a}_R^\dagger = \mathbf{a}_\uparrow^\dagger = \mathbf{a}_{+1/2}^\dagger &= \frac{\mathbf{a}_1^\dagger + i\mathbf{a}_2^\dagger}{\sqrt{2}}, & \mathbf{a}_L^\dagger = \mathbf{a}_\downarrow^\dagger = \mathbf{a}_{-1/2}^\dagger &= \frac{i\mathbf{a}_1^\dagger + \mathbf{a}_2^\dagger}{\sqrt{2}}, \\
 \mathbf{a}_R = \mathbf{a}_\uparrow = \mathbf{a}_{+1/2} &= \frac{\mathbf{a}_1 - i\mathbf{a}_2}{\sqrt{2}}, & \mathbf{a}_L = \mathbf{a}_\downarrow = \mathbf{a}_{-1/2} &= \frac{-i\mathbf{a}_1 + \mathbf{a}_2}{\sqrt{2}}.
 \end{aligned}
 \tag{21.2.6c}$$

It does indeed diagonalize the fundamental ($\nu=1$) or ($j=1/2$) \mathbf{H} -submatrix (21.1.16) for C_2^C symmetry.

$$\begin{aligned}
 \begin{pmatrix} \langle\uparrow|x_1\rangle & \langle\uparrow|x_2\rangle \\ \langle\downarrow|x_1\rangle & \langle\downarrow|x_2\rangle \end{pmatrix} \cdot \begin{pmatrix} \langle x_1|\mathbf{H}|x_1\rangle & \langle x_1|\mathbf{H}|x_2\rangle \\ \langle x_2|\mathbf{H}|x_1\rangle & \langle x_2|\mathbf{H}|x_2\rangle \end{pmatrix} \cdot \begin{pmatrix} \langle x_1|\uparrow\rangle & \langle x_1|\downarrow\rangle \\ \langle x_2|\uparrow\rangle & \langle x_2|\downarrow\rangle \end{pmatrix} &= \begin{pmatrix} \langle\uparrow|\mathbf{H}|\uparrow\rangle & \langle\uparrow|\mathbf{H}|x_2\rangle \\ \langle\downarrow|\mathbf{H}|\uparrow\rangle & \langle\downarrow|\mathbf{H}|\downarrow\rangle \end{pmatrix} \\
 \begin{pmatrix} \frac{1}{\sqrt{2}} & \frac{-i}{\sqrt{2}} \\ \frac{-i}{\sqrt{2}} & \frac{1}{\sqrt{2}} \end{pmatrix} \cdot \begin{pmatrix} 0 & -iC \\ iC & 0 \end{pmatrix} \cdot \begin{pmatrix} \frac{1}{\sqrt{2}} & \frac{-i}{\sqrt{2}} \\ \frac{-i}{\sqrt{2}} & \frac{1}{\sqrt{2}} \end{pmatrix} &= \begin{pmatrix} C & 0 \\ 0 & -C \end{pmatrix}
 \end{aligned}
 \tag{21.2.6d}$$

The resulting wave functions are a complex-conjugate pair of two-dimensional Gaussians.

$$\psi_{1\uparrow 0\downarrow}(x_1, x_2) = \frac{\sqrt{2}(x_1 + ix_2)e^{-(x_1^2 + x_2^2)/2}}{(\pi)^{1/2}}, \quad \psi_{0\uparrow 1\downarrow}(x_1, x_2) = \frac{\sqrt{2}(x_1 - ix_2)e^{-(x_1^2 + x_2^2)/2}}{(\pi)^{1/2}}
 \tag{21.2.7}$$

The two have identical probability distribution which is plotted in Fig. 21.2.2. (Also, recall Fig. 21.1.6.)

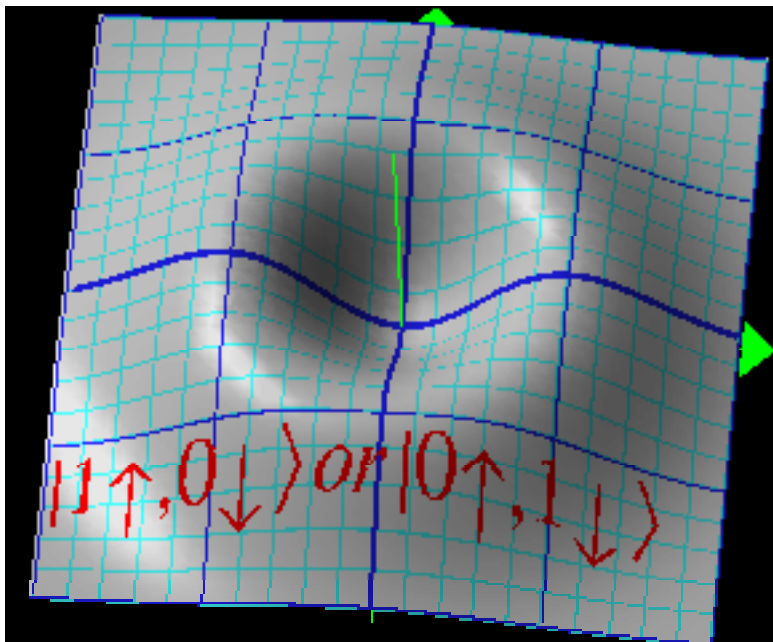


Fig. 21.2.2 2-D Oscillator probability distributions: $|\Psi_{1\uparrow 0\downarrow}(x_1, x_2)|^2$ or $|\Psi_{0\uparrow 1\downarrow}(x_1, x_2)|^2$.

Notice how the probability drops to zero quickly near the origin. This is a general property of an eigentate with non-zero momentum ℓ in ℓ -conserving systems. As a particle approaches the origin with non-zero angular momentum, it gains speed and kinetic energy without limit, like a dust particle in a perfect vortex. However, if energy is also conserved then particles simply must avoid the origin.

(2) 3-Vector base states ($\nu=2$) or ($j=1$)

The preceding procedures may be used to find the eigenvectors of the excited ($\nu=2, 3, 4\dots$) **H**-submatrices. For example, the ($\nu=2$) or ($j=1$) eigenvectors of a C_2^C symmetric **H** must be the following.

$$\begin{aligned}
 |2_{\uparrow 0_{\downarrow}}\rangle &= \frac{\mathbf{a}_{\uparrow}^{\dagger 2}}{\sqrt{2!}}|0\rangle = \frac{(\mathbf{a}_1^{\dagger} + i\mathbf{a}_2^{\dagger})^2}{2\sqrt{2!}}|0\rangle = \frac{\mathbf{a}_1^{\dagger 2} + 2i\mathbf{a}_1^{\dagger}\mathbf{a}_2^{\dagger} - \mathbf{a}_2^{\dagger 2}}{2\sqrt{2}}|0\rangle = \frac{1}{2}|2_1 0_2\rangle + \frac{i}{\sqrt{2}}|1_1 1_2\rangle - \frac{1}{2}|0_1 2_2\rangle \\
 |1_{\uparrow 1_{\downarrow}}\rangle &= \frac{\mathbf{a}_{\uparrow}^{\dagger}\mathbf{a}_{\downarrow}^{\dagger}}{\sqrt{1!\sqrt{1!}}}|0\rangle = \frac{(\mathbf{a}_1^{\dagger} + i\mathbf{a}_2^{\dagger})(\mathbf{a}_1^{\dagger} - i\mathbf{a}_2^{\dagger})}{2}|0\rangle = \frac{\mathbf{a}_1^{\dagger 2} + \mathbf{a}_2^{\dagger 2}}{2}|0\rangle = \frac{1}{\sqrt{2}}|2_1 0_2\rangle + \frac{1}{\sqrt{2}}|0_1 2_2\rangle \quad (21.2.8) \\
 |0_{\uparrow 2_{\downarrow}}\rangle &= \frac{\mathbf{a}_{\downarrow}^{\dagger 2}}{\sqrt{2!}}|0\rangle = \frac{(\mathbf{a}_1^{\dagger} - i\mathbf{a}_2^{\dagger})^2}{2\sqrt{2!}}|0\rangle = \frac{\mathbf{a}_1^{\dagger 2} - 2i\mathbf{a}_1^{\dagger}\mathbf{a}_2^{\dagger} - \mathbf{a}_2^{\dagger 2}}{2\sqrt{2}}|0\rangle = \frac{1}{2}|2_1 0_2\rangle - \frac{i}{\sqrt{2}}|1_1 1_2\rangle - \frac{1}{2}|0_1 2_2\rangle
 \end{aligned}$$

We verify that the resulting vectors are eigenvectors of the 3-by-3 submatrix of (21.1.15c).

$$\begin{aligned}
 (j = \nu/2 = 1) \text{ Eigenvalues: } & 2C, \quad 0, \quad -2C \\
 \begin{pmatrix} \cdot & -iC\sqrt{2} & \cdot \\ iC\sqrt{2} & \cdot & -iC\sqrt{2} \\ \cdot & iC\sqrt{2} & \cdot \end{pmatrix} \cdot \begin{pmatrix} 1/2 \\ i/\sqrt{2} \\ -1/2 \end{pmatrix}, & \begin{pmatrix} 1/\sqrt{2} \\ 0 \\ 1/\sqrt{2} \end{pmatrix}, \begin{pmatrix} 1/2 \\ -i/\sqrt{2} \\ -1/2 \end{pmatrix} \quad (21.2.9)
 \end{aligned}$$

The splitting between neighboring levels is $\Omega = 2C$ as required by (21.1.22)

The ($\nu=2$) eigenfunctions $\langle x_1 x_2 | n_1 n_2 \rangle$ in the **A**-basis are products of 1-D waves (20.3.40).

$$\psi_{2,0_1}(x_1, x_2) = \langle x_1 | 2 \rangle \langle x_2 | 0 \rangle, \quad \psi_{1,1_1}(x_1, x_2) = \langle x_1 | 1 \rangle \langle x_2 | 1 \rangle, \quad \psi_{1,1_1}(x_1, x_2) = \langle x_1 | 0 \rangle \langle x_2 | 2 \rangle$$

$$= Ne^{-(x_1^2 + x_2^2)/2} \sqrt{2} \left(x_1^2 - \frac{1}{2} \right), \quad = Ne^{-(x_1^2 + x_2^2)/2} 2(x_1 x_2), \quad = Ne^{-(x_1^2 + x_2^2)/2} \sqrt{2} \left(x_2^2 - \frac{1}{2} \right)$$

$$(21.2.10a)$$

$$(21.2.10b)$$

$$(21.2.10c)$$

Combining them according to (21.2.8) gives the ($\nu=2$) eigenwaves for a **C**-type Hamiltonian.

$$\psi_{2,0_{\downarrow}} = \frac{1}{2}\psi_{2,0_1} + \frac{i\sqrt{2}}{2}\psi_{1,1_1} - \frac{1}{2}\psi_{0,1_1} = Ne^{-\frac{r^2}{2} \frac{x_1^2 + 2ix_1 x_2 - x_2^2}{\sqrt{2}}} = Ne^{-\frac{r^2}{2} \frac{(x_1 + ix_2)^2}{\sqrt{2}}} \quad (21.2.10d)$$

$$\psi_{1,1_{\downarrow}} = \frac{1}{\sqrt{2}}\psi_{2,0_1} + \frac{1}{\sqrt{2}}\psi_{0,1_1} = Ne^{-\frac{r^2}{2} \frac{\sqrt{2}(x_1^2 + x_2^2 - 1)}{\sqrt{2}}} = Ne^{-\frac{r^2}{2} (x_1^2 + x_2^2 - 1)} \quad (21.2.10e)$$

$$\psi_{0,2_{\downarrow}} = \frac{1}{2}\psi_{2,0_1} - \frac{i\sqrt{2}}{2}\psi_{1,1_1} - \frac{1}{2}\psi_{0,1_1} = Ne^{-\frac{r^2}{2} \frac{x_1^2 + 2ix_1 x_2 - x_2^2}{\sqrt{2}}} = Ne^{-\frac{r^2}{2} \frac{(x_1 - ix_2)^2}{\sqrt{2}}} \quad (21.2.10f)$$

The **A**-type waves $\psi_{2,1,0_2}$ and $\psi_{1,1,1_2}$ plotted in Fig. 21.2.3 have lumps and bumps that are aligned to Cartesian ($x_1 x_2$) coordinates.

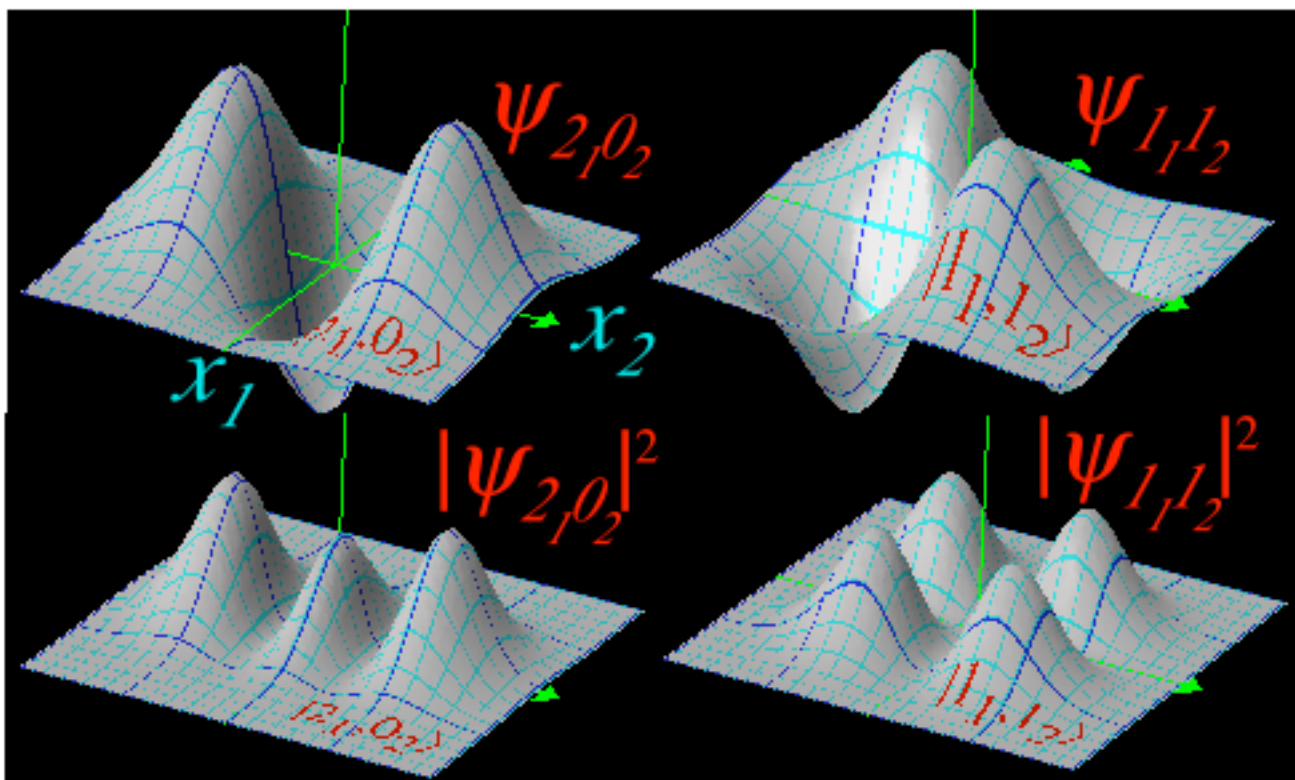


Fig. 21.2.3 ($\nu=2$) Type-A standing waves and distributions: $|\Psi_{2,0,2}(x_1,x_2)|^2$ and $|\Psi_{1,1,2}(x_1,x_2)|^2$.

In contrast, the C-type waves $\psi_{2\uparrow 0\downarrow}$ and $\psi_{1\uparrow 1\downarrow}$ plotted in Fig. 21.2.4 are waves moving around in circular orbits with vibrational angular momentum of ± 2 and 0 .

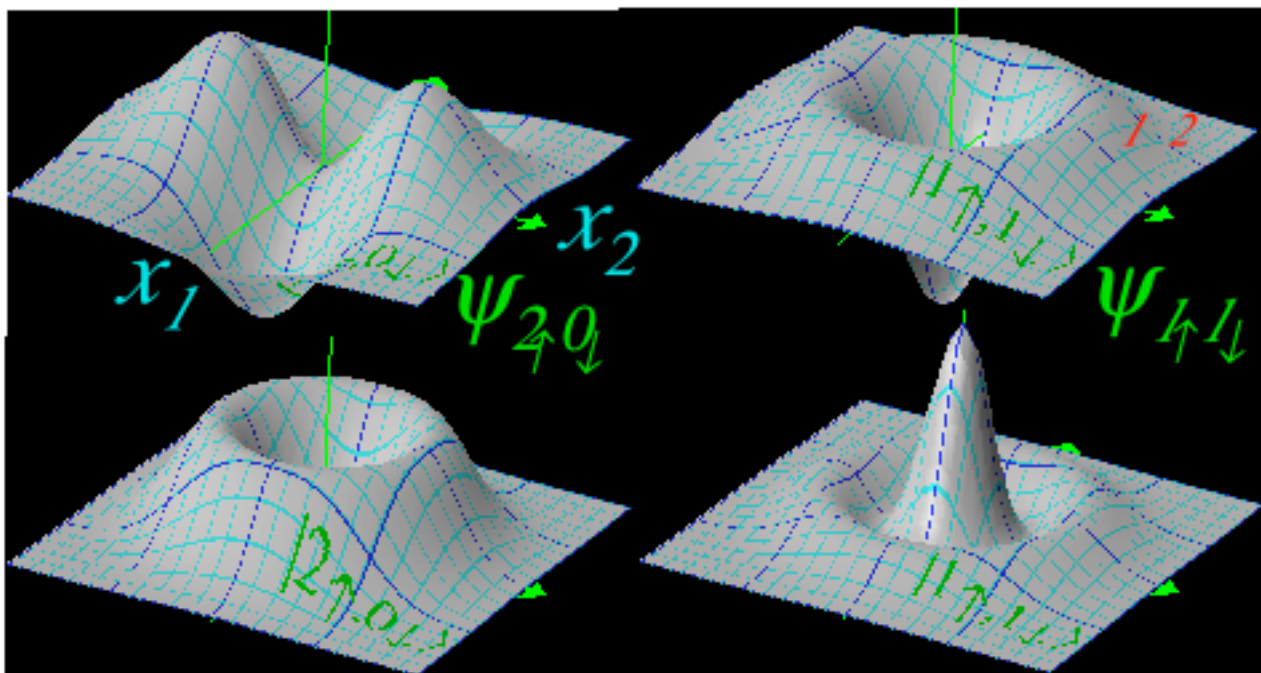


Fig. 21.2.4 ($\nu=2$) Type-C moving waves and distributions: $|\Psi_{2\uparrow 0\downarrow}(x_1,x_2)|^2$ and $|\Psi_{1\uparrow 1\downarrow}(x_1,x_2)|^2$.

The angular momentum structure can be seen by rewriting the wavefunctions in polar coordinates.

$$\psi_{2\uparrow 0\downarrow} = Ne^{-\frac{r^2}{2}} \frac{(x_1 + ix_2)^2}{\sqrt{2}} = \psi_{2m=2}^{j=2} = Ne^{-\frac{r^2}{2}} \frac{r^2 e^{i2\theta}}{\sqrt{2}} \tag{21.2.10d}$$

$$\psi_{1\uparrow 1\downarrow} = Ne^{-\frac{r^2}{2}} (x_1^2 + x_2^2 - 1) = \psi_{2m=0}^{j=2} = Ne^{-\frac{r^2}{2}} (r^2 - 1) e^{i0\theta} \tag{21.2.10d}$$

$$\psi_{0\uparrow 2\downarrow} = Ne^{-\frac{r^2}{2}} \frac{(x_1 - ix_2)^2}{\sqrt{2}} = \psi_{2m=-2}^{j=2} = Ne^{-\frac{r^2}{2}} \frac{r^2 e^{-i2\theta}}{\sqrt{2}} \tag{21.2.10d}$$

Quantum numbers for C-type vibrational states are the *radial quantum number* ($\nu=2j$) and the *vibrational angular momentum quantum number* μ .

$$\nu = 2j = n\uparrow + n\downarrow, \quad \mu = 2m = n\uparrow - n\downarrow \tag{21.2.11}$$

A C-type vibrational eigenstate has μ angular waves and 2μ angular moving wave zeros (two for each wave). For larger angular momentum the wave tends to avoid the origin more and more as shown in Fig. 21.2.5 below in a comparison between a $\mu=1$ and a $\mu=4$ probability distribution.

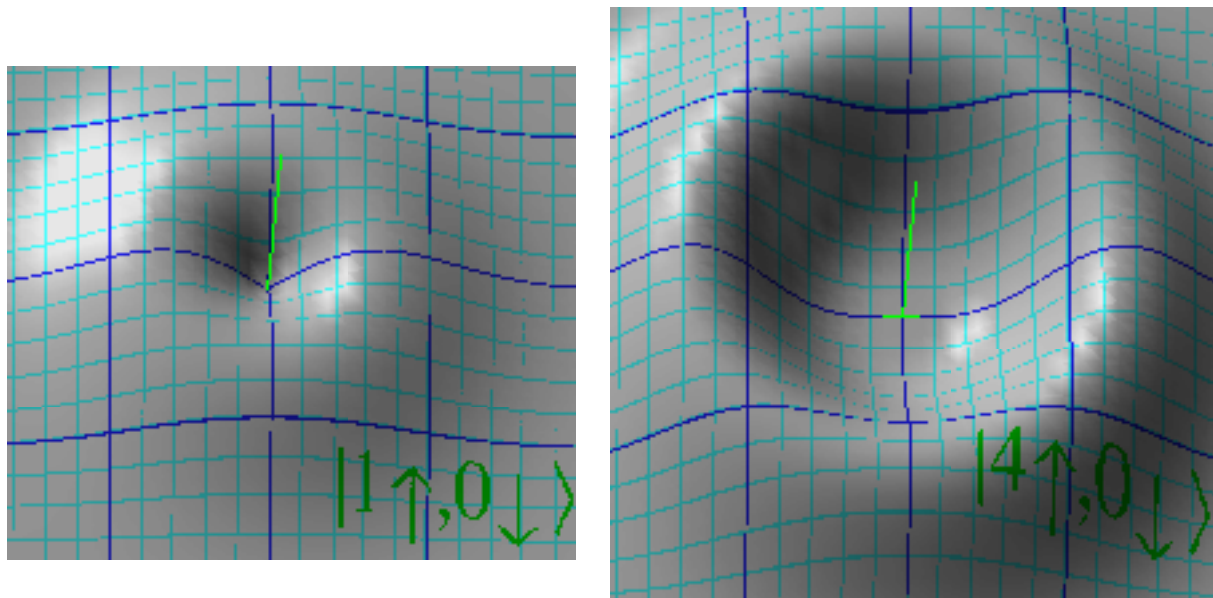


Fig. 21.2.5 ($\nu=2$) Type-C moving wave distributions: $|\Psi_{1\uparrow 0\downarrow}(x_1, x_2)|^2$ and $|\Psi_{4\uparrow 0\downarrow}(x_1, x_2)|^2$.

As the azimuthal angular momentum quantum number $\mu=2m$ increases, the location of the circular orbital radius becomes more and more clearly defined.

(b) Polar coordinates: C_2^C symmetry variable separation

An alternative (and historically much older) way to obtain C -symmetry eigenfunctions is to use coordinates based on circular symmetry, namely, polar coordinates (r, ϕ) instead of Cartesian (x, y) or

$$x = x_1 = r \cos \phi, \quad y = x_2 = r \sin \phi. \quad (21.2.12)$$

The Jacobian transformation between the Cartesian and polar coordinates relates their derivatives.

$$\begin{pmatrix} \frac{\partial}{\partial r} \\ \frac{\partial}{\partial \phi} \end{pmatrix} = \begin{pmatrix} \frac{\partial x}{\partial r} & \frac{\partial y}{\partial r} \\ \frac{\partial x}{\partial \phi} & \frac{\partial y}{\partial \phi} \end{pmatrix} \begin{pmatrix} \frac{\partial}{\partial x} \\ \frac{\partial}{\partial y} \end{pmatrix} = \begin{pmatrix} \cos \phi & \sin \phi \\ -r \sin \phi & r \cos \phi \end{pmatrix} \begin{pmatrix} \frac{\partial}{\partial x} \\ \frac{\partial}{\partial y} \end{pmatrix} \quad (21.2.13a)$$

The inverse (Kajobian) transformation lets us rewrite the Cartesian Schrodinger equation.

$$\begin{pmatrix} \frac{\partial}{\partial x} \\ \frac{\partial}{\partial y} \end{pmatrix} = \begin{pmatrix} \frac{\partial r}{\partial x} & \frac{\partial \phi}{\partial x} \\ \frac{\partial r}{\partial y} & \frac{\partial \phi}{\partial y} \end{pmatrix} \begin{pmatrix} \frac{\partial}{\partial r} \\ \frac{\partial}{\partial \phi} \end{pmatrix} = \begin{pmatrix} \cos \phi & -\frac{1}{r} \sin \phi \\ \sin \phi & \frac{1}{r} \cos \phi \end{pmatrix} \begin{pmatrix} \frac{\partial}{\partial r} \\ \frac{\partial}{\partial \phi} \end{pmatrix} \quad (21.2.13b)$$

The oscillator Schrodinger equation in Cartesian coordinates

$$\frac{\partial^2 \Psi}{\partial x^2} + \frac{\partial^2 \Psi}{\partial y^2} - \frac{2M}{\hbar^2} \left(\frac{M\omega^2}{2} (x^2 + y^2) - E \right) \Psi = 0, \quad (21.2.14a)$$

is rewritten as follows in polar coordinates.

$$\frac{\partial^2 \Psi}{\partial r^2} + \frac{1}{r} \frac{\partial \Psi}{\partial r} + \frac{1}{r^2} \frac{\partial^2 \Psi}{\partial \phi^2} - \frac{2M}{\hbar^2} \left(\frac{M\omega^2}{2} r^2 - E \right) \Psi = 0 \quad (21.2.14a)$$

Separation of coordinate variables r and ϕ into a wavefunction $\Psi(r, \phi) = R(r)\varphi(\phi)$ is similar to the separation $\Psi(x, y) = \psi_x(x)\psi_y(y)$ for Cartesian coordinates and results in the following equation separation.

$$\frac{r^2}{R} \left[\frac{d^2 R}{dr^2} + \frac{1}{r} \frac{dR}{dr} \right] - \frac{2Mr^2}{\hbar^2} \left(\frac{M\omega^2}{2} r^2 - E \right) = -\frac{1}{\varphi} \frac{\partial^2 \varphi}{\partial \phi^2} = \text{const.} = m^2 \quad (21.2.15a)$$

Equality of the two ordinary equations of independent r and ϕ implies both equal a constant. Azimuthal symmetry and boundary conditions $\varphi(\phi) = \varphi(\phi \pm 2\pi)$ force m -quantization, so the constant is the square of azimuthal angular momentum quantum number $m = 0, \pm 1, \pm 2, \dots$

$$\frac{\partial^2 \varphi}{\partial \phi^2} = -m^2 \varphi \quad \text{or:} \quad \varphi(\phi) = Ae^{im\phi} + Be^{-im\phi} \quad (21.2.15b)$$

The radial equation involves the constant m^2 in a more complicated way.

$$\frac{d^2 R}{dr^2} + \frac{1}{r} \frac{dR}{dr} - \left[\frac{M^2 \omega^2}{\hbar^2} r^2 + \frac{2M}{\hbar^2} E - \frac{m^2}{r^2} \right] R = 0 \quad (21.2.15c)$$

C -symmetry makes the angular moving waves in the ϕ -direction independent of the radial wave except through the constant m^2 . Such a constant is called a *separation constant*.

As in the 1-D case of (20.1.12) it helps to factor out a Gaussian scaling function $s(r) = e^{-\alpha r^2}$ such that the factor $\rho(r)$ in the radial wave $R(r) = s(r)\rho(r)$ is a simpler function and preferably an r polynomial.

$$\begin{aligned}
R &= \rho e^{-\alpha r^2} \\
R' &= (\rho' - 2\alpha r \rho) e^{-\alpha r^2} \\
R'' &= (\rho'' - 4\alpha r \rho' + [4\alpha^2 r^2 - 2\alpha] \rho) e^{-\alpha r^2}
\end{aligned} \tag{21.2.16}$$

Dropping the Gaussian converts (21.2.15c) to an equation of similar form.

$$\begin{aligned}
R'' + \frac{R'}{r} - \left[\frac{M^2 \omega^2}{\hbar^2} r^2 - \frac{2M}{\hbar^2} E + \frac{m^2}{r^2} \right] R &= 0 \\
\rho'' + \left[\frac{1}{r} - 4\alpha r \right] \rho' + \left[\left(4\alpha^2 - \frac{M^2 \omega^2}{\hbar^2} \right) r^2 + \frac{2M}{\hbar^2} E - 4\alpha - \frac{m^2}{r^2} \right] \rho &= 0
\end{aligned} \tag{21.2.17a}$$

This simplifies if we use the same Gaussian parameter $\alpha = M\omega/2\hbar$ from (20.1.10b) and set $E = \hbar\omega\varepsilon$.

$$\rho'' + \left[\frac{1}{r} - 4\alpha r \right] \rho' + \left[4\alpha(\varepsilon - 1) - \frac{m^2}{r^2} \right] \rho = 0 = r^2 \rho'' + [r - 4\alpha r^3] \rho' + [4\alpha(\varepsilon - 1)r^2 - m^2] \rho \tag{21.2.17b}$$

Now a polynomial analysis will work by expanding the radial wave and its derivatives. Let $\varepsilon = \varepsilon - l$.

$$\begin{aligned}
\rho &= a_0 + a_1 r + a_2 r^2 + a_3 r^3 + a_4 r^4 + \dots = \sum_{k=0} a_k r^k \\
\rho' &= a_1 + 2a_2 r + 3a_3 r^2 + 4a_4 r^3 + 5a_5 r^4 + \dots = \sum_{k=1} k a_k r^{k-1} \\
\rho'' &= 2a_2 + 6a_3 r + 12a_4 r^2 + 20a_5 r^3 + 30a_6 r^4 + \dots = \sum_{k=2} k(k-1) a_k r^{k-2}
\end{aligned} \tag{21.2.18}$$

Putting this into each term of the radial equation gives series whose grand sum must be zero.

$$\begin{aligned}
-m^2 \rho &= -m^2 a_0 - m^2 a_1 r - m^2 a_2 r^2 - m^2 a_3 r^3 - m^2 a_4 r^4 + \dots = \sum_{k=0} -m^2 a_k r^k \\
4\alpha \varepsilon r^2 \rho &= 4\alpha \varepsilon a_0 r^2 + 4\alpha \varepsilon a_1 r^3 + 4\alpha \varepsilon a_2 r^4 + \dots = \sum_{k=2} 4\alpha \varepsilon a_{k-2} r^k \\
r \rho' &= a_1 r + 2a_2 r^2 + 3a_3 r^3 + 4a_4 r^4 + \dots = \sum_{k=1} k a_k r^k \\
r^2 \rho'' &= 2a_2 r^2 + 6a_3 r^3 + 12a_4 r^4 + \dots = \sum_{k=2} k(k-1) a_k r^k \\
-4\alpha \varepsilon r^3 \rho' &= -4\alpha \varepsilon a_1 r^3 - 8\alpha \varepsilon a_2 r^4 + \dots = \sum_{k=3} -4\alpha(k-2) a_{k-2} r^k
\end{aligned} \tag{21.2.19}$$

The sum of coefficients of each power lying in each column above must vanish. The 0-column gives

$$m^2 a_0 = 0$$

This says that wave amplitude a_0 must vanish for all non-zero momentum m . We noted after Fig. 21.2.5 that orbiting particles avoid the origin. Consider the general column or power- k as listed on the right hand side above. Setting the sum of the k - coefficients to zero leads to a *recursion relation*.

$$[4\alpha \varepsilon - 4\alpha(k-2)] a_{k-2} = -[k(k-1) + k - m^2] a_k \tag{21.2.20a}$$

This may be used as a *bottom-up* relation or else as a *top-down* relation.

$$a_{k+2} = \frac{-4\alpha(\varepsilon_- - k)}{(k+2)^2 - m^2} a_k, \quad a_{k-2} = \frac{m^2 - k^2}{4\alpha(\varepsilon_- - k + 2)} a_k \quad (21.2.20b)$$

The first starts with bottom coefficient a_0 or a_1 and computes the higher ones. The other works down. The bottom-up relation leads to the *quantization condition*

$$\varepsilon_- = N = k_+, \quad (21.2.20c)$$

for some integer *principal quantum number* N in order that the polynomial order is finite and the wave is bounded by the Gaussian. The top-down relation leads to a *centrifugal exclusion condition*

$$k_- = |m|, \quad (21.2.20d)$$

which limits the lowest degree $k_- = m$ allowed by a given angular momentum m . High powers r^k are "center-fleeing" with low radial wave near $r=0$. Momentum magnitude is restricted between zero and N .

$$0 \leq |m| \leq N$$

The quantization condition agrees with the energy spectrum previously derived in (21.1.25).

$$\hbar\omega\varepsilon_- = \hbar\omega(\varepsilon_- - l) = \hbar\omega N,$$

where we use $E = \hbar\omega\varepsilon$ and $\varepsilon_- = \varepsilon - l$ from (21.2.17).

$$E = \hbar\omega\varepsilon = \hbar\omega(N+l) \quad (21.2.20e)$$

Note the principal quantum number N is the total quantum number ν defined previously in (21.1.25).

$$N = \nu = n_1 + n_2$$

The $N=2=\varepsilon_-$ wave for $m=0$ in (21.2.10b) follows from (21.2.20b)

$$a_2 = \frac{-4\alpha\varepsilon_-}{(2)^2 - 0^2} a_0 = -2\alpha a_0 = -\frac{M\omega}{\hbar} a_0 \quad (21.2.21)$$

In units such that $M\omega/\hbar = 1$ or $\alpha = 1/2$ this agrees with (21.2.10b).

$$R(r) = a_0 (1-r^2)$$

21.3 N-Dimensional Oscillator Levels

The quantum levels $(1,2,3,4, \dots, \nu, \dots)$ of a 1D oscillator are singlet levels (no degeneracy). However, an isotropic ($U(2)$ symmetric) 2D oscillator has levels whose degeneracy $\ell = \nu$ equals the principal quantum number. $\nu = n_1 + n_2 = (1,2,3,4, \dots, \nu, \dots)$, as seen in Fig. 21.1.1.

The degeneracies of isotropic ($U(N)$ symmetric) N -D oscillators increase more rapidly. For a $U(3)$ symmetric 3D oscillator the degeneracy numbers are $\ell = (1,3,6,10, \dots, \nu(\nu+1)/2, \dots)$. These are known as *triangular numbers*. Here we consider ways to describe oscillator levels.

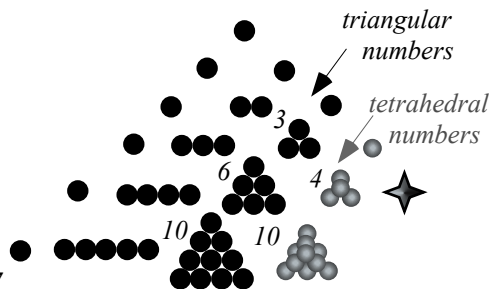
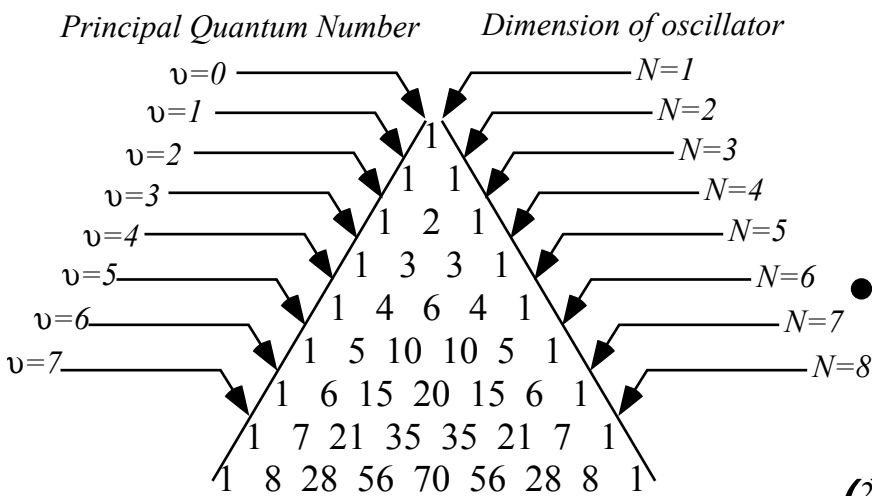
(a) Pascal triangle and $U(N)$ degeneracy

There are some geometric ways to organize and label oscillator degeneracy. The first uses Pascal's triangle of binomial coefficients as shown in Fig. 21.3.1. Each Pascal number is the sum of the two numbers directly above it as shown in Fig. 21.3.1(a). Numbers along a given N -diagonal are the degeneracy ℓ for each quantum number ν listed along the opposing (ν) -diagonal. It's a binomial coefficient $C_\nu^n = \binom{n}{\nu}$ that means the number of combinations of n things taken ν at a time.

$$\ell = C_\nu^{N-1+\nu} = \binom{N-1+\nu}{\nu} = \frac{(N-1+\nu)!}{\nu!(N-1)!} = \binom{N-1+\nu}{N-1} \tag{23.1.1}$$

(a) N -D Oscillator Degeneracy ℓ of quantum level ν

(b) Stacking numbers



(c) Binomial coefficients

$$\frac{(N-1+\nu)!}{(N-1)!\nu!} = \binom{N-1+\nu}{\nu} = \binom{N-1+\nu}{N-1}$$

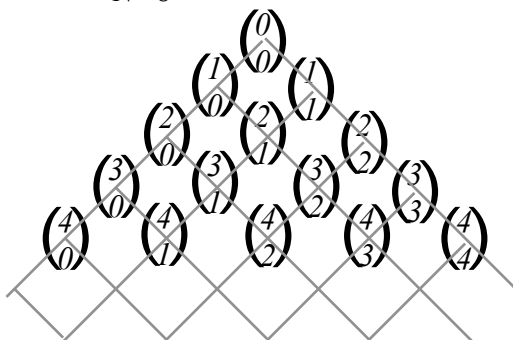
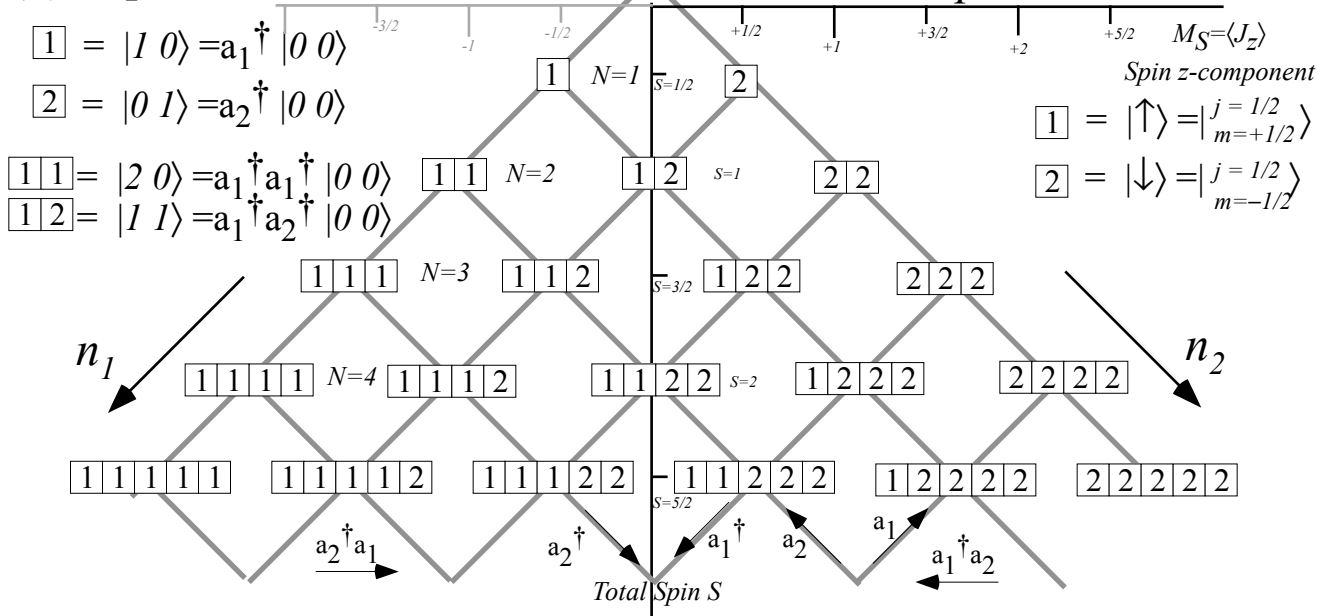


Fig. 21.3.1 Pascal binomial numbers related to oscillator level degeneracy.

The plot in Fig. 21.1.2 of the principal quantum number $\nu = n_1 + n_2$ versus individual $U(2)$ oscillator quantum numbers n_1 and n_2 shows why Pascal's triangular numbers are relevant to oscillator degeneracy. An analogous plot of $\nu = n_1 + n_2 + n_3$ for a $U(3)$ oscillator produces equilateral triangles stacked a diagonal distance $\nu = n_1 + n_2 + n_3$ from the corner of three Cartesian planes defining $n_1, n_2,$ and n_3 axes.

(a) *N*-particle 2-level states $[(\text{vacuum})] = |0 0\rangle$...or spin-1/2 states



(b) *N*-particle 3-level states ...or spin-1 states

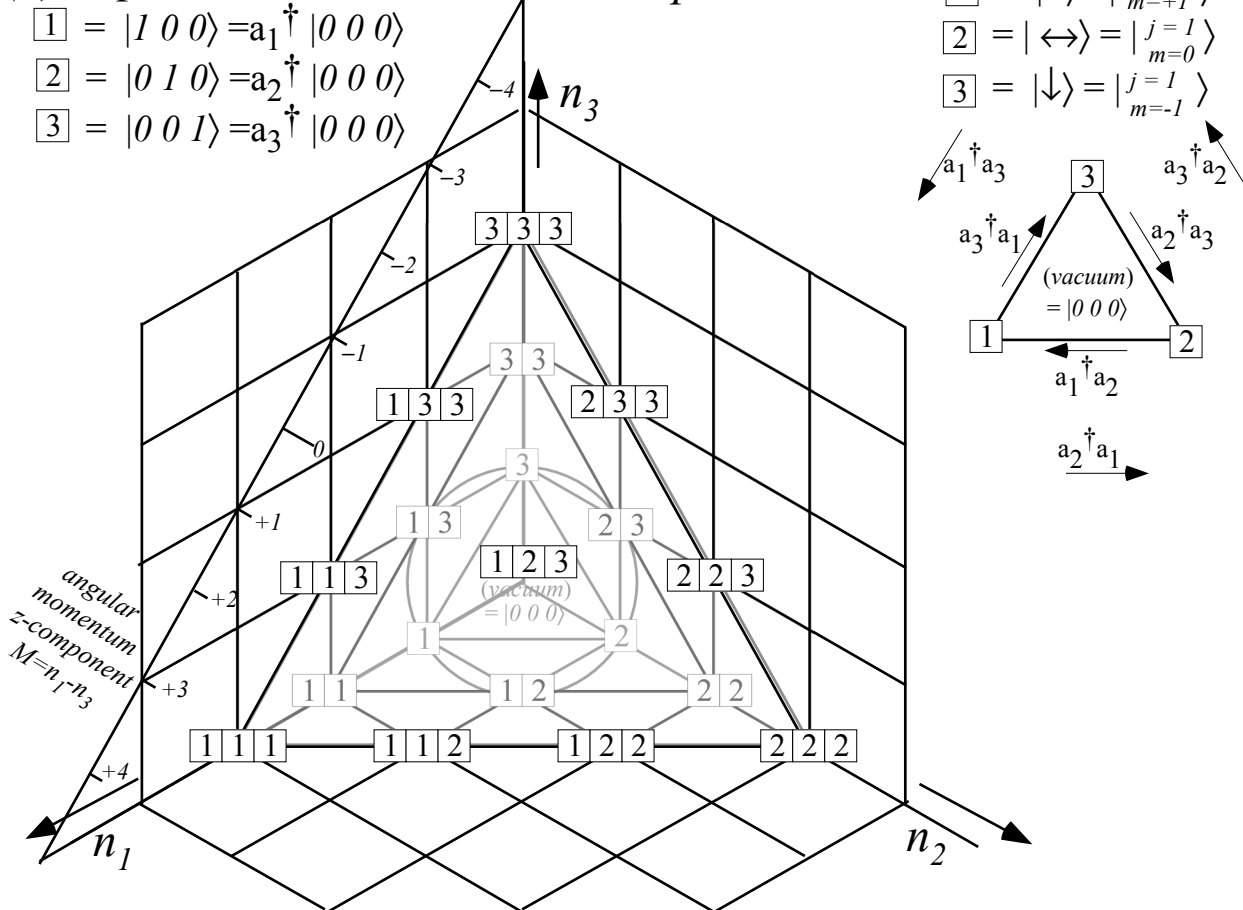


Fig. 21.3.2 *N*-quanta (“particle”) multiplets (a) 2-Levels (“states”) : Spin-1/2. (b) 3-Levels : Spin-1

Fig. 21.1.3(a) displays the 2D oscillator states in a way that is similar but upside down to Fig. 23.1.2(a). Each level has the same total number $N=\nu=n_1+n_2$ of quanta. We may think of each level as an N -particle state where by “particle” we mean a photon, vibron, libron, or any of a number of excitons that occupy our attention in modern physics. It is only important that each “X-on” or “Enr-on” may be created in arbitrary order, that is, has Bose symmetry as stated in (21.1.5) or again below.

$$[\mathbf{a}_m, \mathbf{a}_n] = \mathbf{a}_m \mathbf{a}_n - \mathbf{a}_n \mathbf{a}_m, \quad [\mathbf{a}_m, \mathbf{a}^\dagger_n] = \mathbf{a}_m \mathbf{a}^\dagger_n - \mathbf{a}^\dagger_n \mathbf{a}_m, \quad [\mathbf{a}^\dagger_m, \mathbf{a}^\dagger_n] = \mathbf{a}^\dagger_m \mathbf{a}^\dagger_n - \mathbf{a}^\dagger_n \mathbf{a}^\dagger_m, \\ = \mathbf{0} \qquad \qquad \qquad = \delta_{mn} \mathbf{1} \qquad \qquad \qquad = \mathbf{0} .$$

This is indicated by a *Young Tableaux* notation of boxes holding numbers that indicated the state or X-on numbers. Numbers may be permuted within the rows without changing their meaning. Only the sum

$$N=S/2=\nu=n_1+n_2 \tag{21.3.2}$$

or difference

$$C=S_z/2=n_1-n_2 \tag{21.3.3}$$

Has physical significance. In the following Chapter 22, these numbers will define the photon “spin” that characterizes the intensity N and *one* of the polarization $A, B,$ or C components in a quantum light beam. In Chapter 23, these quantum numbers will define total spin angular momentum S and its z-component S_z in the Schwinger development of rotational quanta.

Fig. 21.1.3(b) displays the 3D oscillator states in an analogous but 3-dimensional way with the 2D oscillator n_1 -axis and n_2 -axis lying on the floor of a Cartesian octant or “room” whose vertical n_3 -axis is the number of quanta or “particles” in the 3rd oscillator state. Again any kind of “X-on” may use this geometry and the total number $N=\nu=n_1+n_2+n_3$ of these “particles” would be marked off on a $(1,1,1)$ -axis coming straight out of this Fig. 21.3.2(b). With three dimensions or quanta $n_1, n_2,$ and n_3 there are lots more ways that they can sum to a given N . That number is one of the triangular numbers $1,3,6,10,..$ listed in Pascal’s triangle on the $N=3$ diagonal of Fig. 21.3.1(a) and indicated in Fig. 21.3.1(b). The triangles for $N=\nu=0, 1, 2,$ and 3 are “stacked” in Fig. 21.3.2(b) with their Young tableaux state labeling.

These stacks make larger and larger tetrahedrons. Such tetrahedrons are just what are needed to make the next higher 4D-oscillator states whose degeneracy (for an isotropic oscillator) will be the tetrahedral numbers $1,4,10,15,..$ listed in Fig. 21.3.1(b). These are the number of cannonballs in an N -sided stack seen sitting dissolutely in Civil War monuments throughout the educationally miasmatic Southern states of a United States so tortured by its apparent need for that and other wars.

In contrast, there is much to learn about the quantum states by considering the geometry and algebra of these curious stacks and considering how it is that the idea of quantum *particles*, on one hand and quantum *states*, on the other, can be clearly defined in some cases and quite mixed up in others.

Problems for Chapter 21

From A to B

21.1.1. Consider a B -type 2D oscillator Hamiltonian:

$$H^B = \frac{A}{2}(\mathbf{p}_1^2 + \mathbf{x}_1^2 + \mathbf{p}_2^2 + \mathbf{x}_2^2) + B(\mathbf{p}_1\mathbf{p}_2 + \mathbf{x}_1\mathbf{x}_2)$$

- Express it in terms of A -basis creation-destruction operators $\mathbf{a}_j = (\mathbf{x}_j + i \mathbf{p}_j)/\sqrt{2}$ ($j=1,2$).
- Compute its A -basis representation for the first five levels: $N=0, 1, 2, 3, 4, \dots$
- Plot the H^B eigenvalues for fixed $A=1$ and varying between $B=-1$ and $B=+1$.
- Diagonalize the representation for the three $N=2$ levels and display the 3-by-3 transformation matrix $T_{B \leftarrow A}$ which effectively transforms from the A -basis to the B -basis. Does T depend on A or B ?

Lines of degeneracy

21.1.2. The eigenvalues in Fig. 21.1.1 exhibit quite a number of degeneracy points as the splitting or beat frequency Ω varies relative to static oscillator frequency ω . Give a sketch of the algebra, geometry, or arithmetic that might shed some light on this. The revival crossings described in Ch. 9 might be relevant.

From B to C

21.1.3. Consider a C -type 2D oscillator Hamiltonian:

$$H^C = \frac{A}{2}(\mathbf{p}_1^2 + \mathbf{x}_1^2 + \mathbf{p}_2^2 + \mathbf{x}_2^2) + C(\mathbf{x}_1\mathbf{p}_2 - \mathbf{x}_2\mathbf{p}_1)$$

- The ($N=2$)-transformation $T_{B \leftarrow A}$ from an A -basis to a B -basis derived in Exercise 21.1.1(d) might also be capable of continuing on from a B -basis to a C -basis. Does $T_{B \leftarrow A} = T_{C \leftarrow B}$? Check this. How is $T_{C \leftarrow A}$ related to these two?
- (For Ch. 23) How are these matrices related to the irreducible representations $D^{(l)}(\varphi, \vartheta, \Theta)$?

From 2 to 3

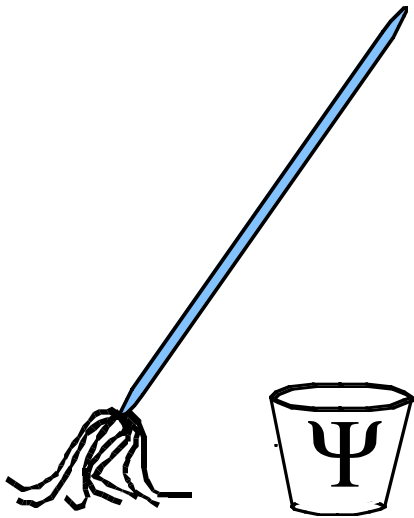
21.3.1. Using a ruler and a compass plot out the N -exciton states of a 3D isotropic harmonic oscillator for $N=3$ and for $N=4$ (as in Fig. 21.3.2(b)). Label each plot with tableaux state labels.

- Show how the energy levels would split for $N=1, 2, 3$, and 4 if oscillator-3 shifted up by 0.1ω .
- Plot the 2D oscillator states (as in Fig. 21.3.2(a)) that belong to each level that splits out.

To 4

21.3.2. How would you plot the states and their tableaux for a *four* dimensional (4D) oscillator?

- Do it for principal quantum number or “X-on” number $N=1, 2$, and 3 .
- Show how the energy levels would split if oscillator-4 shifted up by 0.1ω .



QM for AMOP

Chapter 22

Quantum Electromagnetic Fields

W. G. Harter

The most prevalent example of harmonic oscillator systems are electromagnetic fields, that is, light itself. Light is the genesis of Einstein-Planck quantum theory, and as shown in Unit 2, the putative source of relativity and quantum matter. A single plane em-wave mode is a 2D harmonic oscillator with two orthogonal polarization directions as described in Unit 1. So also is a single mode of a microwave cavity described by classical models in Unit 2 and by semi-classical models of light-matter interaction introduced in Unit 6. In this Unit 7 the light-matter interactions are extended to allow each protagonist, matter and light, to exhibit its quantum wave behavior in concert with the other.

Chapter 22 Quantum Electromagnetic Fields

22.1 QUANTUM ELECTROMAGNETIC FIELDS AND TRANSITIONS 2

- a. Classical Electromagnetic Fields and Operators 3
 - Classical Phasor Energy Relations 3
 - Classical Field Oscillator Variables 5
- b. Quantum Field Operators 6
- c. Electromagnetic Quantum States and Atomic Transitions 8
 - Single-Mode Atomic Dipole Transitions 9
 - Multimode Atomic Dipole Transitions 10
- c. "Impotence" of Photon Number States 13
- d. Coherent Radiation States 16
 - Do low-quantum fields make good coordinate frames? 17

22.2 SPECTRA OF ATOMS IN LASER CAVITY 19

- a. Jaynes-Cummings Hamiltonian 19
- b. Jaynes-Cummings Eigensolutions 22
- c. Transitions in the Jaynes-Cummings Model 24
 - Rayleigh scattering and fluorescence 25
 - Coherent Stokes Raman scattering 25

ADDITIONAL READING 29

22.1 QUANTUM ELECTROMAGNETIC FIELDS AND TRANSITIONS

The fully quantum-mechanical treatment of electromagnetic spectral transitions will be given now. It begins by converting the classical em field equations to harmonic oscillator equations for which the quantum states are well known.

A linearly polarized plane wave may be described by the following classical vector potential derived after (17.1.12) in Unit 6.

$$\mathbf{A} = \mathbf{e}_1 2|a| \sin(\mathbf{k} \cdot \mathbf{r} - \omega t + \phi) . \quad (22.1.1a)$$

This gives the following em fields (We add later the nonradiative or static field $\mathbf{E} = -\nabla\Phi$):

$$\begin{aligned} \mathbf{E} &= -\frac{\partial \mathbf{A}}{\partial t} & \mathbf{B} &= \nabla \times \mathbf{A} \\ &= \mathbf{e}_1 E_0 \cos(\mathbf{k} \cdot \mathbf{r} - \omega t + \phi) & &= (\mathbf{k} \times \mathbf{e}_1) B_0 \cos(\mathbf{k} \cdot \mathbf{r} - \omega t + \phi). \end{aligned} \quad (22.1.1b)$$

The electric E -polarization vector at zero phase is along unit vector \mathbf{e}_1 :

$$E_0 \mathbf{e}_1 = 2|a| \omega \mathbf{e}_1 . \quad (22.1.1c)$$

At the same time the magnetic B -polarization vector is along a unit vector $\mathbf{b}_1 = \mathbf{e}_2$, which is orthogonal to \mathbf{e}_1 and wave vector \mathbf{k} :

$$B_0 \mathbf{b}_1 = B_0 (\mathbf{k} \times \mathbf{e}_1) = \mathbf{e}_2 2|a| \omega / c \quad (\text{Let: } k = \omega / c) \quad (22.1.1d)$$

In preparation for a quantum-mechanical theory we shall rewrite the vector potential \mathbf{A} as follows:

$$\mathbf{A} = a_{k,1} \mathbf{e}_1 e^{i(\mathbf{k} \cdot \mathbf{r} - \omega t)} + a_{k,1}^* \mathbf{e}_1 e^{-i(\mathbf{k} \cdot \mathbf{r} - \omega t)} , \quad (22.1.2a)$$

where the complex phasor amplitude $a = a_{k,1}$ is given by

$$a_{k,1} = -i |a_{k,1}| e^{i\phi_{k,1}} . \quad (22.1.2b)$$

This sets us up to make classical canonical phase-space coordinates (a, a^*) for the field and, eventually, the quantum field operators $(\mathbf{a}, \mathbf{a}^\dagger)$.

It is instructive to calculate the magnitude of the phasor for one quantum of em action. In other words, we need the magnitude of the vector potential for a wave which contains one "photon" in a cavity of volume V . The time averaged em field energy $\langle U \rangle V$ for a plane wave in volume V follows using $\langle \cos^2 \omega t \rangle = \frac{1}{2}$. Average wave energy of E and B fields are equal, yet we think of B as the lesser field.

$$\begin{aligned} \langle U \rangle V &= \left\langle \frac{\epsilon_0}{2} \mathbf{E} \cdot \mathbf{E} + \frac{1}{2\mu_0} \mathbf{B} \cdot \mathbf{B} \right\rangle V = V \left(\frac{\epsilon_0}{2} 4|a|^2 \omega^2 + 4 \frac{|a|^2}{2\mu_0} k^2 \right) \langle \cos^2(\mathbf{k} \cdot \mathbf{r} - \omega t + \phi) \rangle \\ &= 2\epsilon_0 \omega^2 |a|^2 V = 2 \left(k^2 / \mu_0 \right) |a|^2 V \end{aligned} \quad (22.1.3)$$

We relate this to the Einstein-Planck energy-frequency relation ($\langle U \rangle V = \hbar n \omega$) for $n=1$ photon.

$$|a| = \sqrt{\frac{\hbar \omega}{2\epsilon_0 \omega^2 V}} = \sqrt{\frac{\hbar}{2\epsilon_0 \omega V}} = A \quad (\text{for one } (n=1) \text{ photon}). \quad (22.1.4)$$

This is the "photon unit" of quantum field \mathbf{A} . Note that it is an inverse root function of frequency, which in turn is proportional to the magnitude k of wave vector \mathbf{k} through the vacuum dispersion relation $\omega = ck = k/\sqrt{\mu_0 \epsilon_0}$. Again, note that E and B contribute equally in (22.1.3).

a. Classical Electromagnetic Fields and Operators

To completely describe an electromagnetic field in a box or "cavity" we need one phasor term like (22.1.2) for every possible value of \mathbf{k} and for each choice \mathbf{e}_1 or \mathbf{e}_2 of polarization orthogonal to \mathbf{k} . The complete expression for the classical \mathbf{A} is a sum over the possible modes:

$$\mathbf{A} = \sum_{\mathbf{k}} \left[(a_{\mathbf{k}1} \mathbf{e}_1 + a_{\mathbf{k}2} \mathbf{e}_2) e^{i(\mathbf{k} \cdot \mathbf{r} - \omega t)} + \text{c.c.} \right] = \sum_{\mathbf{k}} \sum_{\alpha=1}^2 \left[a_{\mathbf{k}\alpha} \mathbf{e}_\alpha e^{i(\mathbf{k} \cdot \mathbf{r} - \omega t)} + a_{\mathbf{k}\alpha}^* \mathbf{e}_\alpha e^{-i(\mathbf{k} \cdot \mathbf{r} - \omega t)} \right]. \quad (22.1.5a)$$

Here the \mathbf{k} vector satisfies box boundary conditions, that is, periodic conditions .

$$k_\beta = n_\beta \frac{2\pi}{L} \quad (n_\beta = 1, 2, \dots, j, \quad \beta = x, y, z) \quad (22.1.5b)$$

We let L be the length of each side of a cubic box. An \mathbf{A} time derivative gives electric \mathbf{E} field.

$$\mathbf{E} = -\frac{\partial \mathbf{A}}{\partial t} = \sum_{\mathbf{k}} \sum_{\alpha} \left[i a_{\mathbf{k}\alpha} \omega \mathbf{e}_\alpha e^{i(\mathbf{k} \cdot \mathbf{r} - \omega t)} - i a_{\mathbf{k}\alpha}^* \omega \mathbf{e}_\alpha e^{-i(\mathbf{k} \cdot \mathbf{r} - \omega t)} \right]. \quad (22.1.5c)$$

An \mathbf{A} curl gives electric field. magnetic \mathbf{B} field.

$$\mathbf{B} = \nabla \times \mathbf{A} = \sum_{\mathbf{k}} \sum_{\alpha} \left[i a_{\mathbf{k}\alpha} k \mathbf{b}_\alpha e^{i(\mathbf{k} \cdot \mathbf{r} - \omega t)} - i a_{\mathbf{k}\alpha}^* k \mathbf{b}_\alpha e^{-i(\mathbf{k} \cdot \mathbf{r} - \omega t)} \right], \quad (22.1.5d)$$

Where unit vector $\mathbf{b}_\alpha = \mathbf{k} \times \mathbf{e}_\alpha / k$ is orthogonal to \mathbf{k} and \mathbf{E} -polarization unit vector \mathbf{e} .

Classical Phasor Energy Relations

The classical Hamiltonian is a volume V integral of energy density (22.1.3). The electric contribution is

$$U_E V = \frac{\epsilon_0}{2} \int d^3 r \mathbf{E} \cdot \mathbf{E}, \quad (22.1.6a)$$

where

$$\begin{aligned} \mathbf{E} \cdot \mathbf{E} &= \sum_{k'\alpha'} \sum_{k\alpha} \left(i a_{k'\alpha'} \omega' \mathbf{e}_{\alpha'} e^{i(k' \cdot r - \omega' t)} + \text{c.c.} \right) \cdot \left(i a_{k\alpha} \omega \mathbf{e}_{\alpha} e^{i(k \cdot r - \omega t)} + \text{c.c.} \right) \\ &= \sum_{k'\alpha'} \sum_{k\alpha} \left[-a_{k'\alpha'} a_{k\alpha} \omega' \omega \mathbf{e}_{\alpha'} \cdot \mathbf{e}_{\alpha} e^{i(k'+k) \cdot r - i(\omega'+\omega)t} - a_{k'\alpha'}^* a_{k\alpha}^* \omega' \omega \mathbf{e}_{\alpha'} \cdot \mathbf{e}_{\alpha} e^{i(k'+k) \cdot r + i(\omega'+\omega)t} \right. \\ &\quad \left. + a_{k'\alpha'}^* a_{k\alpha} \omega' \omega \mathbf{e}_{\alpha'} \cdot \mathbf{e}_{\alpha} e^{i(k'-k) \cdot r - i(\omega'-\omega)t} + a_{k'\alpha'} a_{k\alpha}^* \omega' \omega \mathbf{e}_{\alpha'} \cdot \mathbf{e}_{\alpha} e^{i(k'-k) \cdot r + i(\omega'-\omega)t} \right] \end{aligned} \quad (22.1.6b)$$

This simplifies if we use wave and polarization normalization conditions:

$$\int d^3 r e^{i(k'+k) \cdot r} = \delta_{k',-k} V \quad \text{and} \quad \mathbf{e}_{\alpha'} \cdot \mathbf{e}_{\alpha} = \delta_{\alpha'\alpha}$$

The result is

$$U_E V = \sum_{k\alpha} \frac{\epsilon_0 V}{2} \left[|a_{k\alpha}|^2 \omega^2 - a_{-k\alpha}^* a_{k\alpha}^* \omega^2 e^{-2i\omega t} - a_{-k\alpha} a_{k\alpha} \omega^2 e^{-2i\omega t} \right] \quad (22.1.7)$$

The magnetic energy $U_B V = \int d^3 r \mathbf{B} \cdot \mathbf{B} / 2\mu_0$ is like (22.1.6) if we do the following substitutions.

$$\mathbf{E} \rightarrow \mathbf{B}, \quad \frac{\epsilon_0}{2} \rightarrow \frac{1}{2\mu_0}, \quad \omega \mathbf{e}_{\alpha} \rightarrow k \mathbf{b}_{\alpha} \equiv \mathbf{k} \times \mathbf{e}_{\alpha}, \quad \omega' \mathbf{e}_{\alpha'} \equiv \mathbf{k}' \times \mathbf{e}_{\alpha'}$$

After integration the cross terms have the opposite sign as they did in (22.1.6b). We get $\delta_{k',-k} k k' = -k^2$ in the $\mathbf{B} \cdot \mathbf{B}$ integral instead of $\delta_{k',-k} \omega \omega' = \omega^2$ which arose in the $\mathbf{E} \cdot \mathbf{E}$ integral. The magnetic energy is

$$\begin{aligned} U_B V &= \sum_{k\alpha} \frac{V}{2\mu_0} \left[2 |a_{k\alpha}|^2 k^2 + a_{-k\alpha}^* a_{k\alpha}^* k^2 e^{2i\omega t} + a_{-k\alpha} a_{k\alpha} k^2 e^{-2i\omega t} \right] \\ &= \sum_{k\alpha} \frac{\epsilon_0 V}{2} \left[2 |a_{k\alpha}|^2 \omega^2 + a_{-k\alpha}^* a_{k\alpha}^* \omega^2 e^{2i\omega t} + a_{-k\alpha} a_{k\alpha} \omega^2 e^{-2i\omega t} \right]. \end{aligned} \quad (22.1.8)$$

The second line uses the optical dispersion relation.

$$\omega^2 = c^2 k^2 = k^2 / (\mu_0 \epsilon_0) \quad (22.1.9)$$

A change of sign makes the electric cross-terms in (22.1.7) cancel the magnetic ones in (22.1.8). Their sum is then just a sum of elementary mode energy density values (22.1.3). That simple formula leads to the basic Hamiltonian needed to set up quantum field theory in terms of quantum oscillators.

$$UV = (U_E + U_B)V = \sum_{\mathbf{k}\alpha} 2\varepsilon_0\omega^2 |a_{\mathbf{k}\alpha}|^2 V. \quad (22.1.10)$$

Each \mathbf{k} and polarization $\mathbf{e}_{\mathbf{k},\alpha}$ labeled mode is described by a classical complex phasor variable $a_{\mathbf{k},\alpha}$. The real and imaginary parts of $a_{\mathbf{k},\alpha}$ can be treated as classical position $Q_{\mathbf{k},\alpha}$ and momentum $P_{\mathbf{k},\alpha}$ of an oscillator of unit mass as described in Chapter 20 in close analogy is to the 2-dimensional *ABCD* oscillator variables (X_α, P_α) defined by (10.1.1).

Classical Field Oscillator Variables

Let us factor the phasor expression for field energy as follows so it becomes 2N dimensional oscillator energy.

$$\begin{aligned} UV &= \sum_{\mathbf{k}\alpha} 2\varepsilon_0 V \omega^2 a_{\mathbf{k}\alpha}^* a_{\mathbf{k}\alpha} = \sum_{\mathbf{k}\alpha} \frac{1}{2} \left[2\omega\sqrt{\varepsilon_0 V} (a_{\mathbf{k}\alpha}^{\text{Re}} - ia_{\mathbf{k}\alpha}^{\text{Im}}) \right] \left[2\omega\sqrt{\varepsilon_0 V} (a_{\mathbf{k}\alpha}^{\text{Re}} - ia_{\mathbf{k}\alpha}^{\text{Im}}) \right] \\ &= \sum_{\mathbf{k}\alpha} \frac{1}{2} [\omega Q_{\mathbf{k}\alpha} + iP_{\mathbf{k}\alpha}] [\omega Q_{\mathbf{k}\alpha} + iP_{\mathbf{k}\alpha}] \\ &= \sum_{\mathbf{k}\alpha} \frac{1}{2} (P_{\mathbf{k}\alpha}^2 + \omega^2 Q_{\mathbf{k}\alpha}^2) \end{aligned} \quad (22.1.11)$$

Note that vacuum dispersion frequency is a linear function $\omega=c\cdot k$ of k , but may be a non-linear function for light-matter waves (polarons) in solids. The canonical phase space variables are

$$Q_{\mathbf{k}\alpha} = 2\sqrt{\varepsilon_0 V} a_{\mathbf{k}\alpha}^{\text{Re}} = \sqrt{\varepsilon_0 V} (a_{\mathbf{k}\alpha} + a_{\mathbf{k}\alpha}^*) \quad (22.1.12a)$$

$$P_{\mathbf{k}\alpha} = 2\omega\sqrt{\varepsilon_0 V} a_{\mathbf{k}\alpha}^{\text{Im}} = \omega\sqrt{\varepsilon_0 V} (a_{\mathbf{k}\alpha} - a_{\mathbf{k}\alpha}^*)/i. \quad (22.1.12b)$$

The inverse of the foregoing gives the original phasor variables and their conjugates in terms of P's and Q's:

$$a_{\mathbf{k}\alpha} = a_{\mathbf{k}\alpha}^{\text{Re}} + ia_{\mathbf{k}\alpha}^{\text{Im}} = \frac{1}{2\sqrt{\varepsilon_0 V}} (Q_{\mathbf{k}\alpha} + iP_{\mathbf{k}\alpha}/\omega), \quad (22.1.13a)$$

$$a_{\mathbf{k}\alpha}^* = a_{\mathbf{k}\alpha}^{\text{Re}} - ia_{\mathbf{k}\alpha}^{\text{Im}} = \frac{1}{2\sqrt{\varepsilon_0 V}} (Q_{\mathbf{k}\alpha} - iP_{\mathbf{k}\alpha}/\omega). \quad (22.1.13b)$$

The cavity energy UV in (22.1.11) shall be the classical electromagnetic field Hamiltonian function $H = H(Q,P)$. H describes a set of independent harmonic oscillators. To obtain a quantum field theory we make these into quantum oscillators. The situation is very similar to molecular or solid state vibration problems in which classical normal modes are quantized to give "phonons" or "polarons."

b. Quantum Field Operators

Oscillator ladder operations \mathbf{a} and \mathbf{a}^\dagger are defined by (20.2.1) in terms of coordinate and momentum operators of a mass- M particle. For each (\mathbf{k}, α) mode this definition, with $M=1$, becomes the following.

$$\mathbf{a}_{\mathbf{k}\alpha} = \sqrt{\frac{\omega}{2\hbar}} (\mathbf{Q}_{\mathbf{k}\alpha} + i\mathbf{P}_{\mathbf{k}\alpha}/\omega), \quad (22.1.14a)$$

$$\mathbf{a}_{\mathbf{k}\alpha}^\dagger = \sqrt{\frac{\omega}{2\hbar}} (\mathbf{Q}_{\mathbf{k}\alpha} - i\mathbf{P}_{\mathbf{k}\alpha}/\omega), \quad (22.1.14b)$$

Here boldface notation $\mathbf{Q}_{\mathbf{k}}$ and $\mathbf{P}_{\mathbf{k}}$ indicates the quantum operators that correspond to the classical phase variables $Q_{\mathbf{k}}$ and $P_{\mathbf{k}}$, respectively.

By comparing (22.1.14) with (22.1.13) we note that the ladder operators are proportional to whatever operator would correspond to the classical phasor amplitude. So with correspondence $\mathbf{Q}_{\mathbf{k}\alpha}$ with $Q_{\mathbf{k}}$ and $\mathbf{P}_{\mathbf{k}}$ with $P_{\mathbf{k}}$ we have the following phasor correspondence relations:

$$\begin{aligned} a_{\mathbf{k}\alpha} &= \frac{1}{2\sqrt{\varepsilon_0 V}} (Q_{\mathbf{k}\alpha} + iP_{\mathbf{k}\alpha}/\omega) \rightarrow \frac{1}{2\sqrt{\varepsilon_0 V}} (\mathbf{Q}_{\mathbf{k}\alpha} + i\mathbf{P}_{\mathbf{k}\alpha}/\omega) = \frac{1}{2\sqrt{\varepsilon_0 V}} \sqrt{\frac{2\hbar}{\omega}} \mathbf{a}_{\mathbf{k}\alpha} = \sqrt{\frac{\hbar}{2\varepsilon_0 \omega V}} \mathbf{a}_{\mathbf{k}\alpha}, \\ a_{\mathbf{k}\alpha}^* &= \frac{1}{2\sqrt{\varepsilon_0 V}} (Q_{\mathbf{k}\alpha} - iP_{\mathbf{k}\alpha}/\omega) \rightarrow \frac{1}{2\sqrt{\varepsilon_0 V}} (\mathbf{Q}_{\mathbf{k}\alpha} - i\mathbf{P}_{\mathbf{k}\alpha}/\omega) = \frac{1}{2\sqrt{\varepsilon_0 V}} \sqrt{\frac{2\hbar}{\omega}} \mathbf{a}_{\mathbf{k}\alpha}^\dagger = \sqrt{\frac{\hbar}{2\varepsilon_0 \omega V}} \mathbf{a}_{\mathbf{k}\alpha}^\dagger, \end{aligned} \quad (22.1.15)$$

The proportionality or scale factor in (22.1.15) is just the “photon amplitude” derived in (22.1.4). Note that coordinate and momentum operators are observables and are self-conjugate ($\mathbf{Q} = \mathbf{Q}^\dagger$ and $\mathbf{P} = \mathbf{P}^\dagger$). The phasor operator \mathbf{a} is a complex combination of observables and thus not a self-conjugate observable itself.

The oscillator Hamiltonian operator for the quantum field is the same form as (20.2.4), namely,

$$H = \sum_{\mathbf{k}\alpha} \hbar\omega_{\mathbf{k}\alpha} \left(\mathbf{a}_{\mathbf{k}\alpha}^\dagger \mathbf{a}_{\mathbf{k}\alpha} + \frac{1}{2} \right). \quad (22.1.16)$$

This is the same for the classical energy (8.5.10) or (22.1.11) except for the extra $\hbar\omega_{\mathbf{k}\alpha}/2$ terms which are each (\mathbf{k}, α) mode's quantum zero-point energy. Number operator ($\mathbf{a}_{\mathbf{k}\alpha}^\dagger \mathbf{a}_{\mathbf{k}\alpha}$)-eigenvalues are the number $n_{\mathbf{k}\alpha}$ of (\mathbf{k}, α) “photons” or field quanta and each $\mathbf{a}_{\mathbf{k}\alpha}^\dagger$ (or $\mathbf{a}_{\mathbf{k}\alpha}$) can raise (or lower) its assigned photon number.

$$\begin{aligned} \mathbf{a}_{\mathbf{k}\alpha}^\dagger \left| \cdots n_{\mathbf{k}\alpha} \cdots n_{\mathbf{k}'\alpha'} \cdots \right\rangle &= \sqrt{n_{\mathbf{k}\alpha} + 1} \left| \cdots n_{\mathbf{k}\alpha} + 1 \cdots n_{\mathbf{k}'\alpha'} \cdots \right\rangle, \\ \mathbf{a}_{\mathbf{k}\alpha} \left| \cdots n_{\mathbf{k}\alpha} \cdots n_{\mathbf{k}'\alpha'} \cdots \right\rangle &= \sqrt{n_{\mathbf{k}\alpha}} \left| \cdots n_{\mathbf{k}\alpha} - 1 \cdots n_{\mathbf{k}'\alpha'} \cdots \right\rangle, \\ \mathbf{a}_{\mathbf{k}'\alpha'}^\dagger \left| \cdots n_{\mathbf{k}\alpha} \cdots n_{\mathbf{k}'\alpha'} \cdots \right\rangle &= \sqrt{n_{\mathbf{k}'\alpha'} + 1} \left| \cdots n_{\mathbf{k}\alpha} \cdots n_{\mathbf{k}'\alpha'} + 1 \cdots \right\rangle, \\ \mathbf{a}_{\mathbf{k}'\alpha'} \left| \cdots n_{\mathbf{k}\alpha} \cdots n_{\mathbf{k}'\alpha'} \cdots \right\rangle &= \sqrt{n_{\mathbf{k}'\alpha'}} \left| \cdots n_{\mathbf{k}\alpha} \cdots n_{\mathbf{k}'\alpha'} - 1 \cdots \right\rangle. \end{aligned} \quad (22.1.17)$$

These relations follow (20.2.13). Here each additional quanta contributes an increase in \mathbf{A} amplitude equal to the scale factor $\sqrt{\hbar/2\varepsilon_0\omega V}$ that appears in the correspondence relation (22.1.15).

The quantum \mathbf{A} -field operator corresponding to the classical field (22.1.5a) is found by replacing $a_{\mathbf{k}\alpha}$ and $a_{\mathbf{k}\alpha}^\dagger$ according to (22.1.15):

$$\mathbf{A} = \sum_{\mathbf{k}\alpha} \sqrt{\frac{\hbar}{2\varepsilon_0\omega V}} \left[\mathbf{a}_{\mathbf{k}\alpha} \mathbf{e}_\alpha e^{i(\mathbf{k}\cdot\mathbf{r}-\omega t)} + \mathbf{a}_{\mathbf{k}\alpha}^\dagger \mathbf{e}_\alpha e^{-i(\mathbf{k}\cdot\mathbf{r}-\omega t)} \right]. \quad (22.1.18)$$

Time dependence of ladder operators is determined by Bloch equations: $i\hbar\dot{\mathbf{O}} = [\mathbf{H}, \mathbf{O}]$ [Recall (10.5.12)]:

$$\begin{aligned} i\hbar\dot{\mathbf{a}}_{\mathbf{k}\alpha} &= [\mathbf{H}, \mathbf{a}_{\mathbf{k}\alpha}] & i\hbar\dot{\mathbf{a}}_{\mathbf{k}\alpha}^\dagger &= [\mathbf{H}, \mathbf{a}_{\mathbf{k}\alpha}^\dagger] \\ &= -\hbar\omega\mathbf{a}_{\mathbf{k}\alpha} & &= \hbar\omega\mathbf{a}_{\mathbf{k}\alpha}^\dagger \end{aligned}$$

Here we use the $\mathbf{a}^\dagger\mathbf{a}$ form (22.1.16) of the field Hamiltonian and the N-dimensional commutation relation (21.1.5) that is repeated in the following [Recall also (20.2.3)]:

$$[\mathbf{a}_{\mathbf{k}\alpha}, \mathbf{a}_{\mathbf{k}'\alpha'}^\dagger] = \delta_{\mathbf{k},\mathbf{k}'}\delta_{\alpha,\alpha'}1. \quad (22.1.19)$$

According to the foregoing $\dot{\mathbf{a}}$ equations the ladder operators have the following time-dependent phases:

$$\mathbf{a}_{\mathbf{k}\alpha} = \mathbf{a}_{\mathbf{k}\alpha}(0)e^{i\omega t}, \quad \mathbf{a}_{\mathbf{k}\alpha}^\dagger = \mathbf{a}_{\mathbf{k}\alpha}^\dagger(0)e^{-i\omega t}$$

The phases cancel time factors in (22.1.18) to give a time-independent field operator.

$$\mathbf{A} = \sum_{\mathbf{k}\alpha} \sqrt{\frac{\hbar}{2\varepsilon_0\omega V}} \left[\mathbf{a}_{\mathbf{k}\alpha}(0) e^{i\mathbf{k}\cdot\mathbf{r}} + \mathbf{a}_{\mathbf{k}\alpha}^\dagger(0) e^{-i\mathbf{k}\cdot\mathbf{r}} \right] \mathbf{e}_\alpha \quad (22.1.20a)$$

The electric and magnetic quantum field operators follow from (22.1.15).

$$\mathbf{E} = \sum_{\mathbf{k}\alpha} \sqrt{\frac{\hbar}{2\varepsilon_0\omega V}} \left[i\omega\mathbf{a}_{\mathbf{k}\alpha}(0) e^{i\mathbf{k}\cdot\mathbf{r}} - i\omega\mathbf{a}_{\mathbf{k}\alpha}^\dagger(0) e^{-i\mathbf{k}\cdot\mathbf{r}} \right] \mathbf{e}_\alpha \quad (22.1.20b)$$

$$\mathbf{B} = \sum_{\mathbf{k}\alpha} \sqrt{\frac{\hbar}{2\varepsilon_0\omega V}} \left[i\mathbf{k}\mathbf{a}_{\mathbf{k}\alpha}(0) e^{i\mathbf{k}\cdot\mathbf{r}} - i\mathbf{k}\mathbf{a}_{\mathbf{k}\alpha}^\dagger(0) e^{-i\mathbf{k}\cdot\mathbf{r}} \right] \mathbf{b}_\alpha \quad (22.1.20c)$$

When atoms are much smaller than the wavelength $\lambda = 2\pi/k$ of the radiation, the fields can be simplified by the *dipole approximation* $e^{i\mathbf{k}\cdot\mathbf{r}} \cong 1$.

$$\mathbf{A} \equiv \sum_{\mathbf{k}\alpha} \sqrt{\frac{\hbar}{2\varepsilon_0\omega V}} \left[\mathbf{a}_{\mathbf{k}\alpha} + i\omega \mathbf{a}_{\mathbf{k}\alpha}^\dagger \right] \mathbf{e}_\alpha = \sum_{\mathbf{k}\alpha} \sqrt{\frac{1}{\varepsilon_0 V}} \mathbf{Q}_{\mathbf{k}\alpha} \mathbf{e}_\alpha, \quad (22.1.20d)$$

$$\mathbf{E} \equiv \sum_{\mathbf{k}\alpha} \sqrt{\frac{\hbar}{2\varepsilon_0\omega V}} i\omega \left[\mathbf{a}_{\mathbf{k}\alpha} - \mathbf{a}_{\mathbf{k}\alpha}^\dagger \right] \mathbf{e}_\alpha = \sum_{\mathbf{k}\alpha} \sqrt{\frac{1}{\varepsilon_0 V}} \mathbf{P}_{\mathbf{k}\alpha} \mathbf{e}_\alpha, \quad (22.1.20e)$$

$$\mathbf{B} \equiv \sum_{\mathbf{k}\alpha} \sqrt{\frac{\hbar}{2\varepsilon_0\omega V}} ik \left[\mathbf{a}_{\mathbf{k}\alpha} - \mathbf{a}_{\mathbf{k}\alpha}^\dagger \right] \mathbf{b}_\alpha. \quad (22.1.20f)$$

Note also the simple connection between the approximate \mathbf{A} and \mathbf{E} and the canonical field coordinates $\mathbf{Q}_{\mathbf{k}}$ and momenta $\mathbf{P}_{\mathbf{k}}$ which follows from (22.1.14).

c. Electromagnetic Quantum States and Atomic Transitions

Consider an atom coupled to an electromagnetic cavity. Suppose this system starts in a state in which the atomic state is $|s\rangle$ and all the photon numbers $n_{\mathbf{k}\alpha}^s$ are definitely known. We consider some of the possible final states and their probabilities as a function of time.

The states of the whole system at the start and finish will be labeled $|S\rangle$ and $|F\rangle$, respectively.

The starting state $|S\rangle$ is a ket-ket product of atomic $|s\rangle$ and radiation $|\cdots n_{\mathbf{k}\alpha}^s \cdots n_{\mathbf{k}'\alpha'}^s \cdots\rangle$ states:

$$|S\rangle = |s\rangle |\cdots n_{\mathbf{k}\alpha}^s \cdots n_{\mathbf{k}'\alpha'}^s \cdots\rangle$$

The final state is written in a similar way:

$$|F\rangle = |f\rangle |\cdots n_{\mathbf{k}\alpha}^f \cdots n_{\mathbf{k}'\alpha'}^f \cdots\rangle$$

One may picture the states by imagining atomic and electromagnetic levels as sketched in Fig.

22.1.1. A typical transition that conserves energy (more or less) can be imagined as going from the state on one side of the figure to the other. There we imagine that the atom jumps *up* from level $|s\rangle$ to $|f\rangle$ while simultaneously one mode number jumps *down* one level. This is an atomic *absorption* process. (The atom appears to swallow a photon.) If this is reversed, or if the atom jumps *down* from level $|s\rangle$ to $|f\rangle$ while a mode number jumps *up*, the process is called an *emission*. (The atom appears to spit out a photon.) As we will see, these two processes are usually the most likely ones.

The derivation of the probabilities for quantum field atomic transitions of the type shown in Fig. 22.1.1 are given now. This derivation uses the first-order perturbation formula that only involves creating or destroying one photon. Higher N^{th} -order processes involve products of the 1^{st} -order factors discussed below and are called N -photon processes for that reason.

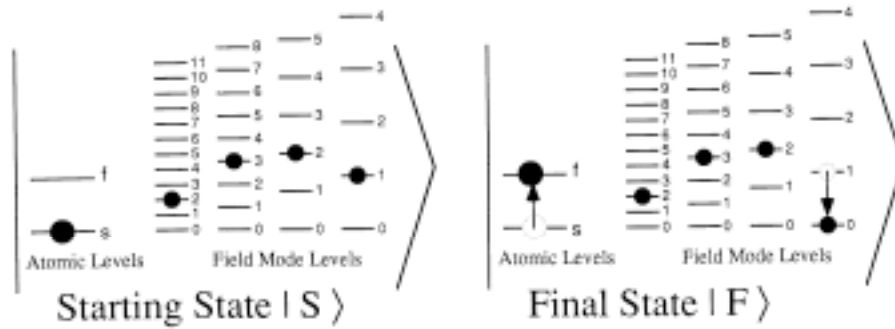


Fig. 22.1.1 Atom-field energy levels for initial and final states in an atomic absorption process involving a single photon from a resonant electromagnetic field mode.

The 1st-order perturbation results of (18.2.5) involve integral terms that is a *spectral functions* $S(\Delta,t)$.

$$c_F^{(1)}(t) = \delta_{FS} + \frac{1}{i\hbar} \int_0^t dt_1 e^{i\omega_{FW}t_1} \langle F | H_I | S \rangle = \delta_{FS} + \frac{1}{i\hbar} S(\omega_{FS}, t) \langle F | H_I | S \rangle \text{ where: } S(\Delta, t) = 2e^{it\Delta/2} \frac{\sin(t\Delta/2)}{\Delta} \tag{22.1.21}$$

The spectral function is plotted Fig. 18.2.1. Here its *detuning parameter* Δ includes the difference of both the atomic and radiation energy.

$$\Delta = \omega_{FS} \equiv \omega_F - \omega_S = \left[\omega_f + \sum_{\mathbf{k}\alpha} \left(n_{\mathbf{k}\alpha}^f + \frac{1}{2} \right) \omega_{\mathbf{k}} \right] - \left[\omega_s + \sum_{\mathbf{k}\alpha} \left(n_{\mathbf{k}\alpha}^s + \frac{1}{2} \right) \omega_{\mathbf{k}} \right]. \tag{22.1.22}$$

For the absorption process depicted in Fig. 22.1.1 the mode number has gone down one step for the (\mathbf{k},α) mode $n_{\mathbf{k}\alpha}^f = n_{\mathbf{k}\alpha}^s - 1$ while the atom went up. Other quanta stay the same, so the detuning is

$$\Delta = \omega_f - \omega_s - \omega_{\mathbf{k}} = \omega_{fs} - \omega_{\mathbf{k}}.$$

Zero detuning means having a mode whose frequency $\omega_{\mathbf{k}\alpha}$ matches the atomic transition frequency ω_{fs} , just like the semi-classical definition (18.2.5g) for absorption resonance. (Compare it to the Δ above.)

Now we see some important differences between quantum field theory calculations and semi-classical ones. For one thing, if you really insist on counting every photon, then the absorption and emission processes become quite distinct.

Single-Mode Atomic Dipole Transitions

A 1st-order S to F transition probability $|c_F|^2$ obtained follows from (22.1.21) assuming $S \neq F$.

$$P_{F \leftarrow S} = |c_F|^2 = \left| \langle F | H_I | S \rangle \right|^2 \frac{\sin^2(t\Delta/2)}{\hbar^2 (\Delta/2)^2}. \tag{22.1.23}$$

We now evaluate the matrix element of the $\mathbf{E} \cdot \mathbf{r}$ interaction operator in (17.1.20)

$$H_I = q\mathbf{E} \cdot \mathbf{r} \cong -q \sum_{\mathbf{k}\alpha} \sqrt{\frac{\hbar}{2\varepsilon_0\omega V}} \left[i\omega \mathbf{a}_{\mathbf{k}\alpha} - i\omega \mathbf{a}_{\mathbf{k}\alpha}^\dagger \right] \mathbf{e}_\alpha \cdot \mathbf{r} \quad (22.1.24)$$

The quantized E field (22.1.20b) is used with the dipole approximation $e^{i\mathbf{k}\cdot\mathbf{r}} \cong 1$. The matrix element consists of a field part followed by the atomic matrix elements $\langle f | \mathbf{r} | s \rangle = (\langle f | x | s \rangle, \langle f | y | s \rangle, \langle f | z | s \rangle)$.

$$\langle F | H_I | S \rangle = q \sum_{\mathbf{k}\alpha} \left[\langle \dots n_{\mathbf{k}\alpha}^f \dots | i\mathbf{a}_{\mathbf{k}\alpha}^\dagger | \dots n_{\mathbf{k}\alpha}^s \dots \rangle - \langle \dots n_{\mathbf{k}\alpha}^f \dots | i\mathbf{a}_{\mathbf{k}\alpha} | \dots n_{\mathbf{k}\alpha}^s \dots \rangle \right] \sqrt{\frac{\hbar\omega}{2\varepsilon_0 V}} \mathbf{e}_\alpha \cdot \langle f | \mathbf{r} | s \rangle.$$

The field part of this matrix element is quite selective. If more than one mode changes its photon number, the whole thing is zero. (Recall that $\langle n | n' \rangle = \delta_{nn'}$.) The only possible nonzero elements occur when a single mode goes up or down by exactly one photon. The two possible types of nonzero matrix elements are listed in the following:

$$\langle F | H_I | S \rangle = \left[i\sqrt{n_{\mathbf{k}\alpha}^s + 1} + 0 \right] \sqrt{\frac{\hbar\omega}{2\varepsilon_0 V}} q \mathbf{e}_\alpha \cdot \mathbf{r}_{fs} \quad \text{if all } n^f = n^s \text{ except } n_{\mathbf{k}\alpha}^f = n_{\mathbf{k}\alpha}^s + 1 \quad (1 \text{ photon emission})$$

$$\langle F | H_I | S \rangle = \left[0 - i\sqrt{n_{\mathbf{k}\alpha}^s} \right] \sqrt{\frac{\hbar\omega}{2\varepsilon_0 V}} q \mathbf{e}_\alpha \cdot \mathbf{r}_{fs} \quad \text{if all } n^f = n^s \text{ except } n_{\mathbf{k}\alpha}^f = n_{\mathbf{k}\alpha}^s - 1 \quad (1 \text{ photon absorption})$$

$$\langle F | H_I | S \rangle = 0, \quad \text{otherwise.} \quad (22.1.25)$$

Field matrix elements follow from (22.1.17). Atomic dipole expectation value is denoted by $\mathbf{r}_{fs} = \langle f | \mathbf{r} | s \rangle$.

If matrix element (22.1.25) allows any transition between $|S\rangle$ and $|F\rangle$ it is an emission or *else* an absorption *but not both*. If it allows one, then the probability for the other is zero. This is very different from the semi-classical transition amplitude (18.2.5) or (18.3.2) in which both processes would simultaneously have non-vanishing probability. The semi-classical amplitude is a sum of a resonant and a non-resonant spectral function. The quantum amplitude (22.1.21) has only one spectral function in the c_F expression. Strict photon counting prevents absorption from interfering with emission.

Multimode Atomic Dipole Transitions

Suppose we accept (or are forced to accept) any of a set of possible final photon states ranging from state $|F\rangle = |f\rangle | \dots n_{\mathbf{k}\alpha} - 1 \dots n_{\mathbf{k}'\alpha'} \dots \rangle$ in which mode (\mathbf{k}, α) lost a photon to state $|F'\rangle = |f\rangle | \dots n_{\mathbf{k}\alpha} \dots n_{\mathbf{k}'\alpha'} - 1 \dots \rangle$ in which mode (\mathbf{k}', α') lost a photon. In each case the atom jumps up from state $|s\rangle$ to state $|f\rangle$, but here we let it accept a photon from a range of cavity modes. It is only necessary that the donor modes have nonzero

photon number and a frequency $\omega_{k\alpha}$ that is close enough to the atomic transition frequency $\omega_f - \omega_s = \omega_{fs}$ so the spectral function $|S|^2$ gives a measurable value.

The total probability for the atomic $f \leftarrow s$ transition will be a sum of probabilities $|c_F|^2 + \dots + |c_{F'}|^2$ as though the contribution of each mode is distinct:

$$P_{f \leftarrow s} = |c_F|^2 + \dots + |c_{F'}|^2 = \sum_{k\alpha} |c_F|^2 = \sum_{k\alpha} \frac{\sin^2(t\Delta/2)}{\hbar^2 (\Delta/2)^2} |\langle H_I \rangle|^2. \quad (22.1.26)$$

Since we are effectively counting the photons from each mode, the amplitudes $c_F \dots c_{F'}$ have random relative phases and interference between them is washed out. Hence the total probability is the sum of their squares $\sum |c_F|^2$ instead of the more complicated square of the sum $|\sum c_F|^2$. (Recall the distinction between incoherent “peeking” and coherent interference in equations (1.3.10) and (1.3.11) of Ch. 1.)

The sum over mode wave vector \mathbf{k} can be converted to an integral over $k = [\mathbf{k}]$ or over mode frequency $\omega = ck$. According to (22.1.5b) the \mathbf{k} sum is a sum over integer values of photon number $n_\alpha = k_\alpha L/2\pi = 1, 2, \dots$, that converts to the following integral.

$$\sum_k = \sum_{n_x} \sum_{n_y} \sum_{n_z} \Delta n_x \Delta n_y \Delta n_z \equiv \int dk_x \frac{\Delta n_x}{\Delta k_x} \int dk_y \frac{\Delta n_y}{\Delta k_y} \int dk_z \frac{\Delta n_z}{\Delta k_z} = \left(\frac{L}{2\pi} \right)^3 \int dk_x \int dk_y \int dk_z.$$

Here the sum is converted to an integral over Cartesian k components using

$$\Delta n_x = 1 = \frac{L}{2\pi} \Delta k_x, \quad \Delta n_y = 1 = \frac{L}{2\pi} \Delta k_y, \quad \Delta n_z = 1 = \frac{L}{2\pi} \Delta k_z.$$

This sum can then be converted to a polar coordinate integral in k space.

$$\sum_k = \left(\frac{L}{2\pi} \right)^3 \int d^3\mathbf{k} = \frac{V}{(2\pi)^3} \int d\Omega_k \int k^2 dk = \frac{V}{(2\pi)^3} \int d\phi_k \int d\theta_k \sin\theta_k \quad (22.1.27)$$

(ϕ_k, θ_k) are azimuth and polar angles of \mathbf{k} , $d\Omega_k$ is the incremental solid angle in k -space, and $V = L^3$ is the cavity volume. This reduces the probability sum (22.1.26) to an integral over solid angle and k or $\omega = ck$.

$$P_{f \leftarrow s} = \sum_\alpha \frac{V}{(2\pi)^3} \int d\Omega_k \int_0^\infty k^2 dk |c_F|^2 = \sum_\alpha \frac{V}{(2\pi)^3} \int d\Omega_k \int_0^\infty \frac{\omega^2}{c^3} d\omega |c_F|^2 = \sum_\alpha \frac{V}{(2\pi)^3} \int d\Omega_k \int d\omega \frac{\omega^2}{c^3} \frac{\sin^2(t\Delta/2)}{\hbar^2 (\Delta/2)^2} |\langle H_I \rangle|^2 \quad (22.1.28)$$

Now we approximate the integral of the spectral function $|S(\Delta, t)|^2$ by assuming that time t is large enough that $|S|^2$ becomes very narrow. (Recall Fig. 18.2.2.) Then most of the probability comes from the neighborhood around zero detuning ($\Delta = 0$). We may set $\omega_{k\alpha} = \omega = \omega_{fs}$ and put all other functions of frequency outside the integral.

$$P_{f \leftarrow s} \cong \sum_{\alpha} \frac{V}{(2\pi)^3} \int d\Omega_{\mathbf{k}} \frac{\omega^2}{\hbar^2 c^3} |\langle H_I \rangle|^2 \int_0^{\infty} d\omega \frac{\sin^2(t\Delta/s)}{\hbar^2 (\Delta/2)^2}$$

The area under the spectral function is simply the elapsed time multiplied by 2π as was noted after the Fermi Golden Rule equation (18.7.10).

$$P_{f \leftarrow s} \cong \sum_{\alpha} \int d\Omega_{\mathbf{k}} \frac{V\omega}{(2\pi)^3 \hbar^2 c^3} |\langle H_I \rangle|^2 2\pi \cdot t \quad (22.1.29)$$

The peak of the spectral function at $\Delta = 0$ goes up quadratically with time, but the area only increases linearly. The width of the peak decreases linearly with time according to the uncertainty relation (18.2.9). As a result the time derivative or rate $R_{f \leftarrow s} = \dot{P}_{f \leftarrow s}$ of the transition probability is a constant in this approximation, the *Fermi golden rule* of constant transition rates. (Recall (18.2.11).)

$$R_{f \leftarrow s} \cong \sum_{\alpha} \int d\Omega_{\mathbf{k}} \rho(\omega_{fs}) |\langle H_I \rangle|^2 \frac{2\pi}{\hbar^2}, \quad (22.1.30a)$$

Here the spectral density of modes $\rho(\omega)$ is defined.

$$\rho(\omega) = \frac{V\omega^2}{(2\pi)^3 c^3}. \quad (22.1.30b)$$

The absorption dipole matrix element (22.1.25) gives the following rate if the photon number in near-resonant modes is $n_{k\alpha}^s \equiv n$:

$$\begin{aligned} R_{f \leftarrow s} &= n \frac{V\omega^2}{(2\pi)^3 c^3} \frac{2\pi}{\hbar^2} \frac{\hbar\omega}{2\epsilon_0 V} q^2 \sum_{\alpha} \int d\Omega_{\mathbf{k}} |\mathbf{e}_{\alpha} \cdot \mathbf{r}_{fs}|^2 \\ &= n \left(\frac{\omega^3}{\hbar c^3} \right) \left(\frac{q^2}{4\pi\epsilon_0} \right) \int d\Omega_{\mathbf{k}} \left(|\mathbf{e}_1 \cdot \mathbf{r}_{fs}|^2 + |\mathbf{e}_2 \cdot \mathbf{r}_{fs}|^2 \right). \end{aligned}$$

The polarization sum and integral is simplified by using the vector relation

$$|r|^2 = |\mathbf{e}_1 \cdot \mathbf{r}|^2 + |\mathbf{e}_2 \cdot \mathbf{r}|^2 + |\hat{\mathbf{k}} \cdot \mathbf{r}|^2.$$

If we let the induced dipole $\mathbf{r} = \mathbf{r}_{fs}$ be along the polar z axis, then $\hat{\mathbf{k}} \cdot \mathbf{r}_{fs} = |\mathbf{r}_{fs}| \cos \theta_k$. The sum and integral is then easily evaluated:

$$\begin{aligned} \sum_{\alpha} \int d\Omega_k |\mathbf{e}_{\alpha} \cdot \mathbf{r}_{fs}|^2 &= \int d\Omega_k \left(|\mathbf{e}_1 \cdot \mathbf{r}_{fs}|^2 + |\mathbf{e}_2 \cdot \mathbf{r}_{fs}|^2 + |\hat{\mathbf{k}} \cdot \mathbf{r}_{fs}|^2 - |\hat{\mathbf{k}} \cdot \mathbf{r}_{fs}|^2 \right) \\ &= \int d\Omega_k (1 - \cos^2 \theta_k) |\mathbf{r}_{fs}|^2 = \int d\phi \int d\theta \sin^3 \theta |\mathbf{r}_{fs}|^2 = \frac{8\pi}{3} |\mathbf{r}_{fs}|^2. \end{aligned}$$

The resulting absorption rate is

$$R_{f \leftarrow s}(\text{absorption}) \equiv nA = n \frac{4\omega^3}{3\hbar c^3} |\mathbf{r}_{fs}|^2 = B. \quad (22.1.31)$$

The corresponding emission rate is similar except $(n + 1)$ replaces n in the matrix element (22.1.25):

$$R_{f \leftarrow s}(\text{emission}) = (n + 1)A = A + B \quad (22.1.32a)$$

The first term is the famous *Einstein-A-coefficient* or *spontaneous decay rate* of an excited atom in a vacuum ($n = 0$):

$$A = \frac{4\omega^3}{3\hbar c^3} \frac{q^2}{4\pi\epsilon_0} |\mathbf{r}_{fs}|^2. \quad (22.1.32b)$$

The second term is the *Einstein-B-coefficient*, which is the *stimulated decay rate* induced by the presence of n resonant photons:

$$B = nA = n \frac{4\omega^3}{3\hbar c^3} \frac{q^2}{4\pi\epsilon_0} |\mathbf{r}_{fs}|^2. \quad (22.1.32c)$$

B is the only contribution to the absorption rate (22.1.31) since spontaneous excitation is impossible in this approximation.

c. "Impotence" of Photon Number States

We noted that the first-order transition amplitude $c_F^{(1)}$ in (22.1.21) could only have an absorption term or else an emission term but not both. This is because the quantum field transition matrix element (22.1.25) cannot be nonzero for both processes at once. We also noted that the semi-classical transition amplitude (18.2.5) does have terms from both processes. In fact, the derivation of resonant excitation of the oscillator expectation value $\langle x \rangle$ depends upon the precise interference between these two terms to reproduce the classical result. [Recall comparison in (18.3.5).] At first this might seem to be a case where quantum theory is failing to approach the correct classical limit. We need to resolve this issue.

The calculation of the atomic position expectation value $\langle \Psi | x | \Psi \rangle$ using quantum field number states is quite different and so are the results. The perturbed atom-field state is

$$|\Psi\rangle = |S\rangle + \sum_{F \neq S} e^{-i\omega_{FS}t} c_F |F\rangle,$$

where the first-order approximation to the amplitude is

$$c_F^{(1)} = \delta_{FS} + \frac{1}{i\hbar} \int_0^t dt_1 e^{i\omega_{FS}t_1} \langle F | H_I | S \rangle,$$

according to the basic time-dependent perturbation formulas (18.2.5). The matrix element is given by matrix elements (22.1.25) between the initial state $|S\rangle = |s\rangle_{\text{atom}} |n_{k\alpha}^s \cdots n_{k'\alpha'}^s\rangle_{\text{field}}$ and final state

$|F\rangle = |f\rangle_{\text{atom}} |n_{k\alpha}^f \cdots n_{k'\alpha'}^f\rangle_{\text{field}}$. The atom part only requires that the induced dipole moment $q\mathbf{r}_{fs} \equiv \langle f | \mathbf{r} | s \rangle q$

be nonzero. The field part is more restrictive; it requires that exactly one mode gain or lose a single photon. The result is a perturbed state of the form

$$\begin{aligned} |\Psi\rangle = |S\rangle = & |s\rangle |n_{k\alpha}^s \cdots n_{k'\alpha'}^s\rangle + d_{k\alpha}^\alpha(f) |f\rangle |n_{k\alpha}^s - 1 \cdots n_{k'\alpha'}^s\rangle + \cdots \\ & + d_{k'\alpha'}^\alpha(f) |f\rangle |n_{k\alpha}^s \cdots n_{k'\alpha'}^s - 1\rangle + \cdots \\ & + d_{k'\alpha'}^e(f) |f\rangle |n_{k\alpha}^s + 1 \cdots n_{k'\alpha'}^s\rangle + \cdots \\ & + d_{k'\alpha'}^e(f') |f'\rangle |n_{k\alpha}^s \cdots n_{k'\alpha'}^s + 1\rangle + \cdots, \end{aligned}$$

Here the transition amplitude to a higher state $|f\rangle$ due to absorption from mode (\mathbf{k}, α) is

$$d_{k\alpha}^\alpha(f) = \frac{e^{-i\omega_f t}}{\hbar} \int_0^t dt_1 e^{i\omega_{fs} t_1} w_k \sqrt{n_{k\alpha} + 1} \mathbf{e}_\alpha \cdot \mathbf{r}_{fs} \quad (\Delta = \omega_{fs} - \omega_k)$$

The transition amplitude to a lower state $|f'\rangle$ due to emission from mode (\mathbf{k}, α) is

$$d_{k\alpha}^e(f') = \frac{e^{-i\omega_{f'} t}}{\hbar} \int_0^t dt_1 e^{i\omega_{fs} t_1} w_k \sqrt{n_{k\alpha} + 1} \mathbf{e}_\alpha \cdot \mathbf{r}_{f's} \quad (\Delta = \omega_{fs} + \omega_k)$$

In each case w_k is the scale factor (22.1.4) times frequency ω and charge q .

$$w_{k\alpha} = \omega_k q \sqrt{\frac{\hbar}{2\epsilon_0 \omega_k V}}$$

If $|s\rangle$ is the atomic ground state, the emission terms with d^e amplitudes are nonexistent. However, there may be several atomic states $|f\rangle, |f'\rangle, \dots$ that can be reached by near-resonant absorption. The same goes for state reached by emission if $|s\rangle$ is an excited state.

Now the expectation value $\langle \Psi | x | \Psi \rangle$ can be evaluated. We write the bra and ket on the left and top, respective, of the box in the following, and we collect the scalar products inside:

$$\langle \Psi | x | \Psi \rangle = \frac{\begin{array}{l} \langle n_{k\alpha}^a \dots | \langle s | x \\ + d_{k\alpha}^{\alpha*} \langle n_{k\alpha}^s - 1 \dots | \langle f | x \end{array}}{\begin{array}{l} |s\rangle | n_{k\alpha}^s \dots \rangle + d_{k\alpha}^a |f\rangle | n_{k\alpha}^s - 1 \dots \rangle + \dots \\ \langle s | x | s \rangle \langle 1 \rangle + d_{k\alpha}^a \langle s | x | f \rangle \langle 0 \rangle + \dots \\ d_{k\alpha}^{\alpha*} \langle f | x | s \rangle \langle 0 \rangle + |d_{k\alpha}^a|^2 \langle f | x | f \rangle \langle 1 \rangle + \dots \end{array}}$$

The sum includes only one field mode and one higher atomic state $|f\rangle$. This is enough to see that all the results must be zero if the atomic states have definite parity $\langle s | x | s \rangle = 0 = \langle f | x | s \rangle$. The orthogonality ($\langle n_k | n_k - 1 \rangle = 0$) of the photon states kills the possibility of any contribution from the induced moment matrix elements $\langle s | x | f \rangle$ or $\langle f | x | s \rangle$, however large they may be.

So photon number states are "impotent"; they cannot create a coherent excitation of an atom. This is consistent with the idea that classical phase is completely uncertain or random for a field oscillator eigenstate that has probability distributed more or less evenly over its phase space. To have a well-defined phase we need a non-stationary coherent oscillator state $|\alpha_{k\beta}\rangle$ for a mode (\mathbf{k}, β) instead of a stationary eigenstate $|n_{k\beta}\rangle$. This will give a wave packet in $(Q_{k\beta}, P_{k\beta})$ phase space or (\mathbf{A}, \mathbf{E}) space which may have well-defined phase as shown in the Sec. 20.3.

Photon number states may be "impotent" but they are not powerless. They can create large fluctuations in expectation $\langle \Psi | x^2 | \Psi \rangle$ even though $\langle \Psi | x | \Psi \rangle$ is identically zero. From the foregoing calculation we get the following:

$$\langle \Psi | x^2 | \Psi \rangle = \langle s | x^2 | s \rangle + |d_{k\alpha}^a|^2 \langle f | x^2 | f \rangle + \dots \tag{22.1.33}$$

The expectation of x^2 is proportional to the photon intensity $v_{\mathbf{k}\beta}$, the square $|\mathbf{r}_{fs}|^2$ of the atomic induced moment, and the mean square x for the final state $|f\rangle$.

d Coherent Radiation States

A much better description of a laser-cavity mode includes the nonstationary coherent or wave packet states $|\alpha_{\mathbf{k}\beta}\rangle$. According to (20.3.25) these may be defined as follows in terms of photon number states $|n_{\mathbf{k}\beta}\rangle$ for a single-cavity mode (\mathbf{k},β) :

$$|\alpha_{\mathbf{k}\beta}\rangle = e^{-|\alpha_{\mathbf{k}\beta}|^2/2} \sum_{n_{\mathbf{k}\beta}} (\alpha_{\mathbf{k}\beta})^{n_{\mathbf{k}\beta}} |n_{\mathbf{k}\beta} 00 \dots\rangle / \sqrt{n_{\mathbf{k}\beta}!}. \quad (22.1.34)$$

The complex parameter $\alpha_{\mathbf{k}\beta}$ is a field phasor expectation value and a quasi-eigenvalue of operator .

$$\mathbf{a}_{\mathbf{k}\beta} |\alpha_{\mathbf{k}\beta}\rangle = \alpha_{\mathbf{k}\beta} |\alpha_{\mathbf{k}\beta}\rangle, \quad \langle \alpha_{\mathbf{k}\beta} | \mathbf{a}_{\mathbf{k}\beta}^\dagger = \langle \alpha_{\mathbf{k}\beta} | \alpha_{\mathbf{k}\beta}^* . \quad (22.1.35)$$

Recall (20.3.25c). Here only the (\mathbf{k},β) mode is excited and all others are in their ground or vacuum states.

The A -field expectation value should equal the classical expression (22.1.2a) we began with:

$$\begin{aligned} \langle \alpha_{\mathbf{k}\beta} | \mathbf{A} | \alpha_{\mathbf{k}\beta} \rangle &= \sqrt{\frac{\hbar}{2\varepsilon_0\omega V}} \left[\langle \alpha_{\mathbf{k}\beta} | \mathbf{a}_{\mathbf{k}\beta} | \alpha_{\mathbf{k}\beta} \rangle + \langle \alpha_{\mathbf{k}\beta} | \mathbf{a}_{\mathbf{k}\beta}^\dagger | \alpha_{\mathbf{k}\beta} \rangle \right] e_\beta \\ &= \sqrt{\frac{\hbar}{2\varepsilon_0\omega V}} \left[\alpha_{\mathbf{k}\beta} + \alpha_{\mathbf{k}\beta}^* \right] e_\beta = \left[\alpha_{\mathbf{k}\beta} e^{-i\omega t} + \alpha_{\mathbf{k}\beta}^* e^{i\omega t} \right] e_\beta \end{aligned}$$

In the last line is the classical value. Note that the dipole approximation $e^{i\mathbf{k}\cdot\mathbf{r}} \cong 1$ is used here. The $_$ has the necessary $e^{-i\omega t}$ time dependence noted in (20.3.29). This gives the non-stationary phase packet motion described by (20.3.34). The relation between $\alpha_{\mathbf{k}\beta}$ and the classical amplitude a involves the phasor and the quantum scale (22.1.4):

$$\alpha_{\mathbf{k}\beta} = a_{\mathbf{k}\beta} e^{-i\omega_{\mathbf{k}} t} \sqrt{\frac{2\varepsilon_0\omega V}{\hbar}} .$$

The $\alpha_{\mathbf{k}\beta}$ expectation value of the $-q\mathbf{E} \cdot \mathbf{r}$ interaction in a coherent state $|\alpha_{\mathbf{k}\beta}\rangle$ then becomes equal to the classical value quoted in (8.4.35a):

$$\langle \alpha_{\mathbf{k}\beta} | H_I | \alpha_{\mathbf{k}\beta} \rangle = -i\omega_{\mathbf{k}} q \mathbf{e}_\beta \cdot \mathbf{r} \left(\alpha_{\mathbf{k}\beta} e^{-i\omega t} - \alpha_{\mathbf{k}\beta}^* e^{i\omega t} \right).$$

It has the positive and negative frequency parts needed to coherently excite an atom.

This might lead you to believe that a coherent quantum field can reproduce the effect on an atom of a classical wave. Indeed, for very high $\alpha_{\mathbf{k}\beta}$ and short enough time the effect of the two are nearly the same. However, eventually the coherent wave produces dephasing and rephrasing effects that are quite remarkable. These coherent decays and "revivals" are discussed in works listed at the end of this chapter. A model of coherent QED by Jaynes and Cummings is discussed next.

Do low-quantum fields make good coordinate frames?

In the meantime, it is interesting to speculate on the ability of quantum fields, in particular, *low - quantum* fields, to make the kind of space-time coordinate grids that were used to develop the quantum theory and relativity in Unit 2.

A fundamental laser mode in a $0.25\mu\text{m}$ cubic cavity such as the E-wave sketched in one half-wave strip of Fig. 22.1.2(c), has green light with $\hbar\omega = 4 \cdot 10^{-19}$ Joule or 2.5eV per photon. The average photon number is thus $\bar{n} = |\alpha|^2 = 10^{10}$ for a laser with mean energy $\bar{E} = \bar{U} \cdot V = \hbar\omega\bar{n} = 4.0\text{ nanoJ}$ in a volume $V = (\frac{1}{4}\mu\text{m})^3$. That amounts to a very intense micro laser! Photon number uncertainty is $\Delta n = |\alpha| = 10^5$ in a coherent state (22.1.34) and it varies inversely to its phase uncertainty which here is a tiny value $\Delta\Phi = \pi/\alpha \sim 3 \cdot 10^{-5}$.

Amplitude expectation value $\langle n|A|n\rangle$ is zero for $|n\rangle$ states due to *incoherence* of phase, but number value $\langle n|\mathbf{a}_k^\dagger \mathbf{a}_k|n\rangle = n$ is exact as is proper frequency ωn due to the phase factor $(e^{-i\omega t})^n$ of $(\mathbf{a}_k^\dagger)^n$. For *any* volume V , these ($n = 10^{10}$)-photons have total energy $E = \hbar\omega n$ or mass $M = E/c^2 = 10^{-25}$ kg equal to that of 59.79 H-atoms, but it's not "real" mass. (Real $e + \bar{e}$ pair-creation means raising ω from 600Thz to $m_e c^2/h$ or 100MegaThz .) Nevertheless, "real" 10^{-25} kg and an "optical" 10^{-25} kg share a hyperbola 10^{10} quanta above the $n=1$ hyperbola in Fig. 5.1.1. Lorentz symmetry demands that.

A coherent-state $|\alpha = 10^5\rangle$ also has a mass $M = 10^{-25}$ kg but with uncertainty $\Delta M = 10^{-30}$ kg. Its *phase* uncertainty $3 \cdot 10^{-5}$ is low enough to plot grids like Fig. 22.1.2(c) or Fig. 22.1.3(a). A low- α wave state such as is used in Fig. 22.1.3(c) has too few photon counts-per-grid to plot sharply. Fig. 22.1.3(d) simulates an n -photon eigenstate $|n\rangle$. It is a wash even for high n since $\Delta n = 0$ has $\Delta\Phi = \infty$.

However, an incoherent space-time "baseball diamond" grid like Fig. 22.1.2(d) is less sensitive to lack of phase coherence and so pure- n photon number states could form diamonds since the coherent interference required for the Cartesian grid of Fig. 22.1.2(c) is not required for a pulse wave diamond grid.

So, do low-quantum fields make good coordinate frames? The answer, you see, is yes or no!

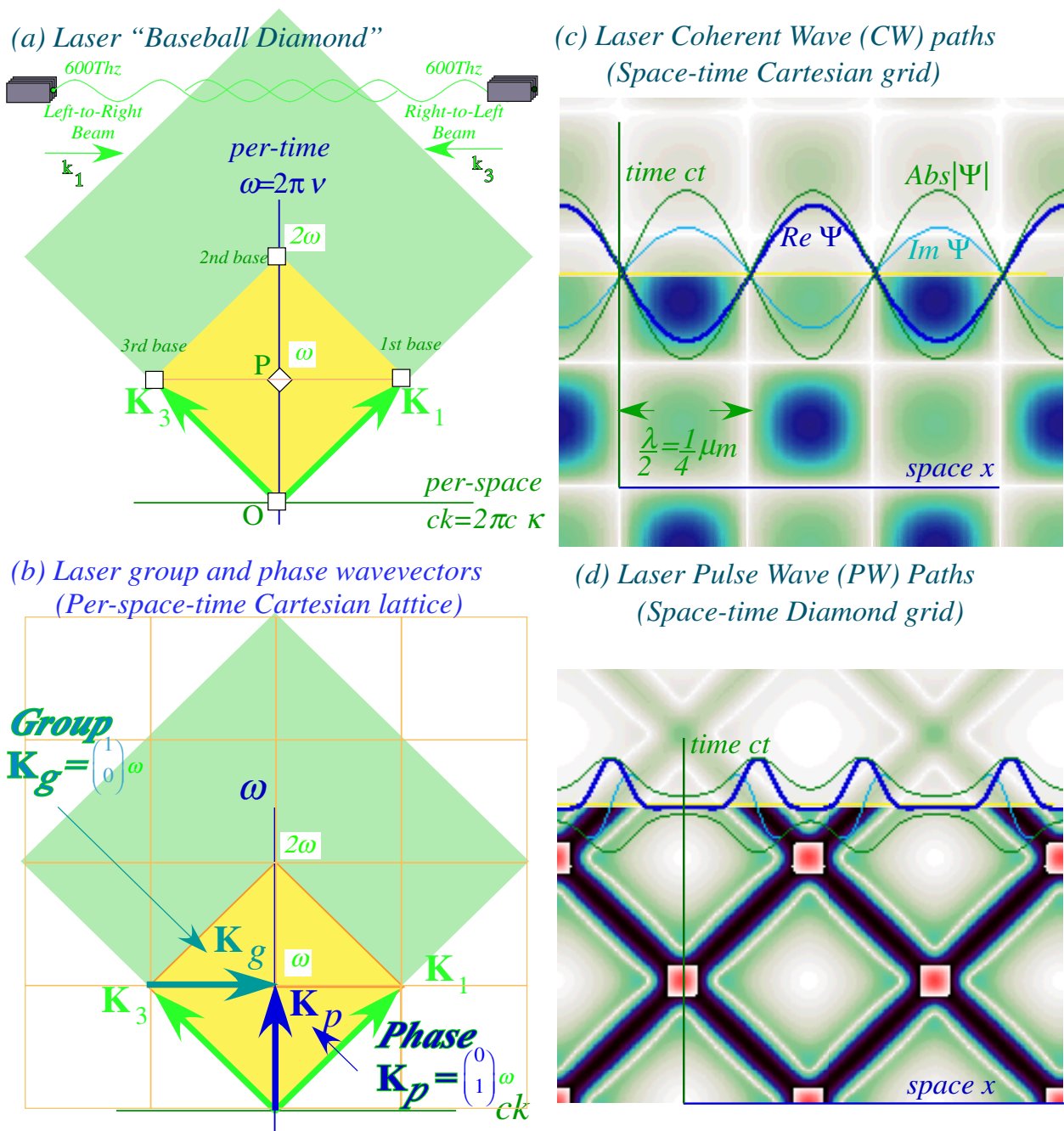


Fig. 22.1.2 Simulated space time wave coordinate grids (a-c) 600Thz Continuous Wave (CW) Cartesian per-space-time (a) and space-time. (b-d) Pulse wave (CW) light waves in per-space-time (b) and space-time (d).

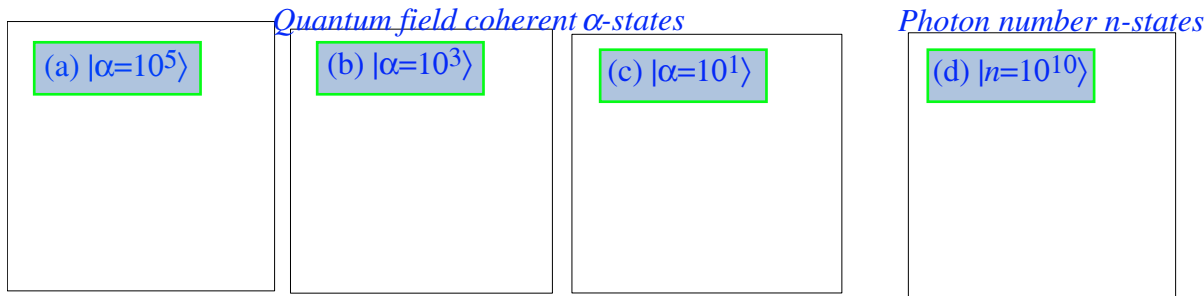


Fig. 22.1.3 Simulated spacetime photon counts for coherent (a-c) and photon-number states (d).

22.2 SPECTRA OF ATOMS IN LASER CAVITY

When atoms interact strongly or resonantly with an electromagnetic field, the distinction between the field and the atom is blurred. Observer and the observed become a single entity that is more than just a sum of its parts. It is as though the atom had become part of a molecule in which the excited levels involve excitation of all the constituent parts. Intra-cavity atomic theory is sometimes called *Cavity Quantum Electrodynamics* or CQED co-opting the more famous acronym QED for quantum field theory.

An atom interacting strongly with a single mode of a simple cavity is described by what is called the *Jaynes-Cummings model*. Here we will give a brief qualitative sketch of states and levels of this model. This is an important model for beginning to understand spectroscopic effects of strong laser fields. It is also a simple solvable example of an atom interacting with something that has a multitude of states. This is also the kind of problem one encounters when atomic motions go together to make a molecular rotation or vibration spectrum that are the subject of Unit 8.

a. Jaynes-Cummings Hamiltonian

In a static electric field the two-level atomic system Hamiltonian has the following representation in the basis of atomic eigenstates given by (10.3.3) in Unit 3 or (19.1.6) in Unit 6:

$$H_{\text{atom}} = H \begin{pmatrix} 1 & 0 \\ 0 & 1 \end{pmatrix} + S \begin{pmatrix} 1 & 0 \\ 0 & -1 \end{pmatrix} - pE \begin{pmatrix} 0 & 1 \\ 1 & 0 \end{pmatrix} = H\mathbf{1} + S\sigma_z - pE\sigma_x. \quad (22.2.1a)$$

The electric field-dipole potential energy factor pE is folded into a Rabi coefficient in (19.1.7).

$$r = pE_z/\hbar \quad (22.2.1b)$$

An oscillating electric field Hamiltonian is transformed into rotating-wave form (19.1.10).

$$H_{\text{RW}} = \frac{\Delta}{2} \begin{pmatrix} 1 & 0 \\ 0 & -1 \end{pmatrix} + \frac{r}{2} \begin{pmatrix} 0 & 1 \\ 1 & 0 \end{pmatrix} = \frac{\Delta}{2} \sigma_z + \frac{r}{2} \sigma_x. \quad (22.2.2a)$$

Detuning factor Δ is the difference between the atomic transition angular frequency ε and the angular frequency Ω of the stimulating laser.

$$\Delta = \varepsilon - \Omega \quad (22.2.2b)$$

In preparation for using a quantum field we need to separate the atomic and radiative contributions to the Hamiltonian. The terms that involve the laser frequency Ω have been collected into the first simple term labeled H_{field} . The atom's two levels H_{atom} and their interaction $H_{\text{interaction}}$ come next.

$$\begin{aligned} H_{\text{RW}} &= \Omega \begin{pmatrix} 0 & 0 \\ 0 & 1 \end{pmatrix} - \frac{\varepsilon + \Omega}{2} \begin{pmatrix} 1 & 0 \\ 0 & 1 \end{pmatrix} + \varepsilon \begin{pmatrix} 1 & 0 \\ 0 & 0 \end{pmatrix} + \frac{r}{2} \begin{pmatrix} 0 & 1 \\ 1 & 0 \end{pmatrix} \\ &= H_{\text{field}} + \frac{\varepsilon}{2} (\boldsymbol{\sigma}_z + \mathbf{1}) + \frac{r}{2} \boldsymbol{\sigma}_x \\ &= H_{\text{field}} + H_{\text{atom}} + H_{\text{interaction}} \end{aligned}$$

In the Jaynes-Cummings model the classical electric field is replaced by an expression using its quantized form. However, only one mode of the field is considered and only the dipole terms (21.1.20e) are used. Also, the unit matrix term dropped. The simplified Hamiltonian is as follows.

$$\begin{aligned} H_{\text{JC}} &= H_{\text{field}} + H_{\text{atom}} + H_{\text{interaction}} \\ &= \Omega \mathbf{a}^\dagger \mathbf{a} + \frac{\varepsilon}{2} (\boldsymbol{\sigma}_z + \mathbf{1}) + i \frac{g}{2} (\mathbf{a}^\dagger - \mathbf{a}) \boldsymbol{\sigma}_x \end{aligned} \quad (22.2.3a)$$

The constant g is the Rabi factor that would correspond to a one-photon laser field. [Recall (22.1.4).]

$$g = \sqrt{\frac{\hbar \Omega}{2 \varepsilon_0 V}} \frac{q \langle 2 | z | 1 \rangle}{\hbar} \quad (22.2.3b)$$

The field amplitude for an N -photon field is proportional to \sqrt{N} , so we have the following relation between the semiclassical and quantum interaction constant.

$$r = g \sqrt{N} \quad (22.2.3c)$$

We let $\mathbf{a}_{\mathbf{k},\alpha} \equiv \mathbf{a}$ since only one laser cavity mode ($\mathbf{k}\alpha$) of frequency $\Omega = \omega$ is being considered. By expressing $\boldsymbol{\sigma}_x$ in terms of spinor raising and lowering operators, $\boldsymbol{\sigma}_x = (\boldsymbol{\sigma}_+ + \boldsymbol{\sigma}_-)$, this becomes

$$H_{\text{JC}} = \Omega \mathbf{a}^\dagger \mathbf{a} + \frac{\varepsilon}{2} (\boldsymbol{\sigma}_z + \mathbf{1}) + i \frac{g}{2} (\mathbf{a}^\dagger - \mathbf{a}) (\boldsymbol{\sigma}_+ + \boldsymbol{\sigma}_-) \quad (22.2.4)$$

A final approximation to the model keeps only the interaction term $\mathbf{a}^\dagger \boldsymbol{\sigma}_-$ for a photon created as the atom drops from the upper-(\uparrow)-level 2 to the lower-(\downarrow)-level 1 and the term $\mathbf{a} \boldsymbol{\sigma}_+$ that does the reverse.

$$H_{\text{JC}} = \Omega \mathbf{a}^\dagger \mathbf{a} + \frac{\varepsilon}{2} (\boldsymbol{\sigma}_z + \mathbf{1}) + i \frac{g}{2} (\mathbf{a}^\dagger \boldsymbol{\sigma}_- - \mathbf{a} \boldsymbol{\sigma}_+) \quad (22.2.5)$$

Let us apply the Hamiltonian (22.2.5) in turn to the radiation-atom product states with $N = 0, 1, 2, \dots$ photons that we label $\{|0\rangle|\downarrow\rangle, |0\rangle|\uparrow\rangle, |1\rangle|\downarrow\rangle, |1\rangle|\uparrow\rangle, |2\rangle|\downarrow\rangle, |2\rangle|\uparrow\rangle, \dots\}$. The following state operations involve operations $a|n\rangle = \sqrt{n}|n-1\rangle$ and $a^\dagger|n\rangle = \sqrt{n+1}|n+1\rangle$ and spin operations $\sigma_-|\uparrow\rangle = |\downarrow\rangle$, and so on.

$$\begin{aligned}
 H_{\text{JCM}}|0\rangle|\downarrow\rangle &= (0 \cdot \Omega + 0)|0\rangle|\downarrow\rangle + i\frac{g}{2}(0 - 0), \\
 H_{\text{JCM}}|0\rangle|\uparrow\rangle &= (0 \cdot \Omega + \varepsilon)|0\rangle|\uparrow\rangle + i\frac{g}{2}(\sqrt{1}|1\rangle|\downarrow\rangle - 0), \\
 H_{\text{JCM}}|1\rangle|\downarrow\rangle &= (1 \cdot \Omega + 0)|1\rangle|\downarrow\rangle + i\frac{g}{2}(0 - \sqrt{1}|0\rangle|\uparrow\rangle), \\
 H_{\text{JCM}}|1\rangle|\uparrow\rangle &= (1 \cdot \Omega + \varepsilon)|1\rangle|\uparrow\rangle + i\frac{g}{2}(\sqrt{2}|2\rangle|\downarrow\rangle - 0), \\
 H_{\text{JCM}}|2\rangle|\downarrow\rangle &= (2 \cdot \Omega + 0)|2\rangle|\downarrow\rangle + i\frac{g}{2}(0 - \sqrt{2}|1\rangle|\uparrow\rangle), \\
 H_{\text{JCM}}|2\rangle|\uparrow\rangle &= (2 \cdot \Omega + \varepsilon)|2\rangle|\uparrow\rangle + i\frac{g}{2}(\sqrt{3}|3\rangle|\downarrow\rangle - 0).
 \end{aligned} \tag{22.2.6}$$

An infinite series of two-by-two matrices represents H_{JCM} in this basis.

$$\begin{array}{c|ccccc}
 & |0\rangle|\downarrow\rangle & |0\rangle|\uparrow\rangle & |1\rangle|\downarrow\rangle & |1\rangle|\uparrow\rangle & |2\rangle|\downarrow\rangle \dots \\
 \hline
 |0\rangle|\downarrow\rangle & 0 \cdot \Omega + 0 & \cdot & \cdot & \cdot & \cdot \\
 |0\rangle|\uparrow\rangle & \cdot & 0 \cdot \Omega + \varepsilon & \frac{-ig\sqrt{1}}{2} & \cdot & \cdot \\
 |1\rangle|\downarrow\rangle & \cdot & \frac{ig\sqrt{1}}{2} & 1 \cdot \Omega + \varepsilon & \cdot & \cdot \\
 |1\rangle|\uparrow\rangle & \cdot & \cdot & \cdot & 1 \cdot \Omega + \varepsilon & \frac{-ig\sqrt{2}}{2} \\
 |2\rangle|\downarrow\rangle & \cdot & \cdot & \cdot & \frac{ig\sqrt{2}}{2} & 2 \cdot \Omega + 0
 \end{array} \tag{22.2.7}$$

The general form of each two-by-two matrix is the following:

$$\langle h_{\text{JCM}} \rangle = \langle N-1 | \langle \downarrow | \begin{array}{c|cc} & |N-1\rangle|\downarrow\rangle & |N-1\rangle|\uparrow\rangle \\ \hline & |N-1\rangle\Omega + \varepsilon & \frac{-ig\sqrt{N}}{2} \\ \langle N | \langle \uparrow | & \frac{ig\sqrt{N}}{2} & N\Omega + 0 \end{array} \tag{22.2.8}$$

In the classical limit of large N the two-by-two matrix begins to look something like the semi-classical matrix (22.2.2a). We can write the two-by-two part of the Hamiltonian as follows:

$$\begin{aligned}
\langle h_{\text{JCM}} \rangle &= (N-1)\Omega \begin{pmatrix} 1 & 0 \\ 0 & 1 \end{pmatrix} + \Omega \begin{pmatrix} 0 & 0 \\ 0 & 1 \end{pmatrix} + \varepsilon \begin{pmatrix} 0 & -i \\ i & 1 \end{pmatrix} \\
&= \left((N-1)\Omega + \frac{\varepsilon + \Omega}{2} \right) \begin{pmatrix} 1 & 0 \\ 0 & 1 \end{pmatrix} + \frac{\varepsilon - \Omega}{2} \begin{pmatrix} 1 & 0 \\ 0 & -1 \end{pmatrix} + \frac{g\sqrt{N}}{2} \begin{pmatrix} 0 & -i \\ i & 0 \end{pmatrix} \\
&= \left((N-1)\Omega + \frac{\varepsilon + \Omega}{2} \right) \begin{pmatrix} 1 & 0 \\ 0 & 1 \end{pmatrix} + \frac{\Delta}{2} \begin{pmatrix} 1 & 0 \\ 0 & -1 \end{pmatrix} + \frac{r}{2} \begin{pmatrix} 0 & -i \\ i & 0 \end{pmatrix} \\
&= \left((N-1)\Omega + \frac{\varepsilon + \Omega}{2} \right) \mathbf{1} + \frac{\Delta}{2} \boldsymbol{\sigma}_z + \frac{r}{2} \boldsymbol{\sigma}_y
\end{aligned} \tag{22.2.9}$$

N -photon-Rabi-factor $r = g\sqrt{N}$ reappears on $\boldsymbol{\sigma}_y$ due to a choice of phase for field operators. The physics is unchanged if we use a modified JCM Hamiltonian that uses $\boldsymbol{\sigma}_x$ instead of $\boldsymbol{\sigma}_y$.

$$H'_{\text{JC}} = \Omega \mathbf{a}^\dagger \mathbf{a} + \frac{\varepsilon}{2} (\boldsymbol{\sigma}_z + 1) + \frac{g}{2} (\mathbf{a}^\dagger \boldsymbol{\sigma}_- + \mathbf{a} \boldsymbol{\sigma}_+)$$

This lets us use semi-classical dressed eigensolutions (19.1.20) to real two-by-two matrices.

$$\begin{aligned}
\langle h'_{\text{JCM}} \rangle &= \begin{array}{c|cc} & |N-1\rangle|\downarrow\rangle & |N\rangle|\uparrow\rangle \\ \hline \langle N-1|\langle\downarrow| & (N-1)\Omega + \varepsilon & \frac{g\sqrt{N}}{2} \\ \langle N|\langle\uparrow| & \frac{g\sqrt{N}}{2} & N\Omega \end{array} = N\Omega \mathbf{1} + \begin{pmatrix} \Delta & r \\ r & 0 \end{pmatrix} \\
&= \left((N-1)\Omega + \frac{\varepsilon + \Omega}{2} \right) \mathbf{1} + \begin{pmatrix} \frac{\Delta}{2} & \frac{r}{2} \\ \frac{r}{2} & -\frac{\Delta}{2} \end{pmatrix} = \left((N-1)\Omega + \frac{\varepsilon + \Omega}{2} \right) \mathbf{1} + \frac{\Delta}{2} \boldsymbol{\sigma}_z + \frac{r}{2} \boldsymbol{\sigma}_x
\end{aligned} \tag{22.2.10}$$

These matrices have the same eigenvectors as the semi-classical matrices. The only difference is that the Rabi factor r depends upon photon number N and there is a level pair for all N greater than zero. The eigenvalues are the similar, too, except for the unit matrix term that yields a ladder of doublet eigenvalues. We examine this ladder of levels now.

b. Jaynes-Cummings Eigensolutions

An attempt to picture the dressed eigenlevels is made in Fig. 22.2.1. A column containing stacks of energy levels is shown for each of three cases of detuning: (a) laser tuned below atomic transition ($\Delta > 0$); (b) at resonance ($\Delta = 0$), and (c) laser tuned higher ($\Delta < 0$). Recall that the detuning parameter is $\Delta = \varepsilon - \Omega$.

Two stacks of horizontal lines on each side of the (a), (b), and (c) columns in Fig. 22.2.1 indicate what the levels would be without any interaction between atom and field ($r = g/\sqrt{N} = 0$). An N -photon level in which the atom is in the first $|1\rangle = |\uparrow\rangle$ or second $|2\rangle = |\downarrow\rangle$ state is labeled $|1, N\rangle$ or $|2, N\rangle$,

respectively. Each of these levels for $N > 0$ is connected to a pair of lines in the center of the column that are shifted up and down by $\pm\delta/2$. The quantity δ is the AC-Stark shift discussed in Section 19.1 (Recall (19.1.20a)). The shifted lines are the “dressed” eigenlevels with interaction turned on ($r = g/\sqrt{N} > 0$). The lines that connect the shorter lines to the zero-field levels indicate the relative the greater of the two amplitudes ($\sin \theta/2$ or $\cos \theta/2$) of the zero-field states in each the dressed eigenstates corresponding to that level. Recall Eqs. (19.1.20c) and (19.1.20d).

Below resonance ($\Delta > 0$) the Hamiltonian rotation vector ω makes an acute angle ($\theta < \pi/2$) with the z -axis. The lower dressed eigenstate $|1^D N + 1, N\rangle$ indicated at the top left-hand side of Fig. 22.2.1 is mostly composed of the atom-field product state $|1, N + 1\rangle$, while the higher-dressed state $|2^D N + 1, N\rangle$ is mostly composed of $|2, N\rangle$.

As the detuning approaches resonance ($\Delta=0$), the zero-field levels get lined up, the AC-shifts reach their maximum, and the rotation angle θ approaches $\pi/2$. One may use the diagrams from Fig. 19.1.6 to quantify the variation. However, caution should be used since the Rabi parameter $r = g\sqrt{N}$ is here a function of N . In other words, the Rabi parameter, which was a constant in the semi-classical theory, is now dependent upon what level you are on. It increases with the laser mode electric field amplitude, which is proportional to the root \sqrt{N} of the photon number.

At resonance ($\Delta=0$) the rotation angle is $\theta = \pi/2$. Then the Hamiltonian rotation vector Ω makes an angle of $\pi/2$ with the z -axis and has its minimum magnitude of $|\Omega| = r$, which is the Rabi frequency. This was shown in Fig. 19.1.3c. The resonance values for the dressed eigenstate amplitudes are $\sin \theta/2 = 1/\sqrt{2}$ and $\cos \theta/2 = 1/\sqrt{2}$. This corresponds to 50-50 mixtures of the atom-field product states $|1, N + 1\rangle$ and $|2, N\rangle$ in the dressed eigenstates $|1^D N + 1, N\rangle$ and $|2^D N + 1, N\rangle$.

Above resonance ($\Delta < 0$) the Hamiltonian rotation vector Ω makes an obtuse angle ($\theta > \pi/2$) with the z -axis. Now the lower-dressed eigenstate $|1^D N + 1, N\rangle$ is mostly composed of $|2, N\rangle$, while the upper-dressed state $|2^D N + 1, N\rangle$ is mostly composed of $|1, N + 1\rangle$, as shown in the upper right-hand side of the Fig. 22.2.1.

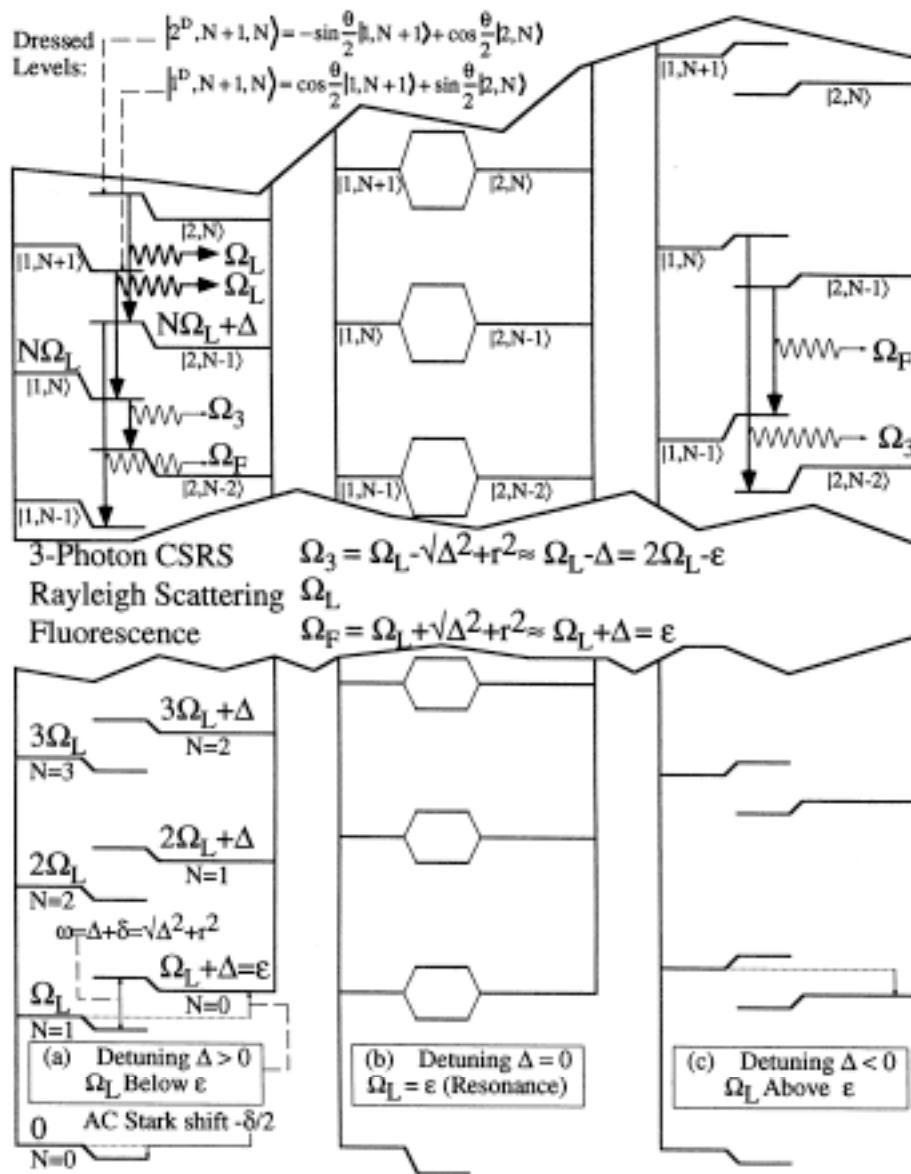


Fig. 22.2.1 Level structure of 2-level atom and 1-mode cavity showing elementary transition processes of fluorescence, Rayleigh scattering, and three-photo coherent Stokes-Raman scattering (CSRS). Transitions are between levels belonging to dressed eigenstates.

c. Transitions in the Jaynes-Cummings Model

The diagram of levels in Fig. 22.2.1 involves just one $\Omega_L = \Omega$ mode interacting with the two-level atom. We have ignored all the other field mode levels such as were sketched in Fig. 22.1.1. We have just concentrated on loading photons into one laser cavity mode whose frequency $\Omega_L = \Omega$ is being tuned close to the value $\epsilon = \omega_f - \omega_s$ of the atomic transition.

However, if these other modes are off-resonance by enough or only have one or two photons, one can treat them using perturbation theory as was discussed in Section 22.1.b. Transition rates between the dressed states of a laser-driven atom can be derived using the Fermi golden rule (22.1.30).

Rayleigh scattering and fluorescence

Some of the commonly observed transitions are indicated by vertical arrows in the Fig. 22.2.1. The strongest transitions involved the so-called *Rayleigh Scattering* processes such as $|1, N+1\rangle \rightarrow |1, N\rangle$ for $N = 0, 1, 2, \dots$ or $|2, N\rangle \rightarrow |2, N-1\rangle$ for $N = 1, 2, \dots$, where only the photon number changes and the system emits one of its laser-mode photons into an external mode of the same frequency Ω_L . These transitions yield light with the frequency of the laser just like classical Rayleigh scattered light.

The other transitions are more complicated. One called *Fluorescence* is a transition between dressed states which involve fundamental transitions such as $|2, N\rangle \rightarrow |1, N\rangle$ or $|2, N-1\rangle$ and $|1, N-1\rangle$. The latter is the major part of the transition indicated by an Ω_F arrow in the upper left-hand side of the figure since the initial (upper) dressed state $|2^D N, N-1\rangle$ is mostly composed of $|2, N-1\rangle$ and $|1^D N, N-1\rangle$ is mostly composed of $|1, N-1\rangle$ in the final (lower) dressed state.

The fluorescence transition angular frequency is the difference between the initial and final dressed eigenlevels connected by the Ω_F arrow. The initial and final eigenvalues are

$$\begin{aligned}\epsilon^D(2, N, N-1) &= N\Omega_L + \Delta + \delta/2, \\ \epsilon^D(1, N-1, N-2) &= (N-1)\Omega_L - \delta/2.\end{aligned}$$

The difference is the fluorescence transition frequency,

$$\Omega_F = \Omega_L + \Delta + \delta = \Omega_L + \sqrt{\Delta^2 + r^2}. \quad (22.2.11)$$

For small Rabi factor ($r \ll \Delta$) or large detuning ($\Delta \gg r$) it becomes the atomic transition frequency.

$$\Omega_F \rightarrow \Omega_L + \Delta = \epsilon \quad (22.2.12)$$

This transition drops the atom from its upper state $|2\rangle$ to its lower state $|1\rangle$ but takes no photons out of the cavity mode since N stays constant. It emits one photon into an external mode of frequency Ω_F .

Coherent Stokes Raman scattering

Another transition called the three-photon process or *Coherent Stokes Raman Scattering* (CSRS) is a transition between dressed states, which mostly involves transitions of the type $|1, N\rangle \rightarrow |2, N-2\rangle$. The latter is the major part of the transition indicated by an Ω_3 arrow in the upper left-hand side of the figure

since the initial (upper) dressed state $|1^D N, N-1\rangle$ is mostly composed of $|1, N\rangle$, and $|2^D N-1, N-2\rangle$ is mostly composed of $|2, N-2\rangle$ in the final (lower) dressed state.

The CSRS transition angular frequency is the difference between the initial and final dressed eigenlevels connected by the Ω_3 arrow. The initial and final eigenvalues are

$$\begin{aligned}\varepsilon^D(1, N, N-1) &= N\Omega_L - \delta/2, \\ \varepsilon^D(2, N-1, N-2) &= (N-1)\Omega_L + \Delta - \delta/2.\end{aligned}$$

The difference is the CSRS transition frequency.

$$\Omega_3 = \Omega_{\text{CSRS}} = \Omega_L - \Delta - \delta = \Omega_L - \sqrt{\Delta^2 + r^2} \quad (22.2.13)$$

For small values of the Rabi factor ($r \ll \Delta$) or large detuning ($r \ll \Delta$) this becomes

$$\Omega_3 = \Omega_{\text{CSRS}} \rightarrow \Omega_L - \Delta = 2\Omega_L - \sqrt{\Delta^2 + r^2} \quad (22.2.14)$$

which is the difference between two laser photons and the atomic transition frequency. This transition raises the atom from its lower state $|1, N\rangle$ to its upper state $|2, N\rangle$. It also takes two photons out of the cavity mode since N decreases by two. It emits one photon into an external mode of frequency Ω_3 , which is approximately the difference between 2Ω and the atomic transition frequency ε .

A direct transition of frequency $\omega\sqrt{\Delta^2 + r^2} = \Delta$ between $|1^D N, N-1\rangle$ and $|2^D N-1, N-2\rangle$ is forbidden by C_2 parity. However, in a system that does not have C_2 symmetry it would be possible to have such a transition as is indicated by the small vertical arrow near the bottom of Fig. 22.2.1(a).

The next Fig. 22.2.2 shows the JTM transitions and their frequency dependence in more detail.

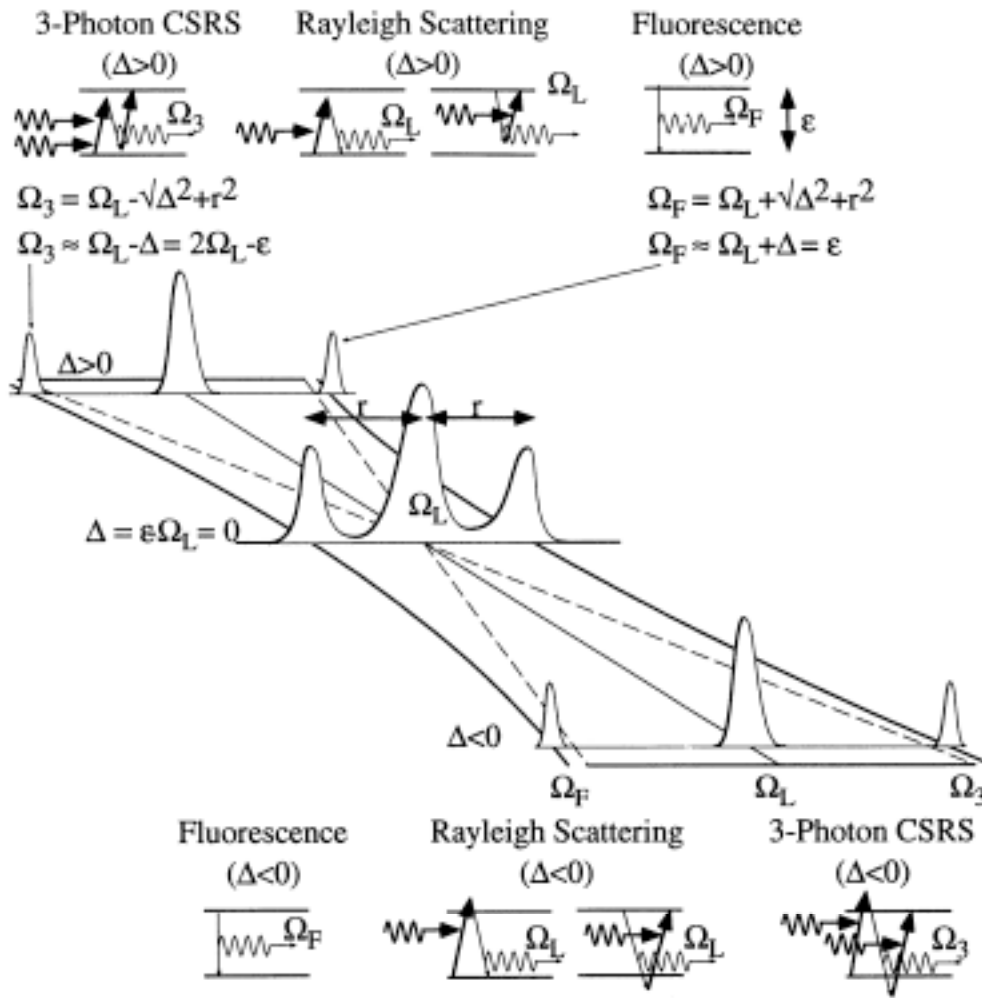


Fig. 22.2.2 Structure of the Mollow spectrum and its elementary processes of fluorescence, Rayleigh scattering, and three-photon coherent Stokes-Raman scattering (CSRS).

The three allowed transitions account for the three main spectral components that may be observed coming out of the sides of a laser atom cavity. It consists of a strong Rayleigh line at $\Omega_L = \Omega$ and two sidebands Ω_F and Ω_3 as shown in Fig. 22.2.2. The triple-pronged spectral line is called the *Mollow Line Shape*. One sideband is centered at $\Omega_F = \Omega + \omega$ which is approximately $\Omega + \Delta$ far from resonance, and the other is at $\Omega_3 = \Omega - \omega$, which is approximately $\Omega - \Delta$.

Near resonance at $\Delta=0$ the sidebands will follow AC Stark shift hyperbolic paths given by (22.2.11) and (22.2.13) rather than simply collapsing upon Ω at $\Delta = 0$. The hyperbolic curves in the semiclassical level diagram in Fig. 19.1.6 are approximate traces of the spectral sidebands for variable detuning Δ around resonance. At resonance ($\Delta=0$) there will still be two sidebands but now they will be

located at $\Omega \pm r$, where r is the Rabi parameter. In general, the sidebands are located at $\Omega \pm \omega$, where $\omega = \sqrt{\Delta^2 + r^2} \approx \Delta$ is the frequency of the Rabi precession or crank rotation shown in Fig. 19.1.3.

The sidebands correspond roughly to fluorescence and CSRS processes, respectively. With positive detuning ($\varepsilon - \Omega = \Delta > 0$) the upper sideband ($\Omega_F = \Omega + \omega \approx \Omega + \Delta$) is due (mostly) to fluorescence while the lower sideband ($\Omega_3 = \Omega - \omega \approx \Omega - \Delta$) is due (mostly) to the three-photon CSRS process. Above resonance the detuning parameter reverses sign ($\varepsilon - \Omega = \Delta < 0$) and the order is reversed. At resonance ($\Delta = 0$) it is not possible to distinguish the two processes since initial states $|1, N\rangle$ and $|2, N-1\rangle$ and $|2, N-2\rangle$ are mixed 50-50 as are the final states $|1, N-1\rangle$ and $|2, N-2\rangle$.

Below resonance ($\Delta > 0$) the CSRS Ω_3 photon has lower frequency than the Ω_F fluorescence photon. It also must come earlier in time. The CSRS process pumps the atom from its lower state-1 into its excited state-2. Only then can it emit a fluorescence photon to put it back into its ground state. Above resonance ($\Delta < 0$) the Ω_3 photon from the CSRS process has higher frequency than the fluorescence Ω_F photon. Then the higher frequency sideband comes earlier. These time correlations have been observed.

This concludes our introduction to the recent fundamental developments in laser spectroscopy. Many details have been left out of this discussion and many new effects will soon be discovered as this new set of tools becomes more widely used. Perhaps the most important development so far lies in the way we are coming to think about the observed object (atom or molecule) and the observer's tool (radiation). In modern laser spectroscopy the distinction between the observer and the observed has practically disappeared, and the atom-radiation-cavity becomes a single quantum object.

ADDITIONAL READING

Discussions of semiclassical quantization and wave-packet dynamics are in the following.

E. J. Heller, *J. Chem. Phys.*, **62**, 1544 (1975); *J. Chem. Phys.*, **68**, 3891 (1978).

M. J. Davis and E. J. Heller, *J. Chem. Phys.*, **71**, 3383 (1979).

S. Y. Lep and E. J. Heller, *J. Chem. Phys.*, **71**, 4777 (1979); *J. Chem. Phys.*, **76**, 3035 (1982).

D. J. Tannor and E. J. Heller, *J. Chem. Phys.*, **77**, 202 (1982).

N. DeLeon and E. J. Heller, *J. Chem. Phys.*, **78**, 4005 (1983); *J. Chem. Phys.*, **81**, 5957 (1984).

M. B. Blanco and E. J. Heller, *J. Chem. Phys.*, **83**, 1143 (1985).

J. R. Reimers and E. J. Heller, *J. Chem. Phys.*, **83**, 516 (1985).

N. DeLeon, *J. Chem. Phys.*, **87**, 4722 (1987); *Comp. Phys. Rep.*, **8**, 321 (1988).

An early paper on action quantization that uses color graphics to approximate quantum wave fronts is

M. J. Davis and E. J. Heller, *J. Chem. Phys.*, **75**, 3916 (1981).

The computer program *Color U(2)* mentioned at the end of Chapter 7 uses color quantization and color animation to show the dynamics of quantum wave fronts.

The idea of wave-packet coherent states can be traced back to Schrödinger.

E. Schrödinger, *Naturwissenschaften*, **14**, 664 (1926).

Their introduction in quantum optics is probably due to Glauber.

R. J. Glauber, *Phys. Rev.*, **131**, 2766 (1966).

Other approaches to semiclassical quantization are found in the following papers (this is by no means an exhaustive list of this large and growing field):

I. C. Percival, *Adv. Chem. Phys.*, **36**, 1 (1977).

D. W. Noid, M. L. Kosykowski, and R. A. Marcus, *Ann. Rev. Phys. Chem.*, **32**, 267 (1981).

- S. A. Rice, *Adv. Chem. Phys.*, **471**, 117 (1981).
- W. Eastes and R. A. Marcus, *J. Chem. Phys.*, **61**, 4301 (1974).
- D. W. Noid and R. A. Marcus, *J. Chem. Phys.*, **62**, 2119 (1975).
- I. C. Percival and N. Pomphrey, *Mol. Phys.*, **31**, 97 (1976).
- S. Chapman, B. C. Garrett, and W. H. Miller, *J. Chem. Phys.*, **64**, 502 (1976).
- C. Jaffe and W. P. Reinhardt, *J. Chem. Phys.*, **71**, 1862 (1979).
- R. T. Swim and J. B. Delos, *J. Chem. Phys.*, **71**, 1706 (1979).
- R. B. Shirts and W. P. Reinhardt, *J. Chem. Phys.*, **77**, 5204 (1982).
- C. C. Martens and G. S. Ezra, *J. Chem. Phys.*, **86**, 279 (1987).
- C. W. Eaker and G. C. Shatz, *J. Chem. Phys.*, **81**, 2394 (1984).
- W. H. Miller, *J. Chem. Phys.*, **81**, 3573 (1984).

References to the original EBK quantization are as follows:

- A. Einstein, *Dent. Ges. Berlin Verh.*, **19**, 9/10 (1917).
- M. L. Brillouin, *J. Phys. Paris (Ser. 6)*, **7**, 353 (1926).
- J. B. Keller, *Ann. Phys. (N.Y.)*, **4**, 180 (1958).
- F. Reiche, *The Quantum Theory*, (Methuen, London, 1922).

A good modern reference to classical, semiclassical, and quantum theory of radiation for spectroscopy is the following:

C. Cohen-Tannoudji, J. Dupont-Roc, and G. Grynberg, *Photons and Atoms* (Wiley Interscience, New York, 1989).

This discusses the $\mathbf{A} \cdot \mathbf{P}$ versus $\mathbf{E} \cdot \mathbf{r}$ perturbations and the Power-Zienau-Wolley transformation. A simplified discussion and other references are in the following paper:

- E. A. Power and T. Thirunamachandran, *Ann. J. Phys.*, **46**, 370 (1976).

An early paper which gave a classical transformation between $\mathbf{E} \cdot \mathbf{r}$ and $\mathbf{A} \cdot \mathbf{p}$ Hamiltonians is by Marie Goeppert-Mayer:

M. Goepfert-Mayer, *Ann. Physik (Lpzg.)*, **9**, 273 (1931).

The first paper to give a quantum mechanical transformation of $\mathbf{E} \cdot \mathbf{r}$ and $\mathbf{A} \cdot \mathbf{p}$ is by Richards. H. S. Synder is credited in the paper.

P. I. Richards, *Phys. Rev.*, **73**, 254 (1948).

A restricted version of this transformation for the case of a magnetic field constant in space and time appears in the following paper:

W. E. Lamb, *Phys. Rev.*, **85**, 259 (1952).

It was used again in the same restricted context by the following authors:

B. R. Johnson, J. O. Hirschfelder, and K. H. Yang, *Rev. Mod. Phys.*, **55**, 109 (1983).

Another discussion of the problem is in the following paper:

J. R. Ackerhalt and P. W. Milonni, *J. Opt. Soc. Am.*, **B11**, 116 (1984).

For an example of some of the confusion surrounding the $\mathbf{A} \cdot \mathbf{p}$ interaction see the following paper:

D. H. Kobe, *Phys. Rev. Lett.*, **40**, 538 (1978).

Some modern treatments of laser-atom lineshape and two-level atom models are listed below. The first papers are seminal ones by B. R. Mollow:

B. R. Mollow, *Phys. Rev.*, **188**, 1969 (1969); *Phys. Rev. A*, **2**, 76 (1969); *Phys. Rev. A*, **12**, 1919 (1969); *Phys. Rev. A*, **13**, 758 (1969).

A discussion that uses the two-level quasi-spin is by Courtens and Szöke, *Phys. Rev. A*, **15**, 1588 (1977).

The two-level atom is presented as a generalization to classical resonance in the following text:

L. Allen and J. H. Eberly, *Optical Resonance and Two-Level Atoms* (Wiley Interscience, New York, 1975).

Applications of radiation theory to laser dynamics is the subject of the following book, which also relates the classical Lorentz model to modern theory:

P. W. Milonni and J. H. Eberly, *Lasers* (Wiley Interscience, New York, 1988).

Recent developments of the problem of an isolated atom-cavity system are based upon the Jaynes-Cummings model.

E. T. Jaynes and F. W. Cummings, *Proc. IEEE*, **51**, 89 (1963).

The phenomenon of “collapse” and “revival” of Jaynes-Cummings solutions is discussed in the following:

J. H. Eberly, N. B. Narozhny, and J. J. Sanchez-Mondragon, *Phys. Rev. Lett.*, **44**, 1323 (1980).

H. J. Yoo, J. J. Sanchez-Mondragon, and J. H. Eberly, *Phys. Rep.*, **118**, 259 (1985).

Recent discoveries have been made about the behavior of the Bloch vector during collapse and revival.

J. Gea-Banacloche, *Phys. Rev. Lett.*, **65**, 3385 (1990); *Phys. Rev. A*, **44**, 5913 (1991); *Optical Commun.* **88**, 531 (1992).

Much of the future work on atoms or molecules in cavities will use so-called driven Jaynes-Cummings models. Some discussions of these have just been published.

P. Alsing and H. J. Carmichael, *Quantum Optics*, **3**, 13 (1991).

P. Alsing, D. S. Guo and H. J. Carmichael, *Phys. Rev. A*, **45**, 5135 (1992).

Time correlation between parts of the resonance spectrum are described in the following paper.

A. Aspect, G. Roger, S. Reynaud, J. Dalibard, and C. Cohen-Tannoudiji, *Phys. Rev. Letters*, **45**, 617 (1980).

Many have contributed to angular momentum coupling besides the originators Wigner, Racah, Clebsch and Gordan. Some have gone on to develop similar formulas for higher unitary groups $U(m)$. Pioneers in this area include Schwinger, Baird, Biedenharn, Bincer, Gelfand, Louck, and Moshinsky.